STUDIES
ON
THE STRUCTURES AND
THE OPTICAL AND ELECTRICAL PROPERTIES OF
SEVERAL ORGANIC SEMICONDUCTORS

TOSHIAKI TAMAMURA

JANUARY, 1974

論文目錄　大阪大学

報告番号・甲第1693号　　玉村敏昭

主論文　Studies on the Structures and the Optical and Electrical Properties of Several Organic Semiconductors

（二・三の半導性有機化合物の構造と光・電気物性に関する研究）

（主論文のうち印刷公表したもの）

1. Electronic Spectra of Organic Charge Transfer Salts of 2-Dicyanomethylene-1,1,3,3-tetracyanopropane

（2-ジシアノメチレン-1,1,3,3-テトラシアノプロパンの有機電荷移動塩の電子スペクトル）

Bulletin of the Chemical Society of Japan 42巻 8号

昭和44年 8月 15日

1. Excimer Emissions of Some Aromatic Vinylpolymers

（いくつかの芳香族ビニルポリマーのエキサイマー発光）

Chemistry Letters 6号

昭和47年 6月 5日

1. Triplet Exciton Migration in Poly-N-vinylcarbazole and its Styrene Copolymers

（ポリ-N-ビニルカルバゾールとそのスチレン共重合体における三重項励起子の移動）

Chemistry Letters　5号

昭和48年 5月 5日

(主論文のうち未公表のもの)

1. Organic Charge Transfer Salts II. Photoconductive and Magnetic Properties of Organic Charge Transfer Salts
(有機電荷移動塩II. 有機電荷移動塩の光電的・磁気的性質)

Bulletin of the Chemical Society of Japan 47巻 2号
昭和49年 2月 15日 掲載予定

1. Crystal Structure of 2,4,6-triphenylpyrylium-1,1,3,3-tetracyanopropenide, $[(C_{23}H_{17}O)^{+}\cdot(C_7HN_4)^{-}]$
(2,4,6-トリフェニルピリリウム-1,1,3,3-テトラシアノプロペナイド $[(C_{23}H_{17}O)^{+}\cdot(C_7HN_4)^{-}]$ の結晶構造)

Bulletin of the Chemical Society of Japan 47巻 3号 又は 4号
昭和49年 3月15日 又は
昭和49年 4月15日 掲載予定

1. Organic Charge Transfer Salts IV. Emission Spectrum of an Organic Charge Transfer Salt, 2,4,6-triphenylthiopyrylium-1,1,3,3-tetracyanopropenide
(有機電荷移動塩IV. 有機電荷移動塩, 2,4,6-トリフェニル-チオピリリウム-1,1,3,3-テトラシアノプロペナイドの発光スペクトル)

Bulletin of the Chemical
Society of Japan 47巻 3又は4号
昭和 49年 3月 15日 又は
昭和 49年 4月 15日 掲載予定

1. Crystal Structure of 2,4,6-triphenylthiopyrylium-1,1,3,3-tetracyanopropenide, $[(C_{23}H_{17}S)^{+}\cdot(C_7HN_4)^{-}]$
(2,4,6-トリフェニルチオピリリウム-1,1,3,3-テトラシアノプロペナイド, $[(C_{23}H_{17}S)^{+}\cdot(C_7HN_4)^{-}]$ の結晶構造)

執筆中
Bulletin of the Chemical
Society of Japan 投稿予定

1. Excimer Formation in Aromatic Vinylpolymers
(芳香族ビニルポリマーにおけるエキサイマー生成)

執筆中
Macromolecules 投稿予定

1. Triplet-Triplet Annihilation in Poly-N-vinylcarbazole and its Alternating Copolymers
(ポリ-N-ビニルカルバゾールとその交互共重合体中の三重項-三重項消失)

執筆中
Journal of Chemical Physics
投稿予定

Organic Charge Transfer Salts II. Photoconductive and Magnetic Properties of Organic Charge Transfer Salts

原稿採用決定御通知

貴下がさきにご投稿になりました報文は 11月 20日開催の編集委員会において採用と決定いたしましたのでご通知申し上げます（原稿番号30682）

題名

題名省略

（上記報文は 49 年 2 月号に掲載の予定です）

昭和 48.11月28日

〒101 東京都千代田区神田駿河台1－5
社団法人 日本化学会編集部
電話東京03(292)6161(代表)

Crystal Structure of 2,4,6-triphenylpyrylium-1,1,3,3-tetracyanopropenide, $[(C_{23}H_{17}O)^{+}\cdot(C_7HN_4)^{-}]$

原稿採用決定御通知

貴下がさきにご投稿になりました報文は 12月 17日開催の編集委員会において採用と決定いたしましたのでご通知申し上げます（原稿番号30727）

題名 題名省略

（上記報文は 49 年 3～4 月号に掲載の予定です）

昭和 48.12.21日

〒101 東京都千代田区神田駿河台1－5
社団法人 日本化学会編集部
電話東京03(292)6161(代表)

Organic Charge Transfer Salts IV. Emission Spectrum of Organic Charge Transfer Salt, 2,4,6-triphenylthiopyrylium-1,1,3,3-tetracyanopropenide

原稿採用決定御通知

B.C.S.J.

貴下がさきにご投稿になりました報文は 12 月 18 日開催の編集委員会において採用と決定いたしましたのでご通知申し上げます (原稿番号 30638)

題名 題名省略

(上記報文は 47 年 3~4 月号に掲載の予定です)

昭和 46. 12. 21 日

〒101 東京都千代田区神田駿河台1－5
社団法人 日本化学会編集部
電話東京03(292)6161(代表)

Preface

The work of this thesis was carried out under the guidance of Professor Hiroshi Mikawa at Faculty of Engineering, Osaka University.

The author is greatly indebted to Professor Hiroshi Mikawa for his continuing guidance and encouragement.

The X-ray crystallographical studies, an important part of this thesis, were done under the guidance of Professor Nobutami Kasai at Faculty of Engineering, Osaka University.

The author is also very grateful to Professor Nobutami Kasai for his kindly guidance.

The author wishes to express his gratitude to Professor Shigekazu Kusabayashi at Yamaguchi University, Assistant Professor Yasuhiko Shirota, Dr. Masaaki Yokoyama, and Dr. Kenichi Okamoto for many helpful discussion and suggestions throughout the work.

He would like to acknowledge Professor Masao Kakudo at Osaka University, Assistant Professor Tamaichi Ashida, and Assistant Professor Noritake Yasuoka for valuable suggestions during the X-ray crystallographical studies.

Thanks are given to the author's co-workers, Dr Takashi Yamane, Mr. Hiroshi Yasuba, Mr. Tatsuro Imai, and Mr. Takeshi Nakano for their assistance.

Finally, the author wishes to thank all the menbers of Mikawa laboratory for their friendship.

Toshiaki Tamamura

List of Publications

The papers published by the author concerning this thesis are as follows.

(1) Electronic Spectra of Organic Charge Transfer Salts of 2-Dicyanomethylene-1,1,3,3-tetracyanopropenide

S. Sakanoue, T. Tamamura. S. Kusabayashi, H. Mikawa, N. Kasai, M. Kakudo, and H. Kuroda

Bull. Chem. Soc. Japan, 42, 2407 (1969).

(2) Organic Charge Transfer Salts II. Photoconductive and Magnetic Properties of Organic Charge Transfer Salts

T. Tamamura, H. Yasuba, K. Okamoto, T. Imai, S. Kusabayashi, and H. Mikawa

Bull. Chem. Soc. Japan, in Press.

(3) Crystal Structure of 2,4,6-triphenylpyrylium-1,1,3,3-tetracyanopropenide, $[(C_{23}H_{17}O)^{+}\cdot(C_7HN_4)^{-}]$

T. Tamamura, T. Yamane, N. Yasuoka, and N. Kasai

Bull. Chem. Soc. Japan, in Press.

(4) Organic Charge Transfer Salts IV. Emission Spectrum of an Organic Charge Transfer Salt; 2,4,6-triphenylthiopyrylium-1,1,3,3-tetracyanopropenide

T. Tamamura, M. Yokoyama, S. Kusabayashi, and H. Mikawa

Bull. Chem. Soc. Japan, in Press.

(5) Excimer Emissions of Some Aromatic Vinylpolymers

M. Yokoyama, T. Tamamura, T. Nakano, and H. Mikawa

Chem. Letters, 499 (1972).

(6) Triplet Exciton Migration in Poly-N-vinylcarbazole

M. Yokoyama, T. Nakano, T. Tamamura, and H. Mikawa

Chem. Letters, 509 (1973).

CONTENTS

GENERAL INTRODUCTION

Organic compounds have been expected as new materials having novel properties, because wide varieties of compounds can be obtained. For the purpose of obtaining new materials for electronics or electrophotography, a number of organic compounds having semiconductivity have been synthesized. One can classify these organic semiconductors from chemical viewpoint as follows.

Class 1 : Conjugated aromotic hydrocarbons.

Class 2 : Molecular complexes.

Class 3 : Photoconductive polymers.

The compounds of Class 1 have usually simple structure, and can be purified on an extremely high level of purity. Anthracene has been exhaustively studied as a most representative material belonging to Class 1, and the results have provided the fundamental and theoretical bases for understanding the electrical conduction in organic materials.[1)]

All compounds belonging to Class 1 are poor semiconductor with very high resistivity, but the conductivity can be improved by means of the formation of molecular complexes. Especially, certain organic molecular complexes belonging to Class 2 such as 7,7,8,8-tetracyanoquinodimethane anion-radical complexes, show extremely low resistivity comparable to those of metals. The main purpose to study the compounds of Class 2 was to obtain these extremely high conductive materials.

On the other hand, the photoconductive polymers are most important

materials for practical purpose, being able to form a photoconductive solid film. Since Poly-N-vinylcarbazole has been successfully utilized as a material for electrophotography, there has been greatly increased interest in these polymers. However, because of the complex structure and the complex feature of the electrical properties, progress in understanding the mechanism of the photoconduction in these polymers seems to be low.

In order to advance the studies on such wide varieties of organic semiconductors, are significantly necessary the research for new material groups and the feed-back of the results obtained to further material research.

In this thesis, the author investigated the structures and the optical and electrical properties of two important groups of organic semiconductive materials. Part I deals with a new kind of organic ionic compounds belonging to Class 2. It should be mentioned that although the extensive studies have been reported on molecular charge-transfer complexes,[2] little attention has been paid to the ionic compounds in which an interionic charge-transfer interaction is present. The author calls this kind of salts organic charge-transfer salts, and has investigated the structures and the physical properties of several organic charge-transfer salts newly prepared here.

On the other hand, among the compounds of Class 3, the vinyl-polymers having large π-electron conjugated system are increasingly important materials for electrophotography.[3] In Part II of this thesis the author has investigated the photophysical processes in these polymers in order to obtain information on the mechanism of photoconduction in this kind of polymers.

References

1) F. Gutman and L. E. Lyons, "Organic Semiconductors", John Wiely & Sons, Inc., New York (1967).

2) R. Foster, "Organic Charge-Transfer Complexes", Academic Press, Inc., London Ltd. (1969).

3) K. Okamoto, S. Kusabayashi, and H. Mikawa, Kogyo Kagaku Zasshi, 73, 1351 (1970).

PART I

STRUCTURES AND PHYSICAL PROPERTIES OF ORGANIC CHARGE-TRANSFER SALTS

INTRODUCTION

The general idea of charge-transfer (abbreviated as CT) interaction was presented theoretically by R. S. Mulliken at 1950.[1,2,3] After that, this idea becomes indispensable both to physical chemistry and to organic chemistry. Organic CT complexes have been extensively investigated from many viewpoints.[4,5]

From a view of organic semiconductor, two approaches have been carried out on organic CT complexes. One is to obtain very highly conductive materials, and other is to obtain the photoconductive materials.

It is well known that although most conjugated aromatic compounds are very poor electrical conductors in the solid state, the conductivity can be fairly improved by the CT complex formation.[6] However, most of the solid CT complexes still have considerably high electrical resistivity. Such complexes are usually composed of relatively weak electron donor or weak electron acceptor molecules. By contrast, solid complexes between strong donors and strong acceptors which show an ion-radical character in the ground state, have low specific resistivity less than 10^5 ohm·cm.

Particularly, the iodine complex with perylene, for example, shows extremely low resistivity, about 3-9 ohm·cm.[7,8] Thus, the very high electrical conduction like metal have been expected for this kind of CT complexes.

On the other hand, in weak CT complexes, a photoconduction due to the broad CT absorption band has been expected, because the dark current is so small that the photocurrent is not swamped by the dark current. In practice, several CT complexes show the photoconduction in the CT absorption region, but in all cases the photocurrent was small and did not show a good reproducibility.[9,10,11,12]

These CT complexes are generally composed of an electron-donating molecule and an electron-accepting molecule. On the other hand, a CT interaction can also be found in certain organic salts which are formed between an electron-donating organic anion and an electron-accepting organic cation. Such an interionic CT interaction was firstly demonstrated with alkylpyridinium iodide salts by E. M. Kosower.[13] Although this type of interaction has been observed in relatively many ionic compounds spectroscopically, no systematic studies on the structures and the physical properties of these organic CT salts has been reported. However, the physical properties of the CT salts are expected to show the characteristic feature differing from those of ordinary molecular CT complexes, since a CT salt has an ionic ground state and a neutral excited state, contrary to molecular CT complex.

Therefore, in Part I, the author has prepared several new organic ionic compounds formed between a pyrylium or thiopyrylium cation and a polycyanoacid anion as shown in Fig. 1, and has investigated the physical properties and the structures of these salts.

In order to demonstrate the existence of the interionic CT interaction in these salts, the absorption spectra (Chapter 1) and emission

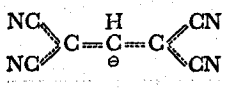

1,1,3,3-tetracyanopropenide anion (TCP)

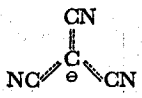

tricyanomethanide anion (TCM)

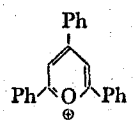

2,4,6-triphenylpyrylium cation (TPP)

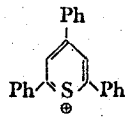

2,4,6-triphenylthiopyrylium cation (TPT)

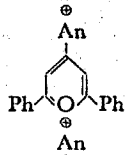

4-anisyl-2,6-diphenyl-pyrylium cation (ADPP)

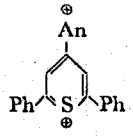

4-anisyl-2,6-diphenylthio-pyrylium cation (ADPT)

Fig. 1.

spectra (Chapter 2) have been examined, and the CT absorption and CT fluorescence bands have been observed both in solution and in the solid state. Moreover, in these chapters, the natures of the ground state and the excited CT state of the salts will be discussed.

Chapter 3 deals with the electrical and magnetic properties of the organic CT salts. The discussion has been concentrated on the relationship between the photoconduction and the paramagnetism and the CT excited state.

Chapter 4 deals with the crystal structures of the organic CT salt in order to obtain further imformation on the CT interaction in the solid state. In this chapter, two organic CT salts prepared here have been investigated by X-ray structure analysis.

References

1) R. S. Mulliken, J. Amer. Chem. Soc., 72, 600 (1950).

2) R. S. Mulliken, ibid., 72, 4493 (1950).

3) W. B. Person and R. S. Mulliken, "Molecular Complexes: A Lecture and Reprint Volume", Wiley, New York, (1969).

4) G. Briegleb, "Electronen-Donator-Acceptor-Komplexe", Springer-Verlag, Berlin (1961).

5) R. Foster, "Organic Charge-Transfer Complexes", Academic Press, Inc. (London) Ltd. (1969).

6) F. Gutman and L. E. Lyons, "Organic Semiconductors", John, Wiely & Sons, Inc., New York (1967).

7) T. Uchida and H. Akamatu, Bull. Chem. Soc. Japan, 34, 1015 (1961).

8) W. H. Bentley and H. G. Drickamer, J. Chem. Phys., 42, 1573 (1965).

9) H. Akamatu and H. Kuroda, ibid., 39, 3364 (1963).

10) H. Kokado, H. Hasegawa and W. G. Schneider, Can. J. Chem., 42, 1084 (1964).

11) M. C. Tobin and D. P. Spitzer, J. Chem. Phys., 42, 3654 (1965).

12) C. K. Prout, R. J. P. Williams, and J. D. Wright, J. Chem. Soc. (A), 747 (1969).

13) E. M. Kosower, J. Amer. Chem. Soc., 77, 3883 (1955).

Chapter 1

ABSORPTION SPECTRA

Introduction

In relatively many ionic compounds, an interionic CT absorption band was observed in solution.[1 - 9] The interionic CT absorption was very sensitive to the nature of solvent, and showed a remarkable blue shift with an increase of the solvent polarity. This behavior has been understood in terms of the strong solvation of the salt in its ionic ground state.[2,3,4] By contrast, few investigations have been reported on the absorption spectra in the solid state of these CT salts, which are necessary for understanding the physical properties and the crystal structures of the CT salts.

This chapter will deal with the absorption spectra of new organic salts composed of the pyrylium or thiopyrylium cation and the polycyanoacid anion both in solution and in the solid state, in order to confirm the presence of interionic CT interaction between the cation and the anion in these salts.[10]

Experimental

Materials. 1,1,3,3-tetracyanopropenide (TCP) and tricyanomethanide (TCM) anions were used as the anions, while 2,4,6-triphenylpyrylium (TPP), 2,4,6-triphenylthiopyrylium (TPT), 4-anisyl-2,6-diphenylpyrylium (ADPP) and 4-anisyl-2,6-diphenylthiopyrylium (ADPT) cations were used as the cations.

1,1,3,3-tetracyanopropenide anion (TCP)

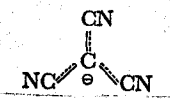

tricyanomethanide anion (TCM)

Anions

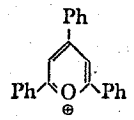

2,4,6-triphenylpyrylium cation (TPP)

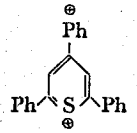

2,4,6-triphenylthiopyrylium cation (TPT)

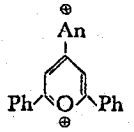

4-anisyl-2,6-diphenyl-pyrylium cation (ADPP)

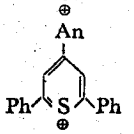

4-anisyl-2,6-diphenylthio-pyrylium cation (ADPT)

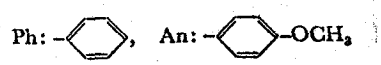

Cations

Sodium-TCP (Na-TCP). Pyridinium-TCP (Py-TCP) was prepared according to Mikawa's method.[11] Na-TCP was obtained from Py-TCP by the use of a cation-exchange resin, Amberlite CG 120 T-1.

Potassium-TCM (K-TCM). This compound was prepared according to Trofimenko's method[12] and was purified by the column chromatography using active carbon as the adsorbent and methanol as the developing solvent.

TPP-perchlorate (TPP-ClO_4), TPT-ClO_4, ADPP-ClO_4, and ADPT-ClO_4. These compounds were prepared according to Ulrich's method.[13]

The organic CT salts were prepared by a double decomposition reaction between corresponding perchlorate salt of the cation and metal salt of the anion, and purified by repeated recrystallizations from methanol-water (4:1), or methanol solution. The organic CT salts prepared thus are listed in Table 1-1 along with their melting points. The results of elemental analysis of these salts showed good agreements with the corresponding calculated value. All the solvents used were purified according to the usual method

of purification.[14)]

Measurements. The absorption spectrum of solution and diffuse reflectance spectrum of the solid were measured with a Hitachi spectrophotometer, EPS 3. The diffuse reflectance spectrum was measured using potassium bromide as a standard; it was then plotted using the Kubelka-Munk function, $f(R) = (1-R^2)/2R$, where R is the reflectance. The spectrum of the solution at low temperatures was measured with a Cary model 14 spectrophotometer. The polarized absorption spectrum in the single crystal was measured with a Shimadzu multipurpose spectrophotometer, MPS-50, with the use of a microspectophotometer attachment.

Results and Discussion

The electronic absorption spectra in solution. The absorption spectrum of TPT-TCP in chloroform has four absorption bands (λ_{max}: 281, 351, 416, and 570 nm), Na-TCP has one absorption band (λ_{max}: 345 nm), and TPP-ClO_4 has three absorption bands (λ_{max}: 281, 372, and 414 nm), as shown in Fig. 1-1. The absorption band of Na-TCP is due to the TCP anion, and the absorption

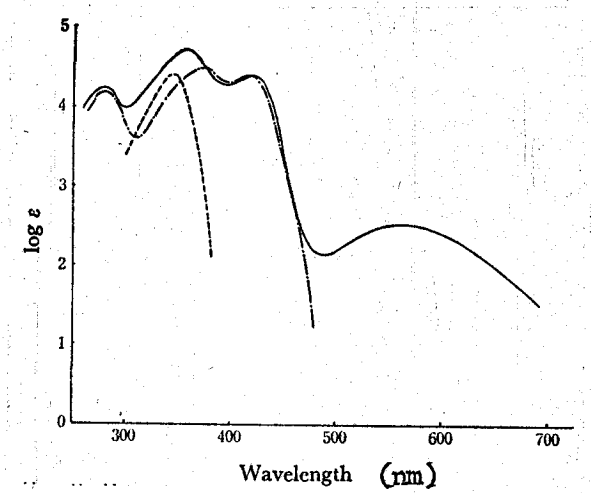

Fig. 1-1. Absorption spectra of TPP-TCP in chloroform and its component ions.
—— TPP-TCP in $CHCl_3$, ---- TPP-ClO_4 in $CHCl_3$ —·— Na-TCP in CH_3OH

Table 1-1 Absorption maxima of CT band in chloroform and in solid state.

Salts	m.p. (°C)	λ_{max} in $CHCl_3$ (nm)	λ_{max} in solid (nm)
TPP-TCP	(203-204)	570	565
TPT-TCP	(142-143)	595	540
ADPP-TCP	(243-245)	540 (S)	530 (S)
ADPT-TCP	(175-177)	570 (S)	560 (S)
TPP-TCM	(197-199)	538	530
TPT-TCM	(156-158)	566	520 (S)
ADPP-TCM	(201-202)	530 (S)	520 (S)
ADPT-TCM	(65- 67)	540 (S)	560 (S)

(S): shoulder

bands of TPP-ClO_4 are due to the TPP cation. Three absorption bands (λ_{max}: 281, 351, and 416 nm) of TPP-TCP salt can be explained in terms of the superposition of the absorption bands of the parent cation and anion, being assigned to the locally excited (LE) absorption bands of the component ions of the salt. The other absorption band (λ_{max}: 570 nm) is characteristic of the TPT-TCP salt, because neither the parent cation nor the parent anion have any absorption in this region. This fact suggests that the new band is an interionic CT band. A new band of this type is also found in the absorption spectra of the other salts. The wavelengths of these new absorption bands are listed in Table 1-1.

The new band is sensitive to the polarity of solvent. The increase in the polarity of solvent causes the absorption maximum to shift toward a shorter wavelength and the apparent molar extinction coefficient (ε_{app}) to decrease.

Figure 1-2 shows the plot of the λ_{max} energies of the new bands of TPT-TCP salt in various solvents versus the Z-value,[2,3,4] the empirical parameter of the solvent polarity. The approximately linear relationship

shows that the absorption maximum shifts to a shorter wavelength with an increase in the solvent polarity. The other salts give similar results. The solvent shift of the absorption bands in these salts can be explained by Kosower's theory presented in his consideration of solvent effect of the absorption spectrum of organic iodides.[2,3,4] That is, the solvent of the absorption maximum depends on the stabilization in the ground state and the destabilization in the excited state. From the above results, it can be concluded again that the new bands of these salts are due to the interionic CT from the anion to the cation.

As these CT bands are due to the interaction between the anion and the cation, both ions must be in the ion-pair form in order to exhibit CT interactions. The salts are in the following equilibrium in solution:

$AD \rightleftharpoons D^- + A^+$, where DA is an organic CT salt in an ion-pair form, and

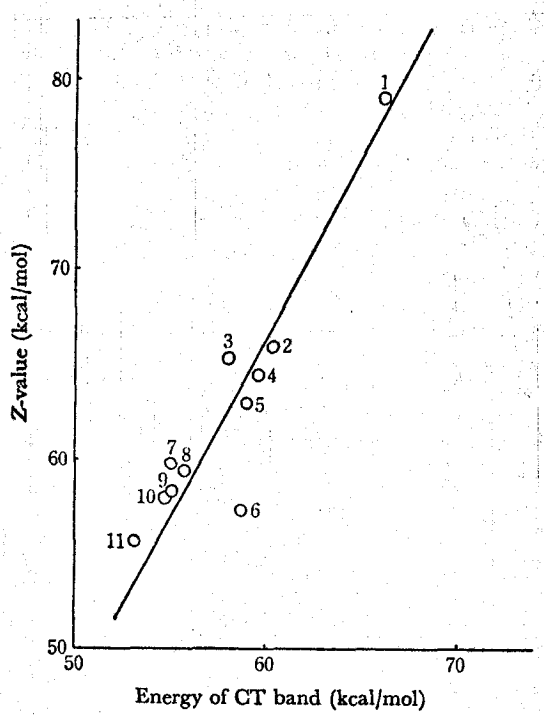

Fig. 1-2. Energies of the charge transfer bands of TPT-TCP against the *Z*-value for the solvents used.
(1) Acetic acid, (2) Methyl acetate, (3) Anisole, (4) Dichloromethane, (5) Chloroform, (6) Ethyl acetate, (7) Bromobenzene, (8) Chlorobenzene, (9) Dioxane, (10) Toluene, (11) Benzene.

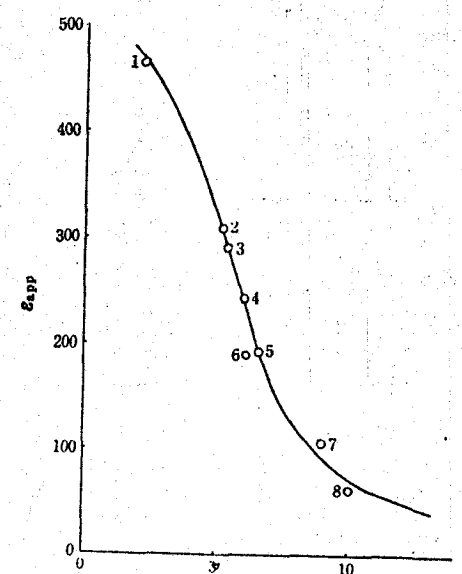

Fig.1-3. Dielectric constant

Apparent molar extinction coefficient of TPT-TCP against the dielectric constants for the solvents used.
(1) Dioxane, (2) Chlorobenzene, (3) Bromobenzene, (4) Methyl acetate, (5) Ethyl acetate, (6) Acetic acid, (7) Dichloromethane, (8) 1,2-dichloroethane.

D^- and A^+ are the component ions. In polar solvents the dissociation of the ion-pair proceeds and the concentration of the ion-pair becomes low, and consequently the apparent molar extinction coefficient (ε_{app}) decreases. At a certain concentration the ε_{app} values were measured in several different solvents. As is shown in Fig. 1-3, the ε_{app} values decrease with the increase in the dielectric constant of the solvent. Although the solvent shift of the interionic CT band can be explained by the term of Z-values, the dissociation of the salt is closely related to the dielectric constant of the solvent.

The interionic CT absorption band is also sensitive to temperature, and shows a considerable blue shift as the temperature is lowered. In Fig. 1-4 are shown, for example, the absorption spectra of TPT-TCP salt in 2-methyltetrahydrofuran (2MTHF) - toluene (9:1) solution at various temper-

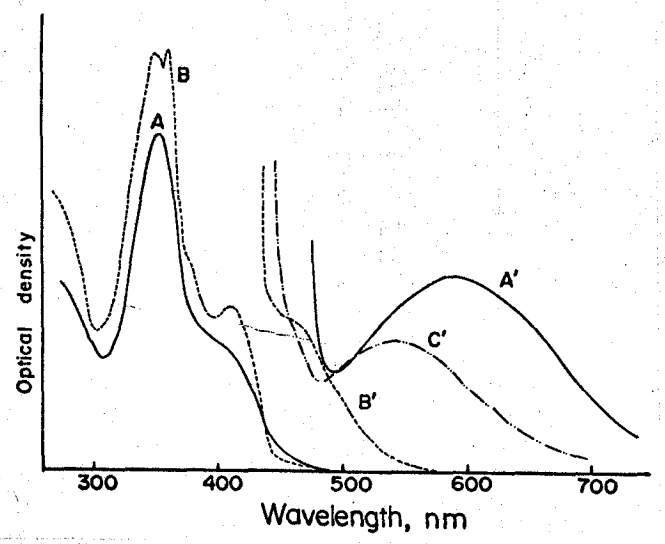

Fig. 1-4. Absorption spectra of TPT-TCP in 2MTHF-toluene (9:1) solution at various temperature.

A: 4.0×10^{-5} mol/l, room temperature,
A': 2.0×10^{-3} mol/l, room temperature,
B: 4.0×10^{-5} mol/l, 77°K, B': 2.0×10^{-3} mol/l, 77°K,
C': 2.0×10^{-3} mol/l, 223°K.

atures. At 77°K, the LE bands of the component ions become sharp, but do not show any shift in maximum wavelength, compared with that at room temperarure. The CT absorption maximum, however, shows a blue shift of 45 nm at 227°K, and 120 nm at 77°K from the position of this band at room temperature. A considreable decrease of the absorbance of the CT band occurs together with this blue shift. This kind of blue shift was observed in CH_2Cl_2 solutions of some alkylpyridinium-halide salts by Brinen et al.,[15] but they did not discuss the reason of this blue shift. This temperature dependence seems to be phenomenologically similar to the solvent effect on the CT absorption.

It is well known that the polarity of solvent increases with the lowering of temperature, because of the enhanced orientation of the solvent dipole. Indeed, Furutsuka et al. reported that the values of the dielectric constant of 2MTHF at 298°, 223°, just above the glass transition temperature (108°K), and below 108°K are 7.0, 9.0, 18.0, and 3.5, respectively.[16] Thus, the dielectric constant increases with the lowering of temperature down to the glass transition temperature. Therefore, even near the glass transition temperature of 2MTHF-toluene (9:1), the solvent molecules around the salt are expected to be in well oriented state. Although the dielectric constant of the solvent is very small below the glass transition temperature, the local solvent orientation around the salt may be kept even in the frozen state. The Z-value of the solvent, therefore, may increase with the lowering of temperature, and may not decrease even in a glass. From the result in Fig. 1-4, the Z-values of 2MTHF-toluene (9:1) at room temperature, 223°, and 77°K can be estimated to be about 64, 72, and 88 kcal/mol. Thus the blue shift and the decrease of the absorbance of the CT band can be accounted for by the increase of the solvent polarity in the low temperature region.

The electronic absorption spectrum in solid. The absorption spectra in a solid were measured by diffuse reflectance spectroscopy. The spectra of TPP-TCM, TPP-TCP, and TPP-ClO_4 are shown in Fig. 1-5. The absorption band is at 530 nm in TPP-TCM and at 565 nm in TPP-TCP. These absorption bands in a solid are considered to correspond to the CT bands in solution. The absorption peaks of other salts are given in Table 1-1.

The CT band in the solid state lies in a somewhat shorter wavelength region than the corresponding CT band in chloroform solution, as shown in Table 1-1. This suggests that the stabilization by the neighboring ions in the solid state is larger than the stabilization by the neighboring solvent molecules in chloroform solution. The data in Table 1-1 also suggest that the stabilization of the TPP system is smaller than that of the TPT system. This difference may be due to the difference in the crystal structure, as stated in Chapter 4 of this part.

The polarized absorption spectra of the single crystals of TPP salts

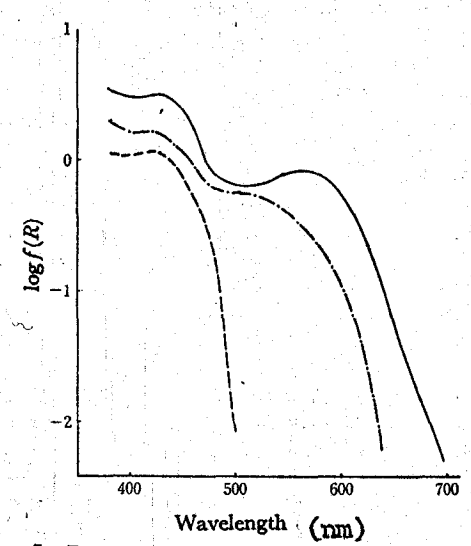

Fig. 1-5. Diffuse reflectance spectra of TPP-TCP (——), TPP-TCM (– – –) and TPP-ClO_4 (——).

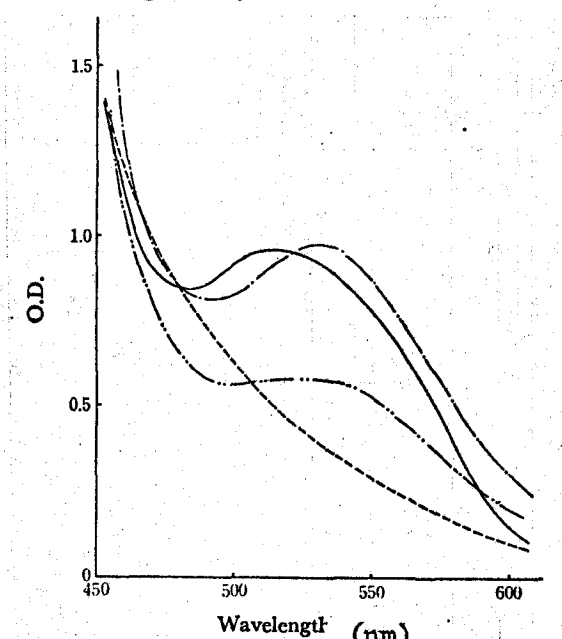

Fig. 1-6. Polarized absorption spectra of single crystals of TPP-TCP and TPP-TCM.
TPP-TCP: – – – 1//, – – – – 1⊥
TPP-TCM: —— 1//, —— 1⊥

show a remarkable dichroism in the CT absorption band, the optical density being large in the direction of the crystal growth (Fig. 1-6). This suggests that the cation and the anion are stacked in an alternating face-to-face arrangement in the crystal growth direction, and that the CT transition occurs from an anion to the nearest cation in this direction, which were confirmed with TPP-TCP salt, as stated in Chapter 4.

Summary

In new organic CT salts formed between a pyrylium or thiopyrylium cation and a polycyanoacid anion, a CT absorption band between the cation an and the anion was observed both in solution and in the crystalline state. The CT absorption band in solution was found to be very sensitive to the nature of solvent due to two different factors. As the solvent polarity increased, (i) the absorbance of the CT band decreased by the proceeding of the dissociation of the salt into component ions, and (ii) the CT absorption peak showed a remarkable blue shift, which was accounted for by the strong solvation of the salt in its ionic ground state. The interionic CT band was also dependent on the temperature as well as on the solvent. In a single crystal, the polarized absorption spectrum showed a remarkable dichroism, which may be closely related to the crystal structure.

References

1) E. M. Kosower, J. Amer. Chem. Soc., 77, 3883 (1955).

2) E. M. Kosower, ibid., 83, 3253, 3261 (1958).

3) E. M. Kosower, and G. S. Wu, ibid., 83, 3142 (1961)

4) E. M. Kosower, G. S. Wu, and T. S. Sorensen, ibid., 83, 3147 (1961).

5) E. M. Kosower, J. A. Skorcz, W. M. Schwarz, and J. W. Pattor, ibid.,

82, 2188 (1960).

6) S. F. Mason, J. Chem. Soc., 1960, 2437.

7) E. L. Goff and R. B. LaCount, J. Amer. Chem. Soc., 85. 1354 (1963).

8) A. T. Balaban, M. Mocanu, and Z. Simon, Tetrahedron, 20, 119 (1964).

9) S. Sakanoue, T. Tamamura, S. Kusabayashi, H. Mikawa, N. Kasai, M. Kakudo, and H. Kuroda, Bull. Chem. Soc. Japan, 42, 2407 (1969).

10) H. Yasuba, T. Imai, K. Okamoto, S. Kusabayashi, and H. Mikawa, ibid., 43, 3101 (1970).

11) A. Taniguchi, K. Suzuki, and H. Mikawa, ibid., 39, 1605 (1966).

12) S. Trofimenko, E. L. Little, an H. F. Mower, J. Org. Chem., 27, 433 (1962).

13) R. Winzinger, and P. Ulrich, Helv. Chim. Acta,39, 5, 207 (1956).

14) J. A. Riddick and E. E. Troops,Jr., "Technique of Organic Chemistry," Vol.7, Organic Solvents, Interscience Publishers, Inc., New York, (1955).

15) J. S. Brinen, J. G. Koren, H. O. Olmsteaed, and R. C. Hirt, J. Phys. Chem.,69, 3791 (1965).

16) T. Furutsuka, T. Imura, K. Kawabe, and T. Kojima, Technology Reports of the Osaka University, 24 (1973).

Chapter 2

EMISSION SPECTRA

Introduction

As mentioned in Chapter 1, the CT absorption spectra of organic CT salts showed a remarkable solvent effect, because the salt in its ground state is ionic. The excited CT state of organic CT salts may consist of two neutral radical species, $D^{\cdot}A^{\cdot}$. The existence of such an excited state can be directly demonstrated by the observation of the emission from this state.

Although the extensive studies have been carried out on the absorption spectra of organic CT salts,[1] few investigations have been reported on the emission spectra.[2] Especially, it seems that the solvent effect on the emission spectrum has not yet been elucidated in a wide range of solvent polarity. Among the salts investigated here, 2,4,6-triphenylthiopyrylium (TPT) - 1,1,3,3-tetracyanopropenide (TCP) salt is fairly soluble in various solvents including non-polar ones such as toluene or p-dioxane. Therefore, using TPT-TCP salt, it is possible to investigate the solvent effect of the emission spectrum of an organic CT salt in detail.

In this chapter, the author will study the emission spectra of TPT-TCP salt, special attention being paied to the solvent effect.

Experimental

For the measurement of the emission spectrum in the solid state, the microcrystalline sample was sealed in a pyrex tube (2mm diameter) under vacuum. Each sample in solution having an appropriate concentration was degassed and sealed in a pyrex tube. All solvents used were purified according to the usual purification method.[3] Emission spectra were recorded on a Hitachi model MPF-3 spectrophotofluorometer equipped with a Xe excitation lamp and an R-446 photomultiplier tube, and delayed emissions were measured with a delayed emission accessory including a cylindrical chopper to eliminate prompt emissions. The spectra obtained were not corrected both for the excitation source and for the photomultiplier response. Phosphorescence lifetimes were estimated from the decay curves on an oscilloscope. Fluorescence lifetimes were measured by the pulse method with an N_2 gas laser excitation (337 nm, 5 nsec half-width).

Results and Discussion

Emission spectrum in the crystalline state. Although sodium-TCP does not emit, TPT-perchlorate salt shows an emission both in solution and in the solid state. Figure 2-1 shows the emission and excitation spectra of TPT-TCP and TPT-perchlorate salts in the solid state at room temperature. The emission of the perchlorate salt in the solid state is also found in fluid solution. This emission is assigned to the fluorescence of TPT cation by its lifetime in solution (a few nsec), the mirror image relationship between the absorption and emission bands of the cation, and the excitation spectrum which approximately agrees with the absorption spectrum.

In TPT-TCP salt in the solid state, the fluorescence of TPT cation

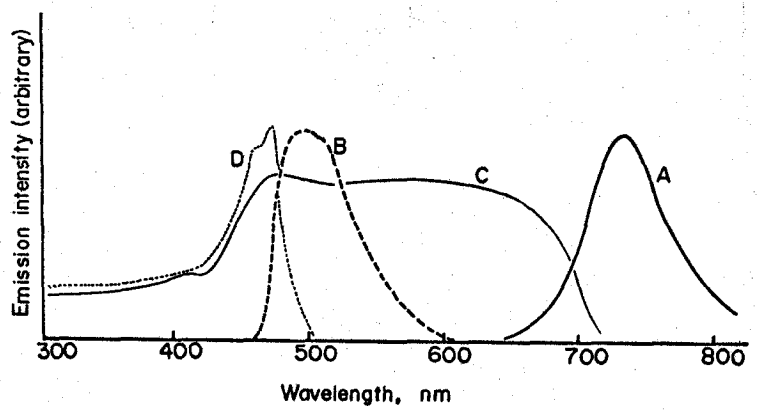

Fig. 2-1. Emission spectra of TPT-TCP and TPT-ClO_4 in solid.

(A) emission spectrum of TPT-TCP, (B) emission spectrum of TPT-ClO_4, (c) excitation spectrum of the emission of TPT-TCP at 740 nm, (D) excitation spectrum of the emission of TPT-ClO_4 at 500 nm.

was not found, and a new emission was observed at 740 nm. This emission can be assigned to an interionic CT fluorescence by the following reasons; (i) the mirror image relationship with the CT absorption is shown, (ii) this emission can be found by irradiation not only in the LE band but also in the CT absorption band, (iii) the lifetime was very shorter than 100 μsec.

Table 2-1 Maxima of the CT fluorescence (λ^F_{max}) and the CT absorption band (λ^A_{max}) in the solid state

Salts	λ^F_{max} (nm)	λ^A_{max} (nm)
TPP-TCP	725	565
TPT-TCP	740	540
ADPP-TCP	640	530 (S)
ADPT-TCP	710	560 (S)
TPP-TCM	680	530
TPT-TCM	620	520 (S)
ADPP-TCM	670	520 (S)

The above assignment is confirmed by the fact that such an emission band is also found in the solid state of other organic CT salts prepared in chapter 1. Table 2-1 gives the maximum wavelengths of the CT absorption and CT fluorescence bands of these salts. An approximately parallel relationship is found between the energies of the absorption and emission bands. Thus, when a CT interaction is present, the fluorescence of the component ion is completely quenched and a CT fluorescence is observed in the solid state.

Emission spectrum in fluid solution. The emission spectrum of TPT-TCP salt in fluid solution was measured in various solvents and at various concentrations at room temperature. In all cases, the fluorescence of TPT cation was observed, but a CT fluorescence could not be found. As shown in

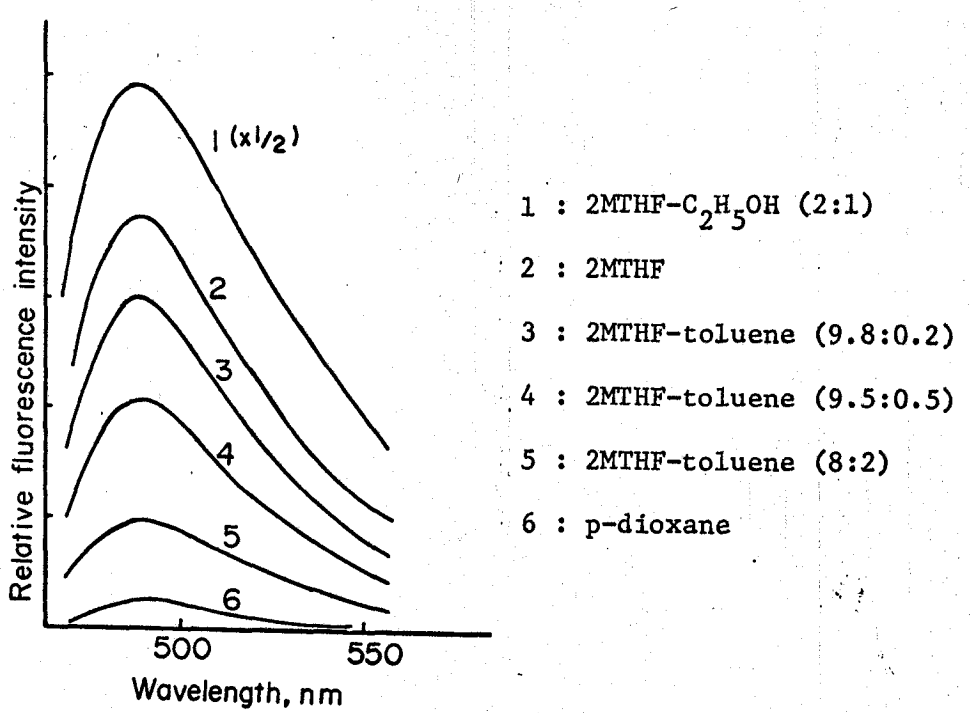

Fig. 2-2. Emission spectra of TPT-TCP in fluid solution at room temp.

Fig. 2-2, the intensity of the fluorescence of the cation was very sensitive to the solvent polarity, and became weak with the decrease of the solvent polarity. This fact suggests that the fluorescence of the cation is emitted only from the free TPT cation present in solution, and that the amount of the free cation produced by the dissociation of the ion-pair becomes small in a less polar solvent. This consideration is supported by the fact that the excitation spectrum of this emission agrees with the absorption of TPT cation.

Thus, in fluid solution TPT-TCP salt shows only the fluorescence of the free TPT cation and no emission from the undissociating ion-pair. This is in sharp contrast with the observation of the CT fluorescence of TPT-TCP salt in the solid state. In fluid solution the excited CT energy may be deactivated radiationlessly because of the interionic CT interaction.[4] Similarly, an ordinary molecular CT complex does not show a CT fluorescence even in non-polar solvents except for a few rare cases, and this seems to be understood in terms of an extremely low transition probability of a CT complex in fluid solution.[5,6,7]

Emission spectrum in rigid solution at 77°K. The emission spectrum of TPT-TCP salt in rigid solution is also affected by the nature of the solvent. In a polar solvent, methanol - ethanol (1:1), the emission spectrum is essentially identical with that of TPT-perchlorate under the same condition, as shown in Fig. 2-3. The emission band at 460 nm is the fluorescence of the cation. An emission band at 540 nm is assigned to the phosphorescence of TPT cation, because this band is found as a delayed emission of the perchlorate salt at 77°K, and its lifetime is about 30 msec. Since in this solvent TPT-TCP salt dissociates completely into two component ions, these two emissions originate from the free TPT cation present in rigid solution.

Figure 2-4 shows the emission spectra of TPT-TCP salt in a less polar

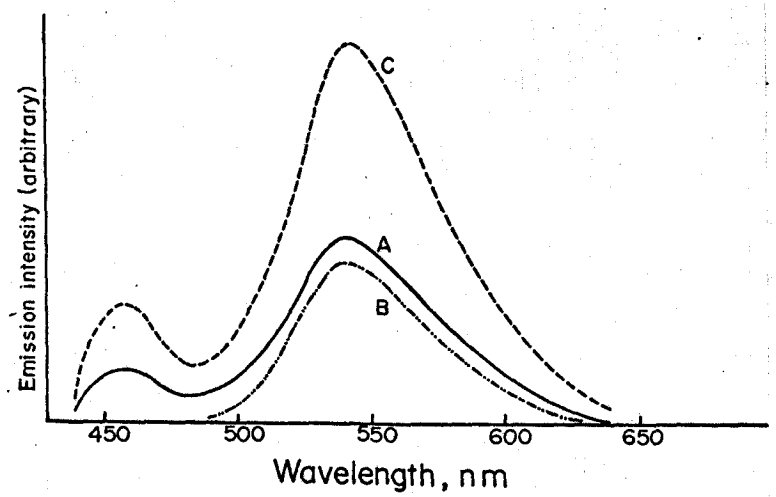

Fig. 2-3. Emission spectra of TPT-TCP and TPT-ClO_4 in CH_3OH-C_2H_5OH (1:1) rigid solution at 77°K.

(A) total emission of TPT-TCP, (B) delayed emission of TPT-TCP, (c) total emission of TPT-ClO_4.

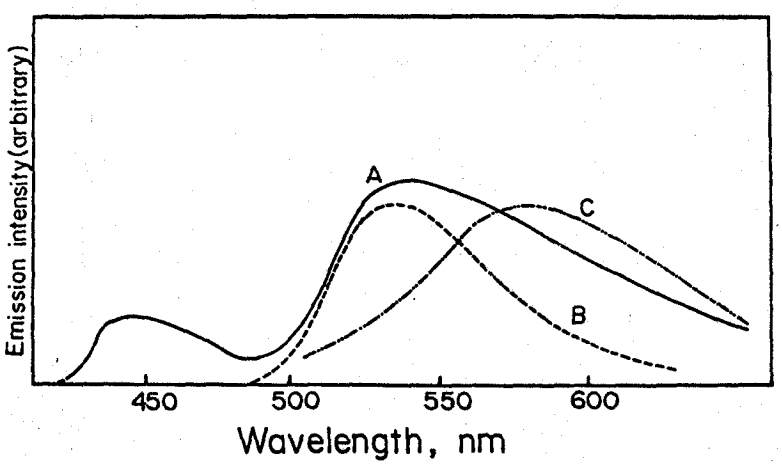

Fig. 2-4. Emission spectra of TPT-TCP in 2MTHF-toluene (9:1) rigid solution at 77°K.

(A) total emission by excitation at 420 nm,
(B) delayed emission by excitation at 420 nm,
(C) total emission by excitation at 470 nm.

2MTHF - toluene (9:1) solution. In the case of the excitation of the LE band of the cation, the emission at 540 nm becomes broad with a new emission around 600 nm. On the excitation of the CT band in rigid solution at 77°K (at 470 nm, as shown in Fig. 1-4), only this new emission band was observed clearly at 585 nm. This band can be assigned to the interionic CT fluorescence of TPT-TCP salt in rigid solution by the following reasons; (i) the lifetime is about 170 nsec, (ii) a mirror image relationship is found between this emission band and the CT absorption band shown in Fig. 1-4, (iii) the Stokes shift of this transition, about 4200 cm^{-1}, is comparable with those of ordinary molecular CT complexes in rigid solution.[8)]

The relative intensities of these three emission bands, i. e., the fluorescence and phosphorescence of the cation and the CT fluorescence, are

Fig. 2-5(a)

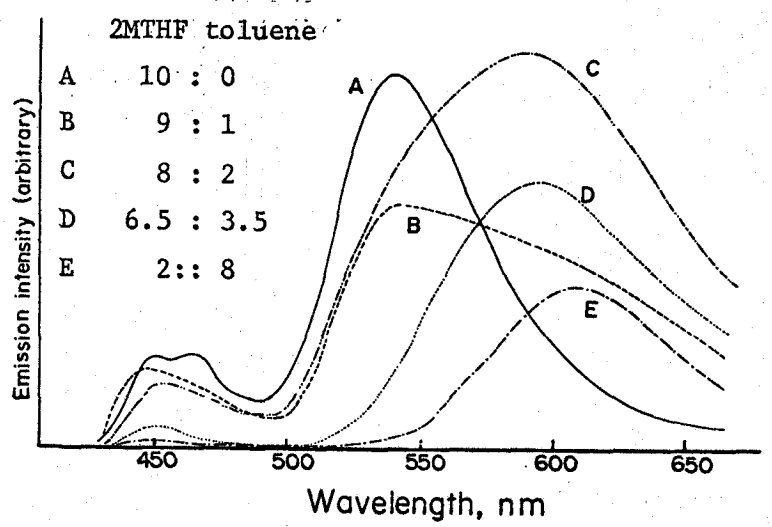

Fig. 2-5 (b)

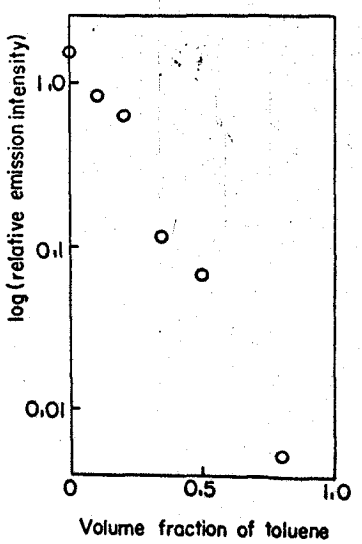

Fig. 2-5.

(a) Emission spectra of TPT-TCP in various compositions of 2MTHF-toluene solvent system at 77°K by 420 nm excitation.

(b) Relative phosphorescence intensity of TPT cation against the solvent composition of 2MTHF-toluene system.

very sensitive to the solvent polarity. The total emission spectra of TPT-TCP salt by 420 nm excitation are shown in Fig. 2-5(a) for various compositions of 2MTHF - toluene solvent system. In a more polar solvent the phosphorescence of the cation is predominant over the CT fluorescence, while in a less polar solvent the CT fluorescence predominates. The relative intensity of the phosphorescence of the cation is plotted against the solvent composition in Fig. 2-5(b). The intensity of the phosphorescence is reduced strikingly with the addition of toluene, but its lifetime remains almost unchanged. Furthermore, upon the direct excitation of the CT absorption band, the phosphorescence of the cation cannot be observed at all. These facts indicate that even in a non-polar solvent the phosphorescence of the cation is emitted only from the dissociated free cation. Therefore, the dependence of the emission spectrum on the solvent polarity shown in Fig. 2-5 can be accounted for by the variation of the relative amount of the free TPT cation. This result shows that the solvent polarity similar to that of 2MTHF - toluene (9:1) is required for the dissociation of the salt in rigid solution. This appears to correspond to the fact that in solution at room temperature the salt dissociates almost completely into two component ions in the solvent of dielectric constant > 10.

As stated above, the solvent polarity is a very important factor in determining the emission spectrum of the interionic CT salt, the degree of dissociation of the salt being primary determined by this factor. The solvent polarity has also effect on the maximum wavelength and the lifetime of the CT fluorescence. The maximum wavelengths and the lifetimes of the CT fluorescence, and the maximum wavelengths of the CT absorption band in various solvents are listed in Table 2-2. Exact maximum of the CT fluorescence is difficult to decide with the excitation in the LE bands, as both the CT fluorescence and the phosphorescence of the cation are observed

Table 2-2 The maximum wavelengths (λ^{F}_{max}) and lifetime (τ_F) of the CT fluorescence at 77°K and the maximum wavelength (λ^{A}_{max}) of the CT absorption band in various solvents

Solvent	λ^{F}_{max} [1] (nm)	τ_F [2] (nsec)	λ^{A}_{max} at 77°K (nm)	λ^{A}_{max} at 293°K (nm)
2MTHF	585	150	460 (S) [3]	585
2MTHF-toluene (9:1)	585	170	470	590
" (8:2)	590	240	-	595
" (6.5:3.5)	596	290	-	603
" (5:5)	600	-	-	625
" (2:8)	610	330	-	635
p-dioxane [4]	635	-	-	635

[1] : By CT absorption band excitation at 470 nm at 77°K.

[2] : By N_2 gas laser excitation at 337 nm at 77°K.

[3] : Shoulder. [4] : In a cloudy solid at 77°K.

simultaneously. Therefore, the maximum wavelengths given in Table 2-2 were determined by the excitation of the CT absorption band. The fluorescence lifetimes, however, were measured on the excitation at 337 nm of an N_2 gas laser.

The increase of the solvent polarity causes a blue shift of the CT fluorescence. The amount of this blue shift is comparable with the amount of the blue shift of the CT absorption maximum with the increase of the solvent polarity in solution at room temperature. A CT fluorescence of organic CT salts in rigid solution has been reported only by Brinen et al. on some alkylpyridinium-halide salts.[2)] They observed the CT fluorescences of these salts in three solvents, that is, water, methanol - ethanol (1:4), and dichloromethane, and indicated that no solvent effect was observed on the

the energy of the CT fluorescence. Therefore, the result observed in the present system is quite different from that in alkylpyridinium salts.

As a CT salt has an ionic ground state, an ion-pair is strongly solvated in the ground state. Even in Franck-Condon state, therefore, the salt is strongly solvated, in spite of the components of the salt being neutral in the excited state. Brinen et al. suggested that the solvent-solute reorientation occurs during the relaxation of the excited state from the Franck-Condon state to a fluorescent CT state even in rigid solution. Recently, Kobayashi et al., however, have shown that in s-tetracyanobenzene complexes this kind of reorientation does not occur sufficiently during the relaxation in rigid solution at 77°K.[7] The present observation of the blue shift of the CT fluorescence, suggests also that the reorientation of the solvent molecules is insufficient at 77°K, and that the salt in the CT fluorescent state is still solvated in the similar fashion as in the ground state. If the CT fluorescence of this salt could be observed in fluid solution, the energy would remain constant independently on the solvent polarity, because the reorientation of the solvent molecules would occur sufficiently in fluid solution.

The lifetime of the CT fluorescence becomes long with the decrease of the solvent polarity. The increase of the lifetime may be caused by the decrease of the radiative transition probability or the decrease of the radiationless transition probability of the excited ion-pair. If the emission probability decreased, the quantum efficiency of the CT fluorescence would show a considerable decrease corresponding to the increase of the fluorescence lifetime. Although the quantum efficiency of the CT fluorescence cannot be decided, because the concentration of the undissociating ion-pair in rigid solution is unknown, such a decrease of the intensity of the CT fluorescence was not observed. This suggests that the dependence of

the fluorescence lifetime is attributable to the decrease of the radiationless transition probability of the excited ion-pair in a less polar solvent.

Summary

The emission spectra of an organic CT salt: 2,4,6-triphenylthiopyrylium-1,1,3,3-tetracyanopropenide (TPT-TCP) were investigated in the solid state and in solution of various solvents. TPT-TCP salt showed exclusively a CT fluorescence, emission from the component ion being quenched. Other CT salts prepared in the chapter 1 also showed this type of emission. This is the first example of the CT fluorescence of organic CT salts in the crystalline state. A CT fluorescence was not observed in fluid solution of TPT-TCP salt, but was again observed in non-polar rigid solution at 77°K. This observation of CT fluorescence clearly demonstrated the presence of the excited CT state of TPT-TCP salt, both in the solid state and in solution.

Although the excited CT state is considered to consist of two neutral radical species, $D^{\cdot}A^{\cdot}$, the CT fluorescence in rigid solution showed remarked solvent effects in its energy and lifetime. This may be due to that the strong solvation in the ionic ground state considerably influences on the orientation of solvent molecules around the salt even in the excited CT state in rigid solution at 77°K.

References

1) R. Foster,"Organic Charge-Transfer Complexes", Chapter 10, 292, Academic Press, Inc., (London) Ltd. (1969).

2) J. S. Brinen, J. G. Koren, H. O. Olmsteaed, and R. C. Hirt, J. Phys. Chem., 69, 3791 (1965).

3) J. A. Riddick, and E. E. Troops,Jr.,"Technique of Organic Chemistry",

Vol. 7, Organis Solvents, Interscience Publishers, Inc., New York (1955).

4) T. G. Beaumont and K. M. C. Davis, J. Chem. Soc. (B), 1970, 456.

5) J. Prochorow and R. Sieogoczynski, Chem. Phys. Lett., 3, 635 (1969).

6) N. Mataga and Y. Murata, J. Amer. Chem. Soc., 91, 3144 (1969).

7) T. Kobayashi, K. Yoshihara, and S. Nagakura, Bull. Chem. Soc. Japan, 44, 2603 (1971).

8) J. Czekalla, G. Briegleb, und W. Herr, Z. Electrochem., 63, 712 (1959).

Chapter 3

ELECTRICAL AND MAGNETIC PROPERTIES

Introduction

In order to elucidate the role of the interionic CT interaction in the electrical properties of organic CT salts, the photoconductive and semiconductive properties as well as the magnetic properties have been investigated in this chapter.

Although the photoconduction has been found in several weak molecular CT complexes having low dark conductivity,[1-4] the photocarrier generation, in most cases, has been considered to be extrinsic in nature, and the intrinsic carrier generation is not proved in any cases. With weak molecular CT complexes, Akamatu and Kuroda discussed the relationship between the conduction state and the excited CT state.[1] They suggested that between these two states, may be present the difference of energy equivalent to that necessary for the separation of the excited CT state into free ions, that is, the separation of a $D^{+\bullet}A^{-\bullet}$ ion-radical pair into two charge carriers, and this large energy may prevent the intrinsic carrier generation. However, in the case of an interionic CT salt, the excited CT state may consist of two neutral radical species, $D^{\bullet}A^{\bullet}$, and consequently, the carrier separation from the CT state will be fairly easier than in the case of a weak molecular CT complex. Thus, in an organic CT salts, is expected the possibility of the intrinsic

carrier generation by the CT excitation.

Actually, all the CT salts investigated here show about ten times larger photocurrent on irradiation at the CT absorption band, when compared with the dark current. Furthermore, a weak esr signal, which seems to originate from the charge carrier in dark conduction, was enhanced on the CT and near IR excitation. On the basis of the results on the electrical and magnetic properties, the auther will discuss in this chapter the mechanism of electrical conduction and the possibility of the intrinsic carrier generation in organic CT salts.

Experimental

Materials. The organic CT salts were purified by repeated recrystallizations at least three times. Vacuum sublimation or zone refining could not be used for the purification due to the decomposition of the salt. Single crystals of the CT salts, dimensions about 2 x 1 x 0.5 mm, were grown from methanol - water (4:1) or methanol solution. However, except for TPT-perchlorate, single crystals of the perchlorate salts of other cations could not be obtained.

Conductivity measurement. The apparatus for the measurements of the dark and photoconduction is depicted in Fig. 3-1. The D.C. conductivity was measured by a Takedariken vibrating reed electrometer, type TR-81. Temperature was controlled by passing cold nitrogen gas or heated air around a single crystal sample, and was monitored by a thermocouple. Light from a 500 W Xe lamp, arc current 20 A, was monochromatized by a monochromator. The energy distribution and the absolute light intensity of the Xe lamp were shown in the previous paper.[5] To investigate the light intensity dependence of the photocurrent, neutral filters of known transmittance were

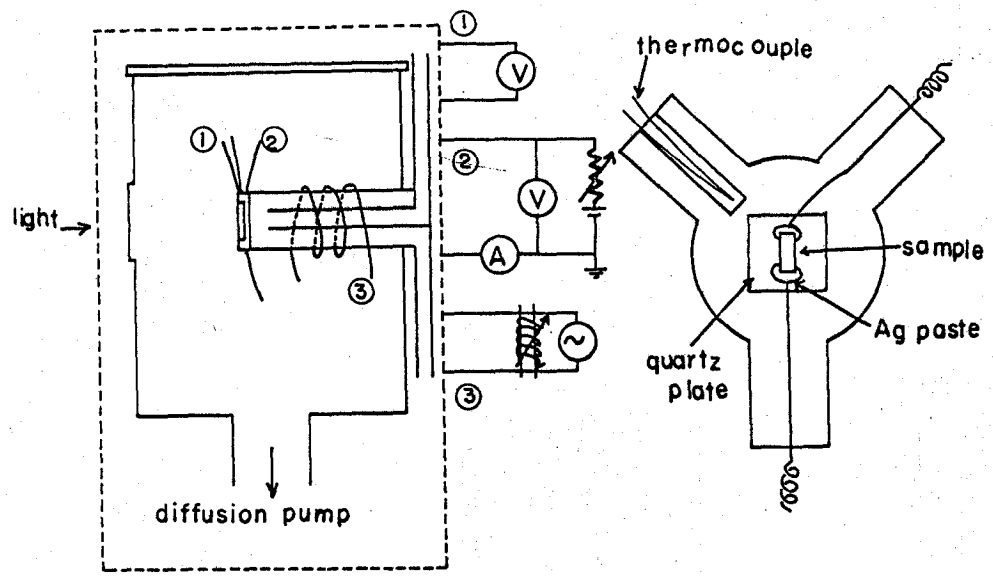

Fig. 3-1. Apparatus for the conductivity measurements.

inserted between a sample and a monochromator. A single crystal was settled on a quartz plate by Ag paste, which was used as electrodes (Fig. 3-1). In the case of TPP-perchlorate, a compressed pellet of powder crystals was used. The voltage-current characteristics were ohmic in all samples up to 200 V applied voltage and no photovoltaic current was observed when no voltage was applied. These facts indicate that the choice of this electrode is adequate, and that carrier injection from or to an Ag paste electrode is negligible. All conductivity measurements were perfomed both in dry air at one atmosphere and in vacuum at 10^{-4} - 10^{-5} mmHg.

Esr measurement. An electron spin resonance measurement was carried out with an X band, JES-ME2X type spectrometer (Japan Electron Optics Laboratory Co., Ltd.) with a double mode cavity. A microcrystalline sample was packed in a quartz tube and measured both in air and in vacuum at 10^{-2} mmHg. The concentration of unpaired spins of a salt was estimated by comparing its intensity with that of a DPPH sample. DPPH (Wako, pure grade) was purified

by repeated recrystallizations from CS_2 or petroleum ether (a fraction of b.p. < 40°C) solution. The benzene solution or the powder sample dispersed in KCl (Merck, ultra pure grade, dried over 2 days at 200°C in vacuum) was used as a sample of known concentration of unpaired spins. Temperature was varied by passing cold nitrogen gas or heated air into the cavity, and was monitored by a thermocouple attached around a sample tube in the cavity. The g-value of the unpaired spins in a salt was determined from the g-value of Mn^+ in a MgO sample.[6] For the measurement of photo-esr absorption, a 500 W Xe lamp of 20A was used. The spectral dependence of the photo-esr absorption was roughly estimated by combining several color glass filters of known transmittance at various wavelengths, as the light from a monochromator was too weak for the observation of esr absorption change.

Results

Dark and photoconductivity. The organic CT salts investigated here are semiconducting with the resistivities in the range of 10^{10} - 10^{12} ohm·cm at room temperature. However, on irradiation with a visible light, a photocurrent of ca. 10 times larger magnitude as compared with the dark current was observed.

The light intensity dependence of the photocurrent obeyed $i_{ph} = \alpha \cdot L^n$, where L is the incident light intensity, α and n are the constants. Figure 3-2 shows this relation and the results are listed in Table 3-1. The value of n appears to be independent of the presence of air, being about 0.5 for all salts.

The spectral dependence of the photoconduction is shown in Fig. 3-3 for several salts, together with the corresponding absorption spectra. Each photoconduction spectrum is normalized to the light intensity at 360 nm.

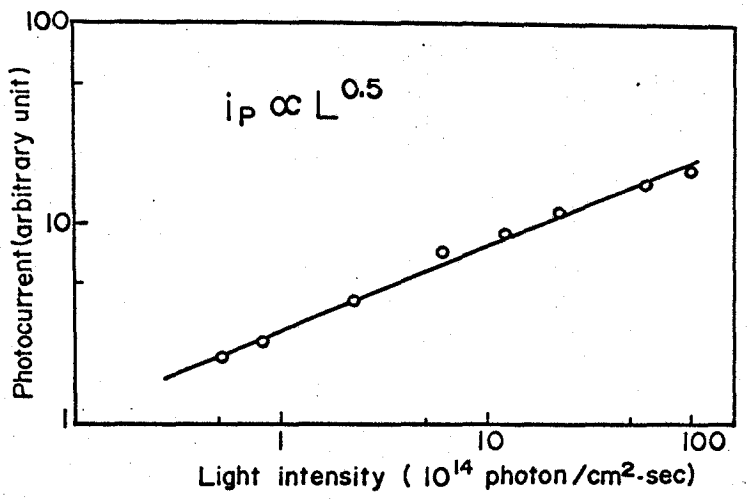

Fig. 3-2. Light intensity dependence of photocurrent at 650 nm of TPT-TCP salt.

Table 3-1 Light intensity dependence of photocurrent of the salts.

Salts	n in $i_p = a \cdot L^n$		λex^1 (nm)
	in vacuum	in air	
TPP-TCP	0.5	0.5	600
TPT-TCP	0.6	0.5	650
TPP-TCM	0.6	0.8	600
TPT-TCM	0.7	0.7	650
ADPP-TCP	-	0.6	600
ADPT-TCP	-	0.5	600
ADPP-TCM	-	0.5	600
TPT-ClO_4	0.4	0.4	500

[1] : wavelength of illuminating light.

Table 3-2 Specific resistivities(ρ_d) in the dark at room temperature, photoconduction maximum wavelengths (λ_{max}^{ph}) and absorption maximum wavelengths (λ_{max}^{ab}) of organic CT salts

Salts	ρ_d (ohm·cm)	λ_{max}^{ph}	λ_{max}^{ab} (nm)	
			CT band[1]	LE band[2]
TPP-TCP	10^{11}	640, 500	565	410
TPT-TCP	10^{11}	640, 500	540	390
TPP-TCM	10^{10}	580	530	410
TPT-TCM	10^{11}	600	520(S)[3]	390
ADPP-TCP	10^{12}	580, 520	530(S)	435
ADPT-TCP	10^{10}	620, 520	560(S)	430
ADPP-TCM	10^{11}	630, 520	520(S)	435
TPP-ClO_4[4]	10^{12}	500	-	410
TPT-ClO_4	10^{12}	500	-	390

[1] : measured by diffuse reflectance spectrum in solid state.
[2] : the lowest LE band of the cation in absorption spectrum in CH_3OH solution. [3] : measured in a compressed pellet of powder crystals. [4] : shoulder.

The resistivity in the dark, and the maximum wavelengths of the photoconduction and the absorption are summarized in Table 3-2. As can be seen in Fig. 3-3 and Table 3-2, a large photoconduction peak is observed in all CT salts in the long wavelength side of the CT absorption band. In TPP-TCP (Fig. 3-3 a) and TPT-TCP (Fig. 3-3 c), another photoconduction peak, which is smaller than the former peak, is observed at the absorption edge of the LE band of the cation. However, TPP-TCM (Fig. 3-3 b) and TPT-TCM (Fig. 3-3 d) did not show this peak clearly, perhaps because this peak is hidden by a large former peak. In TPP-ClO_4 and TPT-ClO_4, in which CT interaction is absent between the cation and the anion, only latter peak was found. This fact indicates that the former photoconduction peak may be the result of the

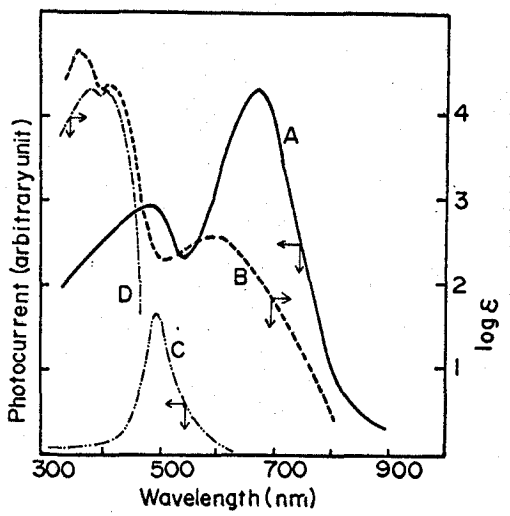

Fig. 3-3(a).

(A): Photoconduction spectrum of TPP-TCP, (B): Absorption spectrum of TPP-TCP in $CHCl_3$, (C): Photoconduction spectrum of TPP-ClO_4, (D): Absorption spectrum of TPP-ClO_4 in CH_3OH.

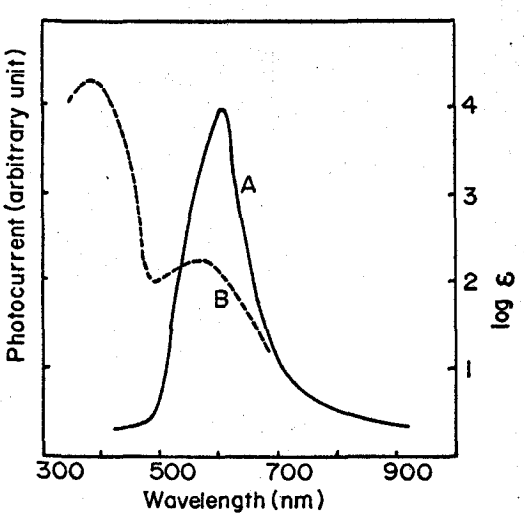

Fig. 3-3(b).

(A): Photoconduction spectrum of TPP-TCM, (B) Absorption spectrum of TPP-TCM in $CHCl_3$

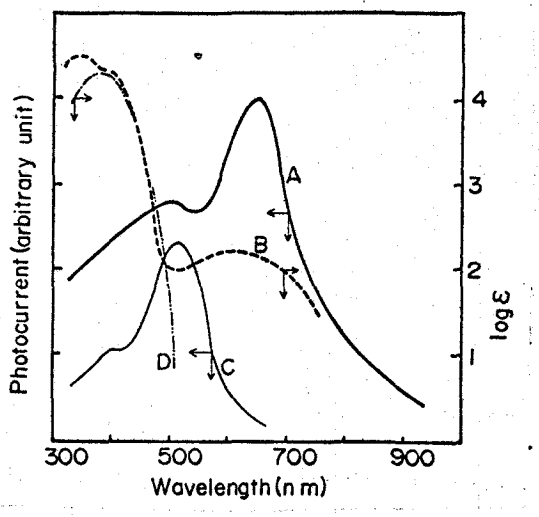

Fig. 3-3(c).

(A): Photoconduction spectrum of TPT-TCP, (B): Absorption spectrum of TPT-TCP in $CHCl_3$, (C) Photoconduction spectrum of TPT-ClO_4, (D): Absorption spectrum of TPT-ClO_4 in CH_3OH.

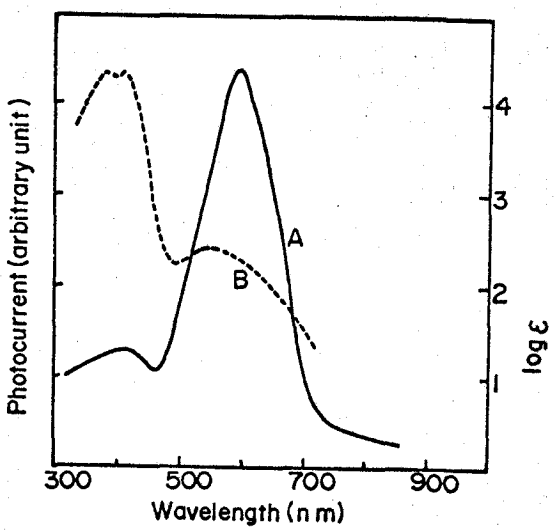

Fig.3-3(d).

(A): Photoconduction spectrum of TPT-TCM, (B): Absorption spectrum of TPT-TCM in $CHCl_3$.

excitation at the CT band, and the latter may be due to the local excitation of the cation. Furthermore, a relatively small photocurrent was observed when a CT salt was illumunated with a light in the near IR region (800 - 1100 nm). This may be due to the presence of deep traps of charge carriers. Spectral dependence curve was reproducible during repeated measurements, and did not depend on the samples of single crystals. The effect of air on the photoconduction spectra was very little.

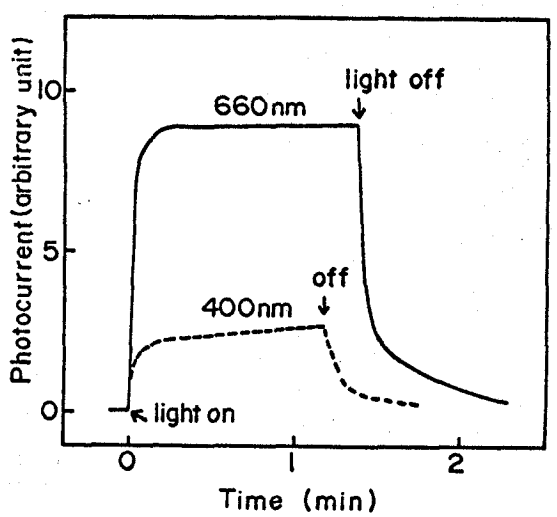

Fig. 3-4. Time response curves of photocurrent of TPT-TCP salt in vacuum at room temperature.

A typical time response curve of the photocurrent is depicted in Fig. 3-4 for TPT-TCP salt. Upon excitation in the CT band (650 nm), the photocurrent increased immediately and reached rapidly a steady state value, and when the excitation was removed, following a rapid decay of the photocurrent, a considerably long tail was observed as the initial value of the dark current was approached. This suggests that the photoconduction by the CT excitation is not strongly limited by charge carrier traps, although shallow traps are present in the crystal. The excitation at 450 nm caused a slightly slower response of the photocurrent.

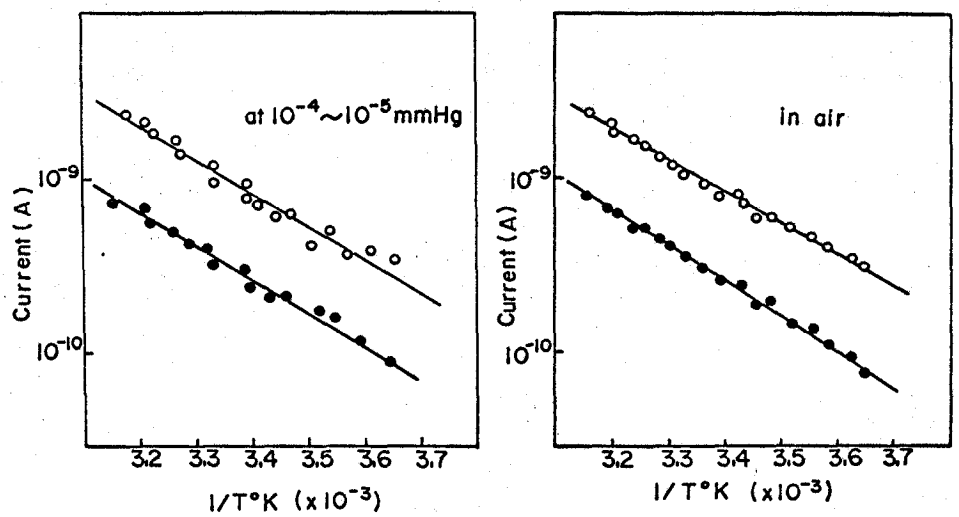

Fig. 3-5. Temperature dependence of dark current and photocurrent at 650 nm of TPT-TCP salt in vacuum and in air.
●—●—● dark current, ○—○—○ photocurrent.

Table 3-3 Activation energies of dark and photoconductivities of the salts.

Salts	Ea_d (eV)		Ea_{ph} (eV)		λex^1
	in vacuum	in air	in vacuum	in air	(nm)
TPP-TCP	0.6	0.5	0.6	0.6	600
			0.6	0.5	1000
TPT-TCP	0.4	0.4	0.45	0.4	650
			0.5	0.5	1000
TPT-TCM	0.9	0.8	0.8	0.7	600
ADPP-TCP	-	0.45	-	0.45	600
ADPT-TCP	-	0.6	-	0.6	600
ADPP-TCM	-	0.45	-	0.35	600
TPT-ClO_4	1.2	0.9	1.2	0.9	500
			1.2	0.9	1000

[1] : wavelength of illuminating light.

The temperature dependence of the dark conduction and photoconduction was investigated between 273° - 323°K. Both for dark and photocurrents, $i = i_o \exp(-Ea/kT)$ holds. A typical result is given in Fig. 3-5 for TPT-TCP salt in vacuum and in air. The activation energy, Ea, of the photocurrent, 0.45 eV in vacuum and 0.4 eV in air, is approximately the same with that of the dark current, 0.4 eV, both in vacuum and in air. Furthermore, the photocurrent at 1000 nm had also essentially the same activation energy, 0.5 eV, as the photocurrent at 650 nm. The other salts also gave essentially the same results (Table 3-3).

Esr absorption. A weak esr signal observed initially in perchlorate salts of TPP and TPT cations disappeared by additional recrystallizations of the salts. Therefore, all CT salts were prepared carefully from the corresponding perchlorate salt which gave no esr signal. Even when prepared in this way, CT salts showed a single broad esr absorption band which did not show a marked change by further recrystallizations. This fact indicates that this absorption is not of impurities. The esr signal of TPT-TCP salt, for example, is depicted in Fig. 3-6. The g-values and the total spin con-

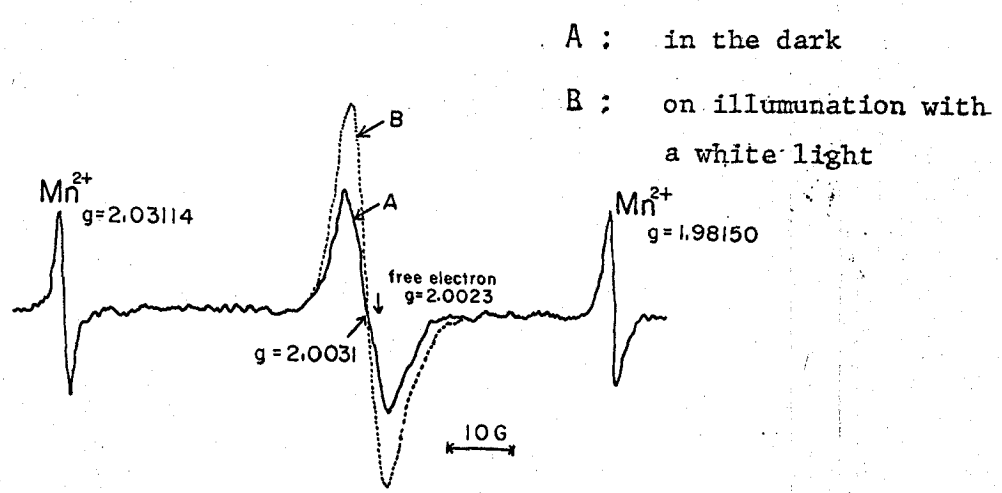

Fig. 3-6. Esr absorption spectra of TPT-TCP salt in vacuum at room temperature.

Table 3-4 g-values, total spin concentration ([S]) and the ratio (R) of esr intensity on illumination with a white light versus that in the dark of organic CT salts.

Salts	g-value	[S] (spins/gram)	R
TPP-TCP	2.00270	1×10^{15}	1.3
TPT-TCP	2.00310	2×10^{15}	1.8
TPP-TCM	2.00295	1×10^{16}	1.3
TPT-TCM	2.00380	5×10^{15}	1.4
ADPT-TCP	2.00530	2×10^{15}	1.5
ADPP-TCM	2.00480	1×10^{15}	1.35

centrations of the CT salts are listed in Table 4. As the value of spin concentration changed somewhat from crystals to crystals, average values are listed. The total spin concentrations, 10^{15} - 10^{16} spins/gram, are much smaller than those observed in many strong molecular CT complexes,[7,8] and almost the same with those measured in weak molecular complexes.[9] These esr signals seem to arise from the defects in the crystal. Upon illumination with a visible light, the intensity of an esr signal increased slightly but the g-value showed no shift (Fig. 3-6). The ratio of esr intensity on excitation by a white light to that in the dark is listed in Table 3-4. When the perchlorate salts of the cation and the alkali metal salts of the anion were irradiated, no esr absorption was observed. The lights in the CT band region and in the near IR region (500 - 1200 nm) were effective on increasing the esr intensity, while those of shorter than 450 nm were ineffective.

The photoresponse curve of an esr signal, for example, of TPT-TCP salt is shown in Fig. 3-7. The curve at room temperature showed a fairly rapid rise and decay, and was quite similar to that of photocurrent shown

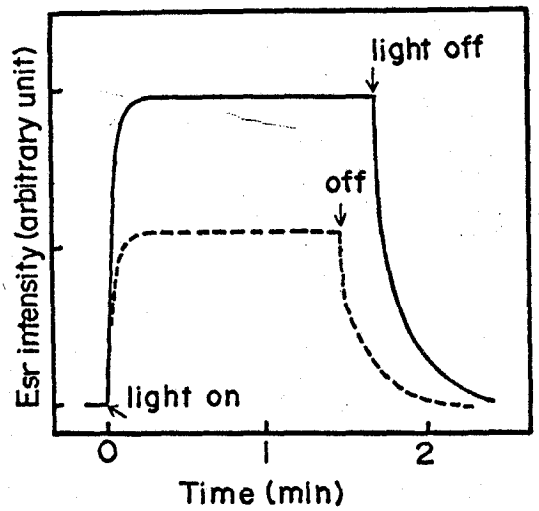

Fig. 3-7. Time response curves of photo-esr absorption of TPT-TCP salt in vacuum at room temperature.

in Fig. 3-4. No significant difference in an esr absorption was found between in vacuum and in air. The spectral response, the time response and the effect of air of the photo-esr absorption suggest the close relationship between the photo-induced paramagnetism and the photoconduction of the CT salts.

The temperature dependence of an esr absorption in the dark and on irradiation was investigated in the range of 213° - 323°K. The total spin concentration and the g-value of an esr signal showed no significant change, when temperature was lowered, indicating that the amount and nature of the paramagnetic species which existed originally in the material are independent of temperature. On the other hand, the photo-esr absorption showed a gradual decrease in its spin concentration with the decrease of temperature, activation energy being slightly negative (< 0.2 eV). Therefore, both paramagnetic species induced by light and those originally present in the crystal in the dark are not produced by the thermal activation process.

Discussion

The general features of the electrical conduction.

(i) All CT salts show a larger photocurrent peak at the long wavelength side of the interionic CT absorption band, and this photoconduction was almost unaffected by the presence of air.

This photoconduction is much larger than that observed in the perchlorate salt of the corresponding cation. A good reproducibility of the photoconduction was observed during several repeated measurements, and even when measured on different single crystals, the behavior of the photoconduction remained almost unchanged. These facts suggest that observed photoconduction in this region is intrinsic and the photo-excitation of the interionic CT band contributes to the photoconduction.

Charge carriers seem to be generated in the bulk rather than on the surface of a crystal. Carrier generation in the bulk can explain the reason why the CT absorption peak does not coincide with the photocurrent peak. That is, the number of photons reaching the bulk of a crystal are larger at the edge of the absorption band than at the absorption peak. Photocurrent, which is insensitive to the presence of air, supports also the bulk carrier generation.

(ii) All CT salts show a smaller photoconduction in the near IR region of 800 - 1100 nm, which is also insensitive to the presence of air.

This result suggests the presence of deep traps at 1.0 - 1.4 eV below the conduction level. As this value is considerably larger than the observed activation energy, the dark current cannot be caused by the thermally activated carrier generation from these deep traps.

(iii) When excited in a LE band of the cation, the photoconduction does not appear significantly.

This may be due to that the photon is absorbed mostly on the surface of a crystal. However, the photon in the absorption edge of the LE band can reach somewhat the bulk of a crystal, and can produce the photocarrier as in the case of CT band excitation as follows,

$$(D^{-}A^{+}) \xrightarrow{h\nu} (D^{-}A^{+*}) \longrightarrow (D^{\cdot}A^{\cdot}) \longrightarrow D^{\cdot} + A^{\cdot}$$

ground state LE state excited CT state photocarrier

(iv) The photocurrent in the CT absorption region is proportional to about the 0.5 power of the incident light intensity.

As the photoconduction in this region seems to be intrinsic, one photon absorption produces two charge carriers. However, if the carriers disappear by the recombination between electrons and holes during its migration, the concentration of the carrier will be proportional to the 0.5 power of the light intensity. Thus, the photoconduction in this system may be recombination limited.

(v) Both dark conductivity and photoconductivity in the CT absorption and in near IR regions have the same activation energy.

As can be seen in Table 3-3, the most striking result of the electrical properties of the organic CT salts is that the values of the activation energy of the dark conduction and photoconduction are the same without any exception with respect to six CT salts investigated. This property seems to be general with this kind of organic salts, and is basically important to frame up the conduction mechanism in the salts in the following.

Mechanism of the electrical conduction in organic CT salts.

As stated above, all CT salts have the same activation energy in dark conduction as well as in photoconduction. This property reminds us immediately a "trapping conduction mechanism" as a most simple model which can explain the agreement of the values of the activation energy of dark conduction and photoconduction. Figure 3-8 shows schematically the trapping con-

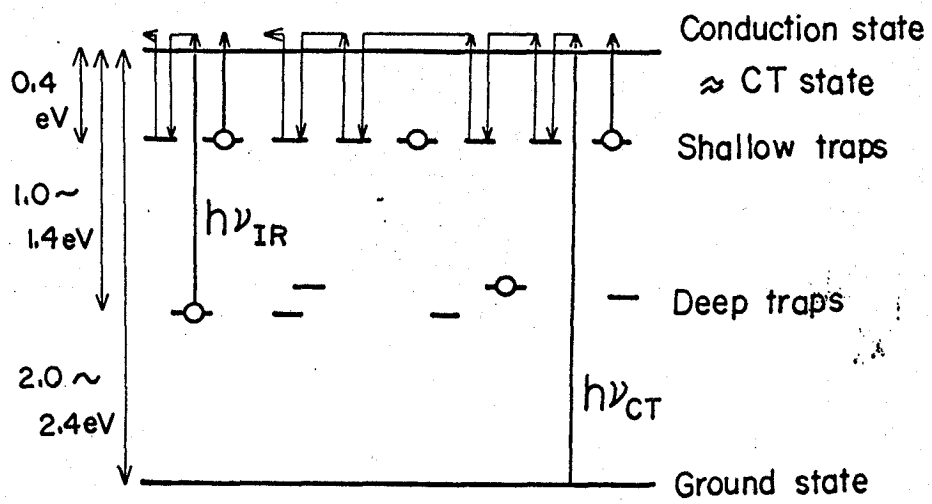

Fig. 3-8. Trapping conduction model in TPT-TCP salt.

duction model with TPT-TCP salt, as an example. With this model, a TPT-TCP crystal has the trapped carriers 0.4 eV below the conduction level and in the dark the trapped carriers are thermally excited up to the conduction level and the carriers generated in this way migrate through the crystal repeating the trapping and detrapping processes. Thus, the activation energy in the dark conduction must be 0.4 eV, the depth of the trap levels below the conduction level, being the energy required for the trapping conduction.

In the case of photoconduction, the photocarriers are spontaneously generated in the conduction level by the absorption of the light in the CT band, because, as discussed later, the energy level of the conduction state may be approximately equal to that of the excited CT state. The photocarriers thus generated migrate by the trapping conduction mechanism. In this mechanism, no activation energy is required for the carrier ganeration, and the activation energy of 0.4 eV as observed must be consumed in the carrier migration process. Thus, both for dark conduction and photoconduction the same amount of activation energy is required, being 0.4 eV for both. Photo-

carriers generated from the deep trap levels by near IR illumination require also the same activation energy for their migration

In the present model, only electron carriers are considered. As the molecular size of the acceptor cation is considerably larger than that of the donor anion, the acceptor radical $A^{\cdot}$, i. e., electron, might contribute predominantly to the photocurrent.

Photoconduction and paramagnetic species.

As stated previously, the investigation of esr of the CT salts revealed that (a) CT salts showed some amount of temperature independent esr absorption even in the dark, (b) the perchlorate salts in which CT interaction is absent gave no esr signal, (c) the total spin concentration was of the order of 10^{15} - 10^{16} spins/gram and this amount changed considerably when measured on the different samples, (d) photo-illumination increased the esr signal and this photo-esr absorption showed similar time response and spectral response with photocurrent, (e) the temperature dependence of the photo-esr absorption showed a slightly negative activation energy, the signal increasing with the lowering of temperature and the time response curve of the photo-esr absorption showed considerably longer rise and decay at lower temperatures.

The temperature independent esr signal in the dark may be due to the charge carriers trapped in shallow traps as shown in Fig. 3-8. This trapped carriers may be generated from crystal defects by CT interaction, because of (b) and (c). Photocarriers and the paramagnetic species of the photo-esr may be the same (d), as can be expected from the model in Fig. 3-8. The slightly negative activation energy of the photo-esr may be understood by the decreasing of the recombination of the paramagnetic species with the lowering of temperature. Actually, the time response curve of the photo-esr absorption shows considerably longer rise and decay at lower temperatures.

As paramagnetic species and the charge carriers are the same, this behavior of the photo-esr signal is in line with the recombination limited photoconconductivity, a photocurrent being proportional to the 0.5 power of the light intensity.

In the case of strong molecular CT complexes, such as perylene - iodine complex, a good coincidence between the values of the activation energy of dark current and of unpaired spin concentration was observed, and this fact was used for the proof of the paramagnetic species observed in the esr spectroscopy being identical with the charge carriers.[7] This kind of coincidence is not necessary in this system, because the thermal activation process in the dark conduction is the carrier migration process. If the carrier concentration in the dark is equal to the spin concentration, about 10^{15} electrons/gram, the mobility of the carrier will be estimated to be 10^{-5} - 10^{-6} $cm^2/Volt \cdot sec$ from the relation of $i = Ne\mu$, where N is carrier concentration, e is electric charge and μ is mobility. This value seems to be very small as compared with the observed mobilities of organic compounds.[10] However, taking account of the facts that a fairly large energy is required for the carrier migration, and that the photoconduction is recombination limited, this small value of mobility may be conceivable.

Another possible mechanism of the electrical conduction.

Although the above mentioned mechanism can well account for the results of the electrical and magnetic properties of organic CT salts, it may be remarked that other mechanisms might also be possible for both the carrier generation and migration. At first, charge carriers can be generated by the interaction between crystal imperfections and CT excitons migrating in a crystal. In this case, the carrier generation is extrinsic. This mechanism is the same as that suggested by Akamatu and Kuroda for the photoconduction of pyrene complexes.[1] Since both mechanism can explain the

spectral, temperature and light intensity dependences of the photocurrent, it is fairly difficult to decide which mechanism is more plausible. However, from the fact that the behavior of the photoconduction shows a good reproducibility when measured on several samples of single crystals, the author thought that the former mechanism is more probable, that is, the intrinsic carrier generation.

With weak molecular CT complexes, Akamatsu and Kuroda suggested that the energy equivalent to the difference of energy between the conduction level and the CT exciton level is required for the separation of a D^+A^- ion-radical pair. Therefore, in this case, CT excitons are impossible to separate spontaneously into charge carriers. However, in interionic salts, the interaction between two neutral radical species, $D^\cdot A^\cdot$, in the CT excited state may be small, and consequently an energy required for the charge separation may be smaller than that in the case of molecular CT complexes, and the photocarriers can be generated from the excited CT state with very small thermal energy compared with the activation energy for the migration. Therefore, the energy level of the conduction state may be approximately equal to that of the excited CT state, and the intrinsic charge carrier generation seems to be possible in organic CT salts.

On the other hand, instead of the trapping conduction, a hopping mechanism may be possible for the carrier migration process. In this case, the charge carrier migrates from an ion to another with an activation energy of 0.4 - 0.8 eV. This value seems to be fairly large as the activation energy for hopping conduction. However, these two mechanisms, i. e., trapping conduction and hopping conduction, can quite well explain the experimental results, and the latter possibility cannot be excluded.

Summary

The single crystals of organic CT salts investigated here are poor semiconductors with the resistivity of 10^{10}- 10^{12} ohm·cm at room temperature, but show about 10 times larger photocurrent upon the excitation in the interionic CT absorption region. From the fact that the photoconduction showed good reproducibility, when measured on several samples of single crystal. The values of the activation energy of the dark conduction and photoconduction were the same without any exception. On the basis of this result, the trapping conduction mechanism was proposed with organic CT salts. The charge carriers in the trapping conduction could be detected by esr measurements. A weak esr signal observed originally in these salts increased on the CT and near IR excitations. This photoinduced paramagnetic species were assigned to the charge carrier in the photoconduction from its time response, spectral dependence and the effect of air.

References

1) H. Akamatu and H. Kuroda, J. Chem. Phys., 39, 3364 (1963).

2) M. C. Tobin and D. P. Spitzer, ibid., 42, 3654 (1965).

3) H. Kokado, H. Hasegawa, and W. G. Sneider, Can. J. Chem., 42, 1084 (1964).

4) C. K. Prout, R. J. P. Williams, and J. D. Wright, J. Chem. Soc. (A), 747, (1966).

5) T. Sano, K. Okamoto, S. Kusabayashi, and H. Mikawa, Bull. Chem. Soc. Japan, 42 , 2505 (1969).

6) D. R. Kearns and M. Calvin, J. Amer. Chem. Soc., 83, 2110 (1961).

7) J. Kommandeur and F. R. Hall, J. Chem. Phys., 34, 129 (1961).

8) D. B. Chesnut and W. D. Phillips, ibid., 35, 1002 (1961).

9) J. W. Eastman, G. M. Andros, and M. Calvin, ibid., 36, 1197 (1962).

10) F. Gutman and L. E. Lyons, "Organic Semiconductors", John Wiely & Sons, Inc., New York (1967).

Chapter 4

CRYSTAL STRUCTURES

Introduction

For the understanding of the physical properties in solid state, it is basically important to have knowledge of the crystal structure. In the previous chapters, the role of interionic CT interaction in the physical properties of organic CT salts have been discussed. In this chapter, the crystal structures of organic CT salts will be discussed.

Many crystallographical studies concerning ordinary molecular CT complexes have clearly demonstrated the effect of CT interaction on the crystal structure.[1,2,3] Especially, most 1:1 solid complexes between π donors and π acceptors have common features in crystal structure, that is, the infinite stacking of parallel donor and acceptor molecules, and a good overlapping between two components.

As compared with these molecular CT complexes in which two components are bounded by CT and van der Waals forces, the influence of interionic CT interaction on the crystal structure is almost unknown, because the lattice energy of organic CT salts is attributed to a very strong electrostatic force between the cation and the anion.

Several organic CT salts have been investigated by the x-ray structure analysis. The crystal structures of the iodide salts with aromatic

planar cations are of particular interest.[4,5,6] The tropylium and N-methylacridinium salts have the structure consisting of infinite columns stacked by ion-pairs in which the iodide ion is located approximately above the center of the aromatic cation plane. By contrast, in 1-ethyl-2-methylquinolinium salt[6] the iodide ion and the planar cation lie roughly on a plane. On the other hand, the quinolinium salt of 2-dicyanomethylene-1,1,3,3-tetracyanopropeniide,[7] one of the salt of polycyanoacid anion, has again the crystal structure of ion-pair type.

In this chapter, therefore, the crystallographic studies on organic CT salts prepared here have been carried out, in order to elucidate the role of interionic CT interaction in the crystal structure. Two organic salts, 2,4,6-triphenylpyrylium-1,1,3,3-tetracyanopropenide (TPP-TCP) and 2,4,6-triphenylthiopyrylium-1,1,3,3-tetracyanopropenide (TPT-TCP), were chosen because the polarized absorption spectra of single crystals of these two salts showed quite different results each other, in spite of the very similarity of their chemical structures.

4-1 CRYSTAL STRUCTURE OF TPP-TCP SALT

Experimental

Crystal data. $[(C_{23}H_{17}O)^{+}\cdot(C_7HN_4)^{-}]$, F.W. = 450.5, monoclinic, a = 13.024, b = 21.357, c = 8.324 Å, β = 94.56°, Z = 4, Dm = 1.38 $g\cdot cm^{-3}$ (CCl_4-C_6H_6), Dx = 1.32 $g\cdot cm^{-3}$, space group : $P2_1/a$, absent spectra : h0l: $h \neq 2n$, 0k0: $k \neq 2n$.

Dark-red, needle crystals of TPP-TCP salt were recrystallized from a methanol solution. Oscillation and Weissenberg photographs showed that the crystals belong to the monoclinic system and the space group is $P2_1/a$. Both the determination of cell constants and the collection of intensity

data were carried out on a Rigaku four-cycle diffractometer.

The crystal used for the intensity measurement had dimensions of 0.32 x 0.45 x 0.15 mm. The crystal was mounted on a goniometer-head along the c axis. Nickel-filtered Cu-Kα_1 radiation was used. The ω-2θ scan technique was applied. The scan range, $\Delta(2\theta)$ of each reflection, was computed by the equation: $\Delta(2\theta) = (2.0° \pm 0.7° \tan\theta_c)$. The starting angle of the scan is $(2\theta_c - 1.0)°$, where θ_c is the calculated value of Bragg angle using λ(Cu-Kα_1) (= 1.5405 Å), and the scanning speed was $4° min^{-1}$. The background was measured at both ends of the each scan range. A total of 3394 independent reflections was obtained. No absorption correction was made (μ = 8.2 cm^{-1} for Cu-Kα_1).

Structure Determination and Refinement

The phases of the reflections were determined by means of the symbolic addition procedure.[8] SIGMA program was used to compute the normalized structure factor magnutude, $|E|$, and to list the Σ_2 relationships for each reflection. Three reflections, 0 3 2, 1 10 6, 11 5 5, were chosen in order to specify the origin, and two other reflections were assigned to have letter phases A and B in order to facilitate the symbolic addition procedure (Table 4-1). The signs of 108 reflections out of 143 reflections ($|E| \geq 2.0$) were determined by hand calculations. TANGENT FORMULA program was then used to calculate the phases of 628 reflections with $|E| \geq 1.3$. From the interaction list the signs of two letter phases A and B were both assigned to be minus.

From the E map, as shown in Fig. 4-1, the positions of all non-hydrogen atoms were found. The oxygen atom in the pyrylium ring was identified by the Fourier synthesis based on these atomic coordinates assuming that all the atoms in the ring are carbon (B = 3.5 $Å^2$), which was later confirmed

Table 4-1

(a) Distribution of normalized structure factor and statistical averages.

	Distribution of $\|E\|$	
	Experimental (%)	Theoretical (centrosymmetric) (%)
$\|E\| \geq 3.0$	0.8	0.5
$\|E\| \geq 2.0$	4.2	5.0
$\|E\| \geq 1.0$	29.0	32.0
$\langle \|E\| \rangle$	0.752	0.798
$\langle \|E\|^2 \rangle$	0.996	1.000
$\langle \|E\|^2 - 1 \rangle$	1.027	0.968

(b) Starting set of application of Σ_2 formula.

h	k	l	$\|E\|$	Phase
0	3	2	4.44	+
1	10	6	4.91	+
11	5	5	3.59	+
0	4	2	5.55	A
9	13	$\bar{2}$	4.83	B

(C) Process of the symbolic addition procedure

Run number	Number of reflections	$\|E\|$	Number of phases determined
0	5		Starting set
1	143	≥ 2.0	108 (hand calculations)
2	628	≥ 1.3	579

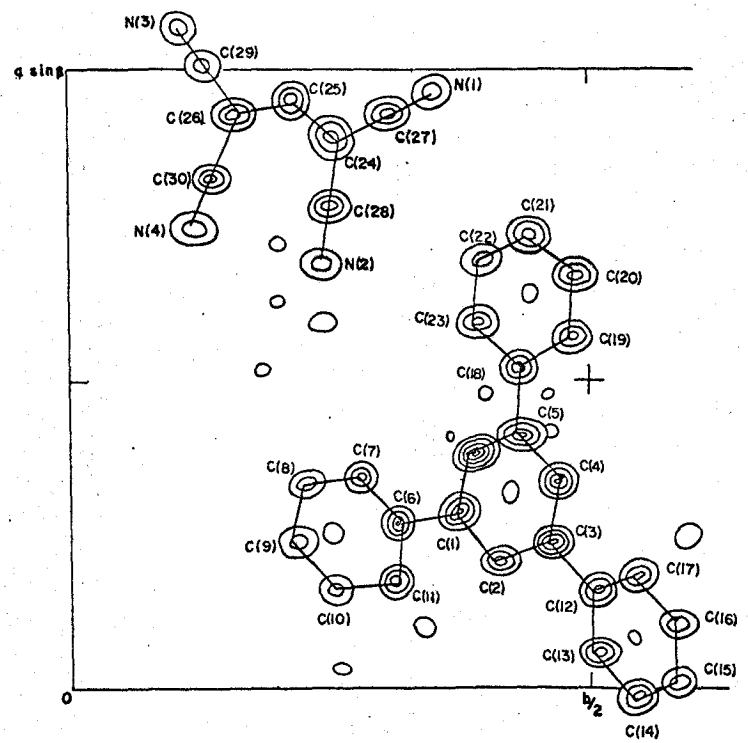

Fig. 4-1. E-map viewed along the c axis.

by the block-diagonal least-squares refinement using FBLS program. Four cycles of isotropic refinement reduced the R value to 0.150. Three cycles of anisotropic refinement using 2867 reflections ($\sin\theta/\lambda \leq 0.53$), reduced the R value to 0.084. The positions of hydrogen atoms were found from the difference Fourier synthesis computed at this stage. Further refinement including hydrogen atoms gave the final R value to 0.053 for non-zero reflections (0.058 for all reflections). In the refinement the function minimized was $\Sigma W(Fo-k|Fc|)^2$, where W = 1.00 for all reflections. The atomic scattering factors were taken from the values determined by Hanson and his co-workers.[9)]

The final positional and anisotropic thermal parameters of non-hydrogen atoms are listed in Table 4-2. The cordinates and isotropic temperature factors of hydrogen atoms are listed in Table 4-3. The numbering of non-

Table 4-2 Positional parameters of non-hydrogen atoms in TPP-TCP along with their standard deviations in parentheses, and their anisotropic thermal parameters ($\times 10^5$), expressed of the form : $\exp[-(\beta_{11}h^2+\beta_{22}k^2+\beta_{33}l^2+\beta_{12}hk+\beta_{13}hl+\beta_{23}kl)]$.

Atom	x	y	z	β_{11}	β_{22}	β_{33}	β_{12}	β_{13}	β_{23}
O	0.3831(2)	0.3841(1)	0.9618(3)	476	202	1655	12	77	60
C(1)	0.2826(3)	0.3723(2)	0.9807(4)	471	210	1409	-76	160	-179
C(2)	0.2089(3)	0.4100(2)	0.9053(4)	443	200	1461	-20	11	-45
C(3)	0.2366(3)	0.4616(2)	0.8153(4)	472	196	1321	-16	33	-197
C(4)	0.3418(2)	0.4718(2)	0.8022(4)	425	186	1346	29	-18	-76
C(5)	0.4139(3)	0.4325(2)	0.8728(4)	515	182	1308	-63	137	-43
C(6)	0.2671(3)	0.3181(2)	1.0825(4)	510	196	1342	-64	6	-86
C(7)	0.3486(3)	0.2785(2)	1.1292(4)	647	234	1639	14	35	150
C(8)	0.3331(3)	0.2272(2)	1.2262(5)	755	269	2094	28	-51	133
C(9)	0.2375(3)	0.2152(2)	1.2788(5)	866	252	1863	-136	-106	167
C(10)	0.1554(3)	0.2548(2)	1.2328(5)	693	286	2084	-232	139	58
C(11)	0.1694(3)	0.3062(2)	1.1351(5)	564	247	1839	-64	35	129
C(12)	0.1590(3)	0.5048(2)	0.7371(4)	441	189	1477	-1	-70	-170
C(13)	0.0582(3)	0.5052(2)	0.7858(5)	492	260	2118	44	222	22
C(14)	-0.0143(3)	0.5453(2)	0.7115(5)	485	275	2689	77	143	-57
C(15)	0.0105(3)	0.5838(2)	0.5881(5)	584	230	2458	80	-363	-133
C(16)	0.1091(3)	0.5828(2)	0.5387(5)	726	265	2058	67	-225	211
C(17)	0.1833(3)	0.5437(2)	0.6125(5)	547	234	1752	2	51	97
C(18)	0.5257(2)	0.4360(2)	0.8651(4)	431	185	1354	5	141	-54
C(19)	0.5689(3)	0.4831(2)	0.7782(5)	555	249	1717	30	219	180
C(20)	0.6755(3)	0.4859(2)	0.7703(5)	585	282	1903	-91	472	100
C(21)	0.7376(3)	0.4415(2)	0.8477(5)	540	287	2080	88	235	161
C(22)	0.6959(3)	0.3953(2)	0.9359(5)	584	274	2403	194	72	162
C(23)	0.5904(3)	0.3921(2)	0.9462(5)	501	242	2076	89	107	183
C(24)	0.3866(3)	0.2438(2)	0.7116(4)	428	213	1610	-1	-9	-147
C(25)	0.4501(3)	0.2833(2)	0.6323(4)	406	221	1573	15	-22	-202
C(26)	0.4260(3)	0.3355(2)	0.5401(4)	394	231	1683	34	122	-117
C(27)	0.4289(3)	0.1928(2)	0.8027(5)	461	239	1796	-69	75	-76
C(28)	0.2785(3)	0.2507(2)	0.7078(5)	397	292	1844	-88	52	-75
C (29)	0.5052(3)	0.3679(2)	0.4661(5)	541	244	2052	104	249	83

Table 4-2 (continued)

Atom	x	y	z	β_{11}	β_{22}	β_{33}	β_{12}	β_{13}	β_{23}
C(30)	0.3261(3)	0.3616(2)	0.5066(5)	515	231	1562	16	-37	-89
N(1)	0.4621(3)	0.1507(2)	0.8756(5)	649	283	2548	-30	68	230
N(2)	0.1913(3)	0.2563(2)	0.7064(5)	505	471	2924	-112	120	75
N(3)	0.5770(3)	0.3947(2)	0.4040(5)	723	341	3265	93	837	626
N(4)	0.2487(3)	0.3855(2)	0.4769(5)	602	342	2498	223	-219	-73

Table 4-3 The atomic coordinates and isotropic temperature factors for hydrogene atoms.

Atom	x	y	z	B ($\AA^2$)
H(3)	0.130	0.400	0.913	1.8
H(5)	0.366	0.510	0.735	1.6
H(7)	0.424	0.287	1.089	1.9
H(8)	0.396	0.196	1.260	2.2
H(9)	0.226	0.176	1.353	1.9
H(10)	0.081	0.245	1.275	2.2
H(11)	0.106	0.337	1.101	1.9
H(13)	0.038	0.475	0.883	1.9
H(14)	-0.090	0.546	0.750	2.0
H(15)	-0.047	0.614	0.531	2.3
H(16)	0.129	0.613	0.440	2.3
H(17)	0.259	0.543	0.573	2.1
H(19)	0.520	0.517	0.715	2.3
H(20)	0.708	0.523	0.703	2.3
H(21)	0.819	0.443	0.840	2.1
H(22)	0.745	0.361	0.997	2.3
H(23)	0.558	0.355	1.016	2.1
H(25)	0.529	0.272	0.644	1.6

Each hydrogene atom is numbered as its number is the same as that of the carbon atom attached. The average estimated standard deviations are $\sigma(x) = 0.002$, $\sigma(y) = 0.001$, and $\sigma(z) = 0.003$, and $\sigma(B) = 0.6$ $\AA^2$.

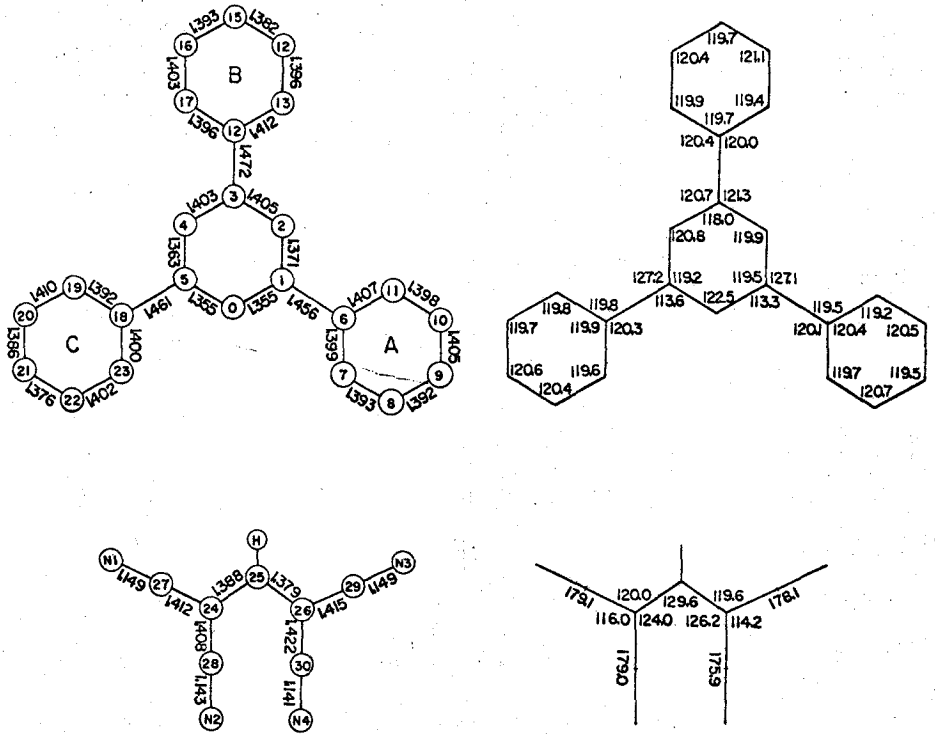

Fig. 4-2. Bond lengths (Å) and bond angles (°) in TPP-TCP salt.

hydrogen atoms is already shown in Fig. 4-1.

Results and Discussion

Structure of TPP cation. The bond lengths and bond angles are given in Fig. 4-2. The dimensions of the pyrylium ring, which contains 6π electrons as well as benzene and pyridinium ring, have not yet been reported hitherto. The pyrylium ring is almost planar with a maximum deviation of 0.015 Å from the best plane (Table 4-4). The bond angle of oxygen is 122.5 (3)° and two C-O bond lengths are both 1.355 (4)Å, which are slightly shorter than that for a conjugated O-heterocyclic, furan (1.371 (5)Å).[10] The bond lengths of C(1)-C(2) and C(4)-C(5) are significantly shorter, however, those of C(2)-C(3) and C(3)-C(4) are slightly longer than the value accepted for benzene

ring (1.397 Å).

Three C-C bond lengths connecting the benzene rings with the pyrylium ring (1.456 (5), 1.472 (5) and 1.461 (5)Å) are all expected values for single bond between two sp^2 hybridized carbon atoms. The considerably small angles of O-C(1)-C(6) and O-C(5)-C(18), 113.6 (3) and 113.3 (3)° may be due to the absence of a hydrogen atom bonded with the oxygen atom. Three benzene rings are planar within experimental error, but tilt from the plane of the pyrylium ring, tilt angle being 10.4, 18.0, and 2.3° for A, B, and C-rings, respectively. No unusual bond lengths and bond angles are found in them.

Structure of TCP anion. TCP anion is also approximately planar, the maximum deviations from the least-spuares plane being 0.053 Å (above) for N(2) and -0.051 Å (below) for N(4). In the anion, however, two $C-C(CN)_2$ groups are respectively planar within 0.007 Å, and they are both tilted by 1.3° from the best plane of the anion. The large bond angle of C(24)-C(25)-C(26), 129.6°, presumably indicates a steric repulsion between $C(CN)_2$ groups. The conjugated O-C bonds between two sp^2 carbon atoms, C(24)-C(25) = 1.388 (5) and C(25)-C(26) = 1.379 (5)Å, are significantly shorter than the C-C bond associated with the CN group, average 1.41 Å. The molecular orbital calculation shows that the bond order for the former is 0.61, which is larger than that of 0.49 for the latter. This result is consistent with the observed bond lengths. The average C≡N bond length, 1.145 Å, is in agreement with those observed in other polycyanoacid anions.[7,11,12,13,14]

Crystal structure. The packings of cations and anions in the unit cell viewed along the c and a axes are respectively shown in Figs. 4-3 and 4-4. Interionic atomic contacts less than 3.6 Å are given in Table 4-5.

The crystal structure consists of parallel columns of infinite length along the c axis in which the cations and anions stack alternately, as shown in Fig. 4-4. The least-squares planes of the cation and the anion are almost

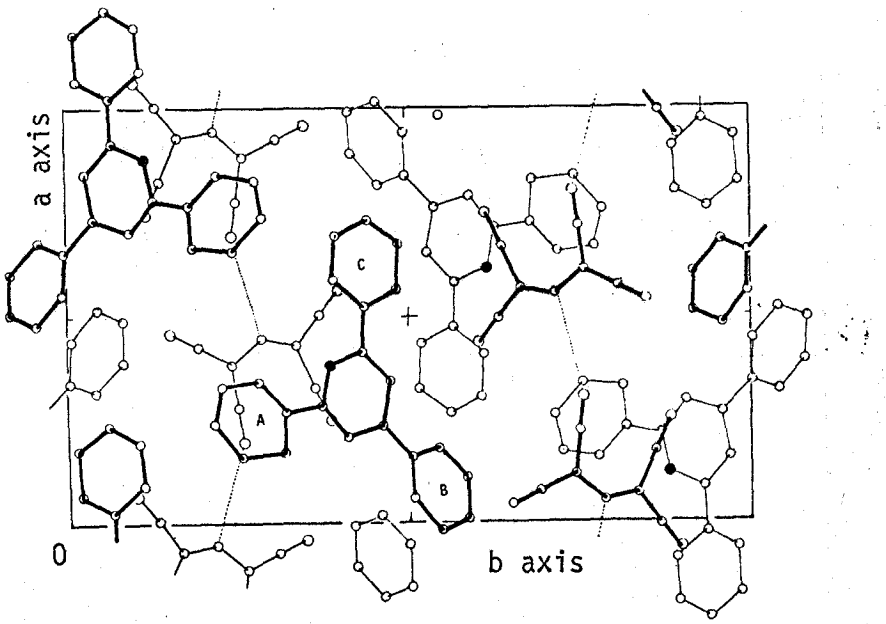

Fig. 4-3. The crystal structure viewed along the c axis.

The dotted lines show the presence of the hydrogen bonding.

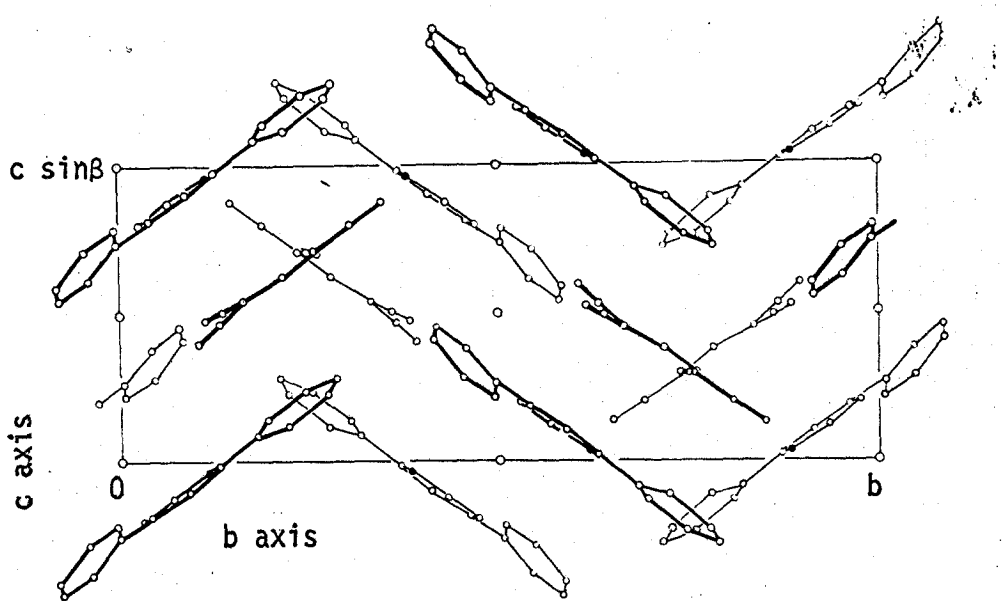

Fig. 4-4. The crystal structure of TPP-TCP viewed along the a axis.

The benzene ring-B in each TPP cation (shown in Fig. 4-4) is omitted.

Table 4-4 Least-squares planes and deviations of the atoms in TPP-TCP.

Equation of the plane : $AX + BY + CZ = D$, where $X = ax + cz \cdot \cos\beta$, $Y = by$, $Z = cz \cdot \cos\beta$.

(I) Best plane through TPP cation

$0.0168X + 0.5961Y + 0.8027Z = 4.7142$

O	-0.005 Å	C(1)	0.041 Å	C(2)	0.078 Å	C(3)	0.013 Å
C(4)	-0.052	C(5)	-0.037	C(6)	0.058	C(7)	0.234
C(8)	0.245	C(9)	0.069	C(10)	-0.112	C(11)	-0.119
C(12)	0.010	C(13)	-0.306	C(14)	-0.306	C(15)	0.018
C(16)	0.338	C(17)	0.329	C(18)	-0.060	C(19)	-0.086
C(20)	-0.092	C(21)	-0.055	C(22)	-0.040	C(23)	-0.049

(II) Best plane through pyrylium ring

$-0.0205X + 0.5773Y + 0.8163Z = 4.3721$

O	-0.002 Å	C(1)	-0.012 Å	C(2)	0.015 Å	C(3)	-0.003 Å
C(4)	-0.011	C(5)	0.014				

(III) Best plane through benzene ring-A

$0.1608X + 0.5625Y + 0.8110Z = 4.9282$

C(6)	0.001 Å	C(7)	-0.003 Å	C(8)	0.003 Å	C(9)	-0.001 Å
C(10)	-0.001	C(11)	0.001				

(IV) Best plane through benzene ring-B

$0.2160X + 0.7150Y + 0.6649Z = 6.7314$

C(12)	-0.000 Å	C(13)	0.005 Å	C(14)	-0.004 Å	C(15)	-0.000 Å
C(16)	0.004	C(17)	-0.004				

(V) Best plane through benzene ring-C

$0.0196X + 0.5815Y + 0.8138Z = 4.6481$

C(18)	0.006 Å	C(19)	0.001 Å	C(20)	-0.008 Å	C(21)	0.007 Å
C(22)	0.001	C(23)	-0.007				

Table 4-4 (continued)

(VI) Best plane through TCP anion

0.0680X + 0.5773Y + 0.8138Z = 8.1201

C(24)	-0.001 Å	C(25)	-0.012 Å	C(26)	-0.015 Å	C(27)	-0.020 Å
C(28)	0.036	C(29)	0.012	C(30)	-0.024	N(1)	-0.020
N(2)	0.053	N(3)	0.042	N(4)	-0.051		

Table 4-5 Interionic atomic contacts (less than 3.6 Å)

Within an ion-pair (Å).

C(26)···C(5)	3.472(5)	C(27)···C(7)	3.504(5)	C(28)···C(1)	3.449(5)
C(28)···C(6)	3.450(5)	C(30)···C(4)	3.400(5)	C(30)···C(5)	3.511(5)
N(2)····C(1)	3.512(5)	N(2)····C(6)	3.468(5)	N(4)····C(3)	3.267(5)
N(4)····C(4)	3.417(5)	N(4)····C(12)	3.588(5)		

Between ion-pairs (Å).

$N(4)^{1}\cdots C(11)^{2}$ 3.401(5)

Between anions (Å).

$C(25)^{1}\cdot\cdot N(2)^{4}$ 3.265(5)

Between cations (Å).

$C(5)^{1}\cdots C(19)^{3}$	3.411(5)	$C(3)^{1}\cdots C(21)^{3}$	3.480(5)	$O^{1}\cdots\cdots C(19)^{3}$	3.480(5)

Between non-overlapping anion and cation (Å).

$N(3)^{1}\cdots C(4)^{3}$	3.579(5)	$N(3)^{1}\cdots C(17)^{3}$	3.520(6)	$N(3)^{1}\cdots C(19)^{3}$	3.438(6)
$N(1)^{1}\cdots C(2)^{4}$	3.457(5)	$N(1)^{1}\cdots C(11)^{4}$	3.446(5)	$N(3)^{1}\cdots C(9)^{5}$	3.446(6)
$N(1)^{1}\cdots C(21)^{6}$	3.517(6)	$N(4)^{1}\cdots C(15)^{7}$	3.439(6)		

Codes for superscripts

^{1} x, y, z, ^{2} x, y, -1+z, ^{3} 1-x, 1/2-y, 1-z,

^{4} 1/2+x,1/2-y, z, ^{5} 1/2+x,1/2-y, -1+z, ^{6} -1/2+x, 1/2-y, z,

^{7} -x, 1-y, 1-z,

parallel to the a axis, and the former inclined to the c axis by 53.0° and the latter 53.7°, the dihedral angle between them being 3.2°. In the column, although the TCP anion is sandwitched by TPP cations and vice versa, the TCP anion has larger overlap and closer contact with one of the cation than the other. Therefore, TCP anion and TPP cation can be considered to form an "ion-pair" in the crystal as a stacking unit.

The relative arrangement between the cation and the anion in the column is shown in Fig. 4-5. In the ion-pair the anion overlaps mainly with the pyrylium ring of the cation. The average interplanar spacing between the best planes of the anion and the pyrylium ring is 3.31 Å, and the closest atomic contact is N(4)···C(3), 3.267 (5)Å. These are slightly shorter than the corresponding van der Waals distances. In addition to the alternate arrangement and the close contact of two components characteristic in organic CT complexes, the overlap between the highest occupied molecular orbital of the anion and the lowest vacant molecular orbital of the cation can be considered as a measure of the CT interaction. The shapes of these orbitals, charge distributions and bond orders were calculated by Huckel M. O. method using ω-technique,[15] which are given in Fig. 4-6. However, the shapes of calculated orbitals can not explain well the observed overlapping between the cation and the anion in terms of the interionic CT interaction. Furthermore, in Fig. 4-5 the coincident overlaps between atoms are only slightly observed. These facts do not indicate an appreciable contribution of CT force on the relative arrangement of the cation and the anion.

Fig. 4-6(b) shows that the negative charge in the anion is significantly distributed on four nitrogen atoms, whereas the positive charge in the cation is localized at the oxygen and neighboring carbon atcms in the pyrylium ring. The observed overlap of the cation with the anion in which the oxygen atom of the cation is located approximately above the center of

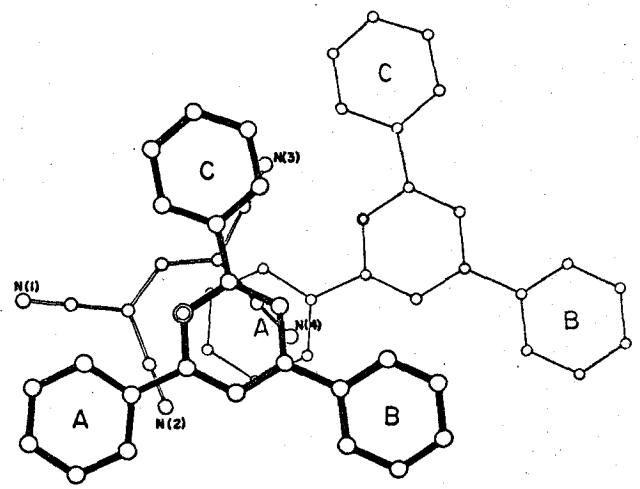

Fig. 4-5. The relative arrangement between the cation and the anion in the column.

Fig. 4-6(a).

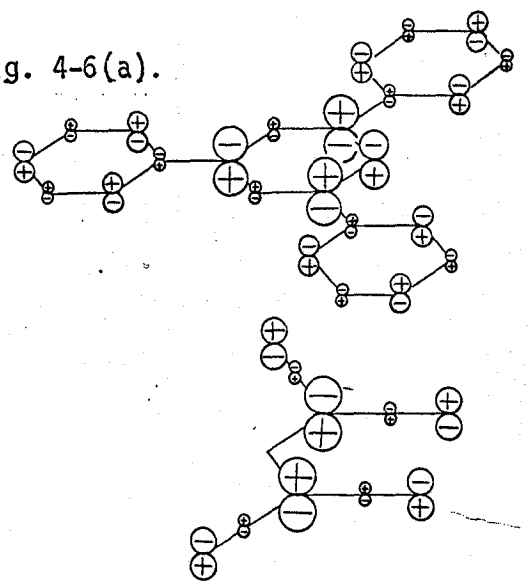

Fig. 4-6(b).

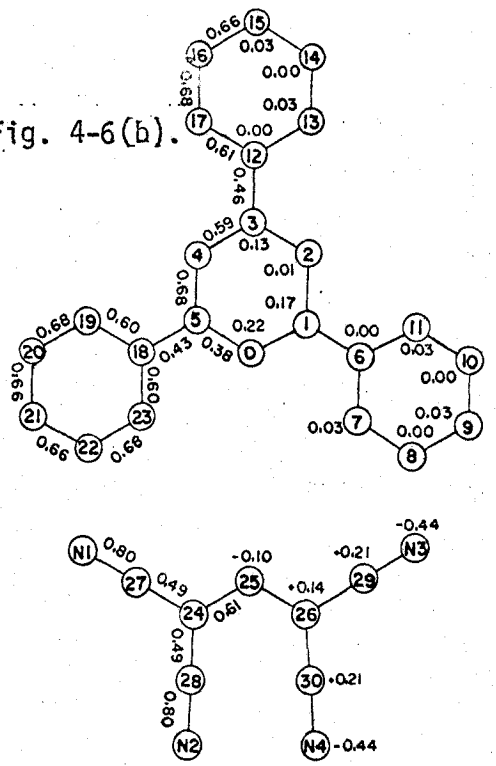

Fig. 4-6(a). The shapes of the lowest vacant molecular orbital of TPP cation and the highest occupied molecular orbital of TCP anion calculated by Huckel M. O. method using ω-technique.

Fig. 4-6(b). The charge distributions (shown in the right half of the molecule) and the bond orders (shown in the left half of the molecule) calculated by Huckel M. O. method using ω-technique.
The parameters were assumed as follows: the resonance integrals are $0.9\beta_o$ for C-O bond, and $1.2\beta_o$ for C-N bond, and the Coulombic integrals are $\alpha_o + 2.5\beta_o$ for O atom and $\alpha_o + 1.0\beta_o$ for N atom, and $\omega = 1.4$.

the anion, therefore, can be explained mainly by the electrostatic interaction.

A short atomic contact between the C(25) atom of a TCP anion and the N(2) atom of the adjacent TCP anion along the a axis, which is shown by a dotted line in Fig. 4-3, indicates an existence of strong interaction like hydrogen bond between anions in the neighboring columns. The C(25)···N(2)^4 and H(25)···N(2)^4 distances and C(25)-H(25)···N(2)^4 angle are 3.265 (5) and 2.185 (5)Å and 170°, respectively. The C-H···N hydrogen bond has been observed scarecely, however, in the present case, this type of short atomic contact is present, which is probably caused by the activation of H(25) atom by four electron-withdrawing cyano groups. The relative arrangement of the anion seems to be affected by this interaction.

The tilt angles of three benzene rings from the pyrylium ring may be affected by the degree of the overlap with TCP anion. The C-ring, with least tilt angle, overlaps with the anion in the ion-pair where the interplanar spacing is fairly short. However, the contact between the A-ring and the anion is in van der Waals distance, which may restrict the free rotation of benzene ring slightly (Fig. 4-5). On the other hand, little overlap observed between the B-ring and the anion allows the rotation of the B-ring.

The polarized absorption spectrum of a single crystal of this salt is given in Fig. 4-7. The optical density of the absorption band at 535 nm, which is usually assigned as interionic CT band, is about 1.65 times higher in the C-polarization spectrum than the other. Assuming that the direction of the transition moment is perpendicular to the planes of the anion and the cation, which is inclined to the C axis by ca. 37°, the ratio of two components of the dipole moment parallel and perpendicular to the C axis is given by cos37°/cos53° (=1.32). The dichroism ration, therefore, is (cos37°/cos53°)^2, 1.74. This value approximately agrees with the observed dichro-

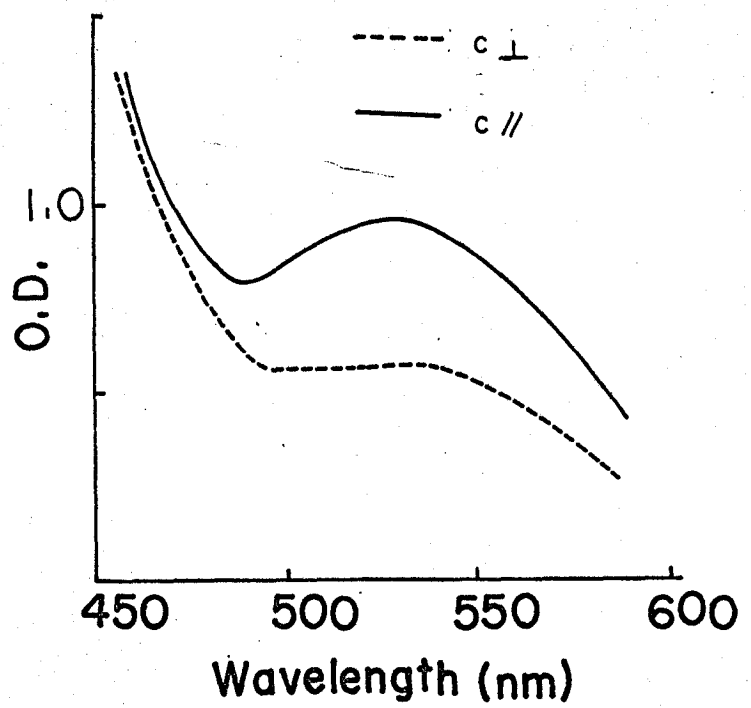

Fig. 4-7. Polarized absorption spectra of TPP-TCP salt.

ism ratio. Thus the polarized absorption spectrum can be explained well in terms of the crystal structure.

4-2 CRYSTAL STRUCTURE OF TPT-TCP SALT

Experimental

TPT-TCP salt, recrystallized from a methanol solution, forms dark-red, needle crystals. The crystal system and appropriate cell parameters were determined from Oscillation and Weissenberg photographs. The cell constants were determined precisely using a diffractometer, The crystallographic data are as follows.

Crystal data. $[(C_{23}H_{17}S)^{+}\cdot(C_7HN_4)^{-}]$, F.W. = 466.6, monoclinic, a = 17.838,

b = 7.762, c = 17.225 Å, β = 93.06°, Z = 4, Dm = 1.39 g·cm^{-3}(CCl_4-C_6H_6), Dx = 1.41 g·cm^{-3}, space group: $P2_1/a$, absent spectra: h0l; h + l ≠ 2n, 0k0; k ≠ 2n.

Intensity data were collected from a crystal of dimensions, 0.51 x 0.22 x 0.10 mm, on a Rigaku four-cycle diffractometer, using Nickel-filtered Cu-Kα_1 radiation. The monoclinic b axis of the crystal was set parallel to the ψ axis of the diffractometer. Integrated intensities were measured by the ω scan method, with a scanning speed of 2° per min. The scan width for each reflection was 3.0°. The back-ground was measured for 5 seconds at each end of the scan range. 2989 independent reflections with 2θ < 110° were obtained and were corrected for Lorentz and polarization factors, but no absorption correction was made (μ = 21.8 cm^{-3}).

Structure Determination and Refinement

The structure was solved by the heavy atom method. Two sets of the coordinates of a sulfur atom in an asymmetrical unit were satisfied with a sharpened Patterson map. On the basis of one set of the coordinates, several atoms around sulfur atom were found in a successive Fourier map. All non-hydrogen atoms were sorted out from the third Fourier map. Four cycles of isotropic least-squares refinement with a block diagonal program FBLS reduced the R value to 17.0 %. The successive refinement using anisotropic temperature factors with all atoms reduced the R value to 14.0 %. The function minimized was $\Sigma w(Fo - |Fc|)^2$. In the early stages of refinement, the weight, w, was assigned to 1.0 for all the observed reflections.

Further refinements did not improve the R value. This may be due to a disorder in the crystal. At this stage, all the bond lengths were reasonable except for those in the thiopyrylium ring. That is, the C^{sp^2}-C^{sp^2}

conjugated double bond lengths in the thiopyrylium ring were extraordinary longer than the expected value. Moreover, the β_{11}, β_{22} and β_{33} components of the anisotropic temperature factors of sulfur atom were fairly large, while these values of C(2) and C(4) were unusually small, as compared with the other atoms. Especially, β_{22} and β_{33} of C(4) were negative. These anomalies suggested that there exist some sort of disorder regarding with the thiopyrylium ring. The sulfur atom in the crystal may locate mainly the S site determined above, but may also locate partially at the C(2) and C(4) sites with less probabilities. The distribution of the sulfur atom in thiopyrylium ring was determined by means of trial and error method so that the anomalous temperature factors of S, C(2), C(4) atoms could be improved. These calculation showed that the probabilities of the sulfur atom at S, C(2), and C(4) sites were 0.6, 0.1 and 0.3,respectively. That is, at the S-site the cabon atom may also be present with the probability of 0.4, and consequently the occupancy with respect to sulfur atom may be 0.75. The occupancies at C(2), and C(4) sites will be 1.167 and 1.50 with respect to carbon atom, respectively. Assumed that the other atoms were fixed at corresponding sites, the refinement was continued on the basis of these new occupancies. This refinement reduced the R value to 12.0 %.

In order to proceed the further refinement, 3 cycles of the full matrix least-squares refinement were carried out, and reduced the value to 9.8 %. The weights for the reflections were : $\sqrt{w} = 1.0$ for $0 < Fo \leq 25$, $\sqrt{w} = 25/Fo$ for $Fo > 25$.

The difference Fourier synthesis calculated at this stage revealed the positions of the hydrogen atoms except for those in thiopyrylium ring. The further refinement including hydrogen atoms gave the final R value 7.3 % for non-zero reflections.

Table 4-6 Positional parameters of non-hydrogen atoms in TPT-TCP salt along with their standard deviations in parentheses, and their anisotropic thermal parameters (x 10^5), expressed of the form : $\exp[-(\beta_{11}h^2+\beta_{22}k^2+\beta_{33}l^2+\beta_{12}hk+\beta_{13}hl+\beta_{23}kl)]$.

Atom	x	y	z	β_{11}	β_{22}	β_{33}	β_{12}	β_{13}	β_{23}
S	0.5792(1)	0.2674(3)	0.5550(1)	394	2565	481	-165	-38	-270
C(1)	0.5259(3)	0.2846(7)	0.4764(3)	354	1302	308	115	0	-192
C(2)	0.5417(2)	0.3458(5)	0.3986(2)	327	1038	321	-193	434	-93
C(3)	0.6223(3)	0.3971(7)	0.3915(3)	323	1493	338	147	62	-266
C(4)	0.6916(2)	0.3858(4)	0.4509(2)	432	1116	165	125	-163	61
C(5)	0.6625(3)	0.3284(7)	0.5309(3)	314	1261	367	-74	49	-225
C(6)	0.4467(3)	0.2277(6)	0.4889(3)	349	1470	325	67	29	-290
C(7)	0.4277(3)	0.1521(7)	0.5581(3)	447	1978	345	-92	169	135
C(8)	0.3537(3)	0.0982(7)	0.5664(3)	476	2332	504	-172	359	38
C(9)	0.2994(3)	0.1184(7)	0.5074(3)	398	1874	636	-105	187	-213
C(10)	0.3179(3)	0.1936(7)	0.4378(3)	373	2374	568	-179	8	-223
C(11)	0.3910(3)	0.2495(7)	0.4279(3)	382	2129	420	-252	-58	-59
C(12)	0.4625(2)	0.4598(6)	0.3147(3)	269	1680	389	100	83	-123
C(13)	0.6045(3)	0.3989(7)	0.2474(3)	317	2095	365	64	3	-78
C(14)	0.6237(3)	0.4572(7)	0.1745(3)	414	2340	398	285	150	-15
C(15)	0.6800(3)	0.5800(8)	0.1674(3)	426	2723	462	230	274	159
C(16)	0.7173(3)	0.6404(8)	0.2355(3)	515	2665	504	-547	333	122
C(17)	0.6993(3)	0.5817(7)	0.3081(3)	393	1914	496	-315	133	96
C(18)	0.7217(2)	0.3190(6)	0.5944(2)	311	1743	303	105	2	-117
C(19)	0.7846(3)	0.4245(7)	0.5911(3)	312	2135	429	-151	12	-75
C(20)	0.8411(3)	0.4149(8)	0.6498(3)	358	2803	464	-136	-64	46
C(21)	0.8351(3)	0.3014(8)	0.7107(3)	475	2676	437	92	-143	77
C(22)	0.7728(3)	0.1952(8)	0.7146(3)	522	2494	416	-87	-51	194
C(23)	0.7144(3)	0.2041(7)	0.6568(3)	434	2017	345	16	-32	19
C(24)	0.4644(3)	0.1033(7)	0.8642(3)	304	2560	396	266	-23	13
C(25)	0.5028(3)	0.2349(7)	0.9035(3)	298	2108	456	345	-13	-143
C(26)	0.5512(3)	0.3580(7)	0.8752(3)	378	2381	323	233	-32	-426
C(27)	0.4128(3)	-0.0019(8)	0.9037(3)	399	2613	581	245	46	-532
C(28)	0.4755(3)	0.0542(8)	0.7863(3)	448	2681	355	33	-186	-9

Table 4-6 (continued)

Atom	x	y	z	β_{11}	β_{22}	β_{33}	β_{12}	β_{13}	β_{23}
C(29)	0.5876(3)	0.4739(8)	0.9288(3)	459	2619	362	235	89	29
C(30)	0.5623(3)	0.3859(7)	0.7953(3)	385	2439	347	221	107	-224
N(1)	0.3700(3)	-0.0811(7)	0.9357(3)	552	3307	797	-418	470	-812
N(2)	0.4873(3)	0.0062(7)	0.7252(3)	856	3397	364	-182	-122	-269
N(3)	0.6158(3)	0.5665(7)	0.9734(3)	658	3349	442	-559	6	-546
N(4)	0.5702(3)	0.4168(7)	0.7315(2)	548	3470	400	148	123	-162

Table 4-7 The atomic coordinates and isotropic temperature factors for hydrogen atoms in TPT-TCP salt.

Atom	x	y	z	B ($Å^2$)
H(7)	0.474	0.120	0.602	4.4
H(8)	0.346	0.045	0.623	4.8
H(9)	0.245	0.074	0.513	5.1
H(10)	0.280	0.208	0.386	4.7
H(11)	0.410	0.316	0.375	5.1
H(13)	0.560	0.307	0.254	3.8
H(14)	0.595	0.397	0.123	3.6
H(15)	0.689	0.609	0.108	3.4
H(16)	0.756	0.749	0.231	7.2
H(17)	0.731	0.626	0.360	4.5
H(19)	0.788	0.516	0.544	4.2
H(20)	0.884	0.494	0.639	6.1
H(21)	0.874	0.287	0.754	6.7
H(22)	0.765	0.118	0.767	4.2
H(23)	0.665	0.128	0.666	4.3
H(25)	0.510	0.759	0.035	3.1

Each hydrogen atom is numbered as its number is the same as that of the carbon atom attached. H(3) and H(5) atoms could not be found from the difference Fourier synthesis. The average e.s.d. are $\sigma(x) = 0.003$, $\sigma(y) = 0.007$, and $\sigma(z) = 0.003$, and $\sigma(B) = 1.3$ $Å^2$.

Tables 4-6, 7 give final atomic parameters. The scattering factors were taken from the values determined by Hanson and his co-workers.[9] The dispersion correction form $\Delta f'$ for the sulfur scattering factor was taken from Tnternational Tables for X-Ray Crystallography.[16]

Results and Discussion

Molecular Structure. The bond lengths and the bond angles in TPT-TCP salt are shown in Fig. 4-8. As mentioned above, thiopyrylium ring in TPT-TCP cation has extraordinary dimensions, due to the disorder of TPT cation in a crystal. This ring, however, seems to be roughly planar with a maximum standard deviation of 0.038 Å, as shown in Table 4-8. All three substituent benzene rings are planar within experimental error, and no unusual bond lengths and bond angles are observed in them. Three phenyl groups tilt to the thiopyrylium ring considerably, the tilt angles being 6.6, 31.8, and 25.4°,

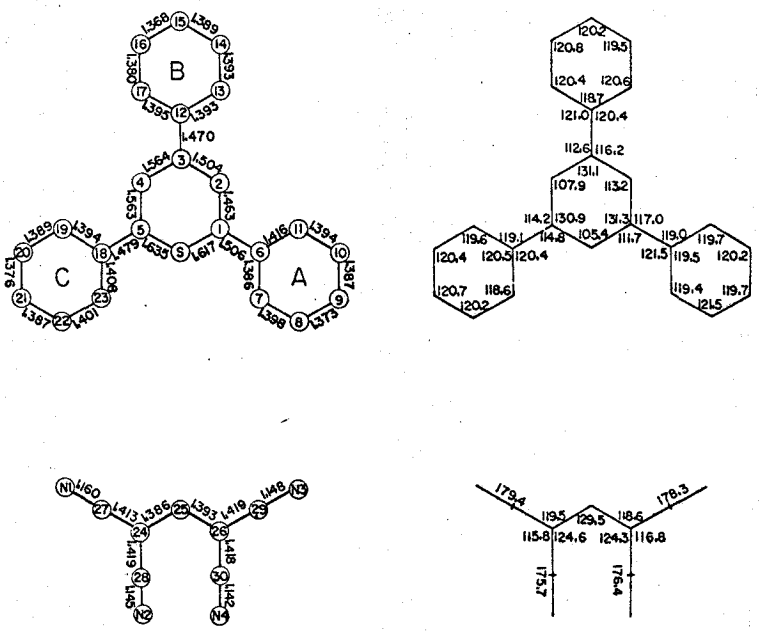

Fig. 4-8. Bond lengths (Å) and bond angles (°) in TPT-TCP salt.

for A, B, and C benzene rings, respectively.

Two dicyanomethylene groups, $C(CN)_2$ in TCP anion are both approximately planar as shown in Table 4-8, but these two planes are twisted by 17.8°, indicating that the anion in TPT-TCP salt is not planar. The bond lengths and bond angles of TCP anion in TPT-TCP are in good agreement with the corresponding values in TPP-TCP salt.

Crystal structure. The packings of TPT-TCP salt in a unit cell viewed along b, c, and a axes are depicted in Figs. 4-9, 4-10 and 4-11, respectively. The crystal structure of the thiopyrylium salt is quite different from that of the pyrylium salt. The structure of TPT-TCP salt is built up from infinite columns in which the same ions are stacked, independently. TPT cations are stacked approximately parallel to the b-plane, forming an infinite column along the b axis. In the column, thiopyrylium ring in one

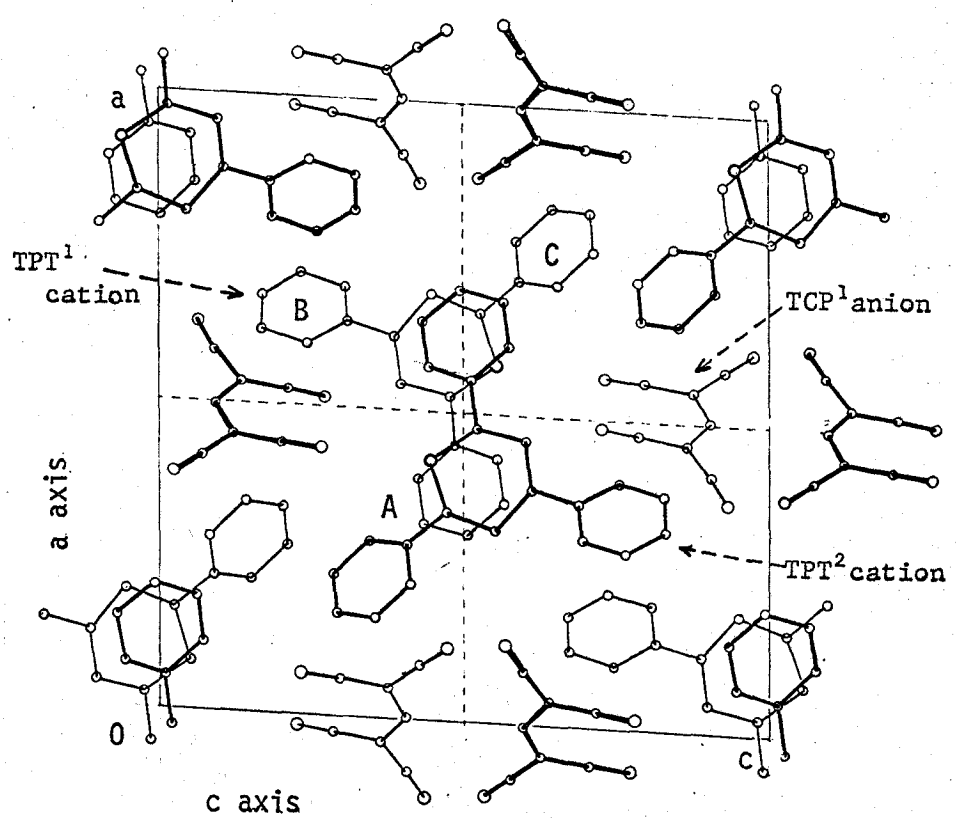

Fig. 4-9. The crystal structure of TPT-TCP viewed along the b axis.

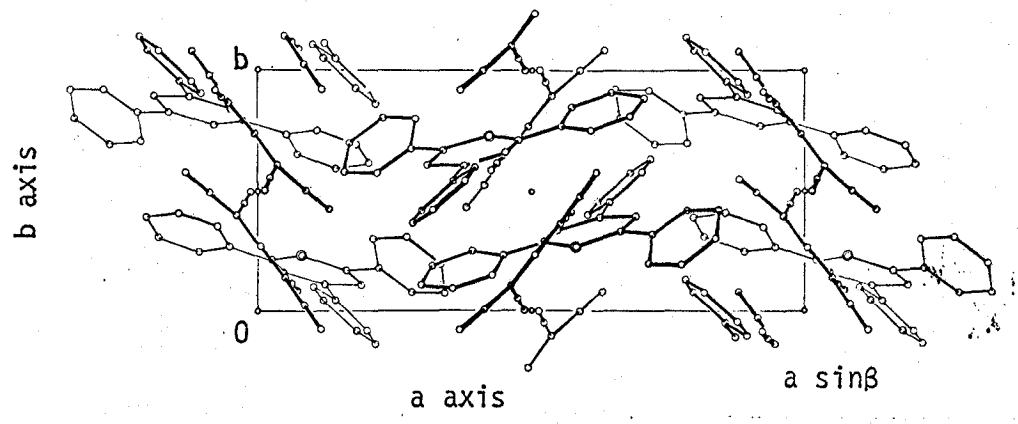

Fig. 4-10. The crystal structure of TPT-TCP viewed along the c axis.

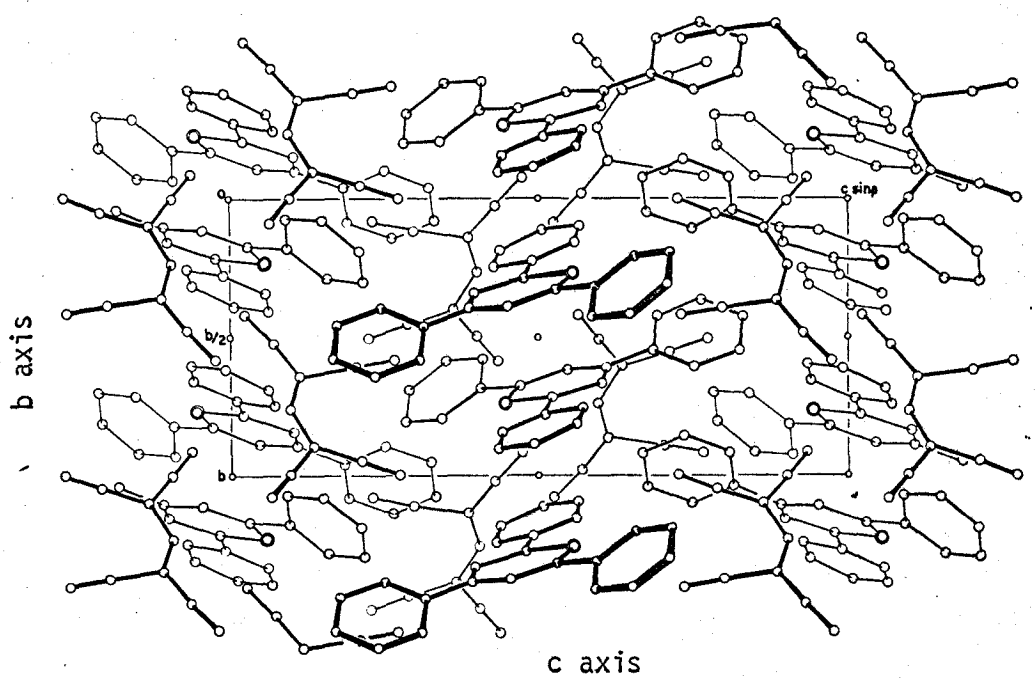

Fig. 4-11. The crystal structure of TPT-TCP viewed along the a axis

TPT cation overlaps with the benzene ring-A in other TPT cation, and vice versa. Since in a TPT cation, the tilt angle between the thiopyrylium ring and the benzene ring-A is only 6.6°, these two planes can be considered to lie roughly on a plane. The interplanar spacings of the least-squares planes involving thiopyrylium ring and the A-ring are alternately 3.6 and 3.8 Å, and the shortest interionic atomic diatance between two cations

Table 4-8 Least-squares planes and deviations of the atoms in TPT-TCP salt.

Equation of the plane : $AX + BY + CZ = D$, where $X = ax + cz \cdot \sin\beta$, $Y = by$, $z = cz \cdot \cos\beta$.

(I)	Best plane through thiopyrylium ring					
	$-0.213X + 0.942Y + 0.260Z = 2.326$					
	S	-0.010 Å	C(1)	0.028 Å	C(2)	0.003 Å
	C(3)	-0.032	C(4)	0.038	C(5)	-0.026
(II)	Best plane through benzene ring-A					
	$-0.246X + 0.900Y + 0.361Z = 2.774$					
	C(6)	0.001 Å	C(7)	0.000 Å	C(8)	-0.001 Å
	C(9)	-0.001	C(10)	0.003	C(11)	-0.003
(III)	Best plane through benzene ring-B					
	$0.677X - 0.734Y - 0.055Z = 4.649$					
	C(12)	-0.001 Å	C(13)	0.006 Å	C(14)	-0.007 Å
	C(15)	0.004	C(16)	0.000	C(17)	-0.002
(IV)	Best plane through benzene ring-C					
	$-0.484X + 0.707Y + 0.516Z = 1.070$					
	C(18)	0.005 Å	C(19)	0.00[illegible] Å	C(20)	-0.004 Å
	C(21)	-0.001	C(22)	0.00[illegible]	C(23)	-0.008
(V)	Best plane through $C(CN)_2$ group [illegible]olving C(24) atom					
	$0.734X - 0.584Y + 0.347Z = 3.680$					
	C(24)	0.014 Å	C(27)	0.008 Å	C(28)	-0.031 Å
	N(1)	-0.006	N(2)	0.016		
(VI)	Best plane through $C(CN)_2$ group involving C(26) atom					
	$0.814X - 0.579Y + 0.048Z = 3.635$					
	C(26)	-0.011 Å	C(29)	0.003 Å	C(30)	0.020 Å
	N(3)	-0.001	N(4)	-0.011		

is 3.463(8) Å for C(8) - C(17). These results suggest that this overlap is in van der Waals contact.

On the other hand, the packing of the anion is also very strange. One TCP anion has close contacts with other TCP anion related by a symmetrical center. The shortest atomic distance between two anions is 3.439 (7) Å for C(25) - N(3), and no other close atomic contact less than 3.7 Å is found between any two anions, indicating that these two anions make a pair in a crystal. This pair is packed in the spaces among the cation columns. The ideal plane of TCP anion makes angles of 52, 36, and 10° with the a, b, and c axes, respectively. Therefore, the pairs of two anions which are approximately parallel to the c-plane, are stacked and form an endless column along the b axis, as shown in Fig. 4-11.

The relative arrangement between the cation and the anion is complex. In Fig. 4-9 TPT^1 cation has close contacts with TCP^1 anion. This anion tilts to the thiopyrylium ring of the cation by ca. 48°. Sulfur atom in the thiopyrylium ring is located between two cyanogroups, C(28)-N(2) and C(30)-N(4), in anion. The shortest atomic distances between the cation and the anion are 3.223 (8) Å for N(2) - C(7) and 3.266 (7) Å for N(4) - S, which are slightly shorter than the corresponding van der Waals distances. Since between N(2) - C(7), the hydrogen atom, H(7), is present and N···H distance 2.293 Å, is significantly shorter the van der Waals distance, a weak interaction like hydrogen bong might participate in the close contact. According to the results on molecular orbital calculations using ω-technique, a considerable amount of a positive charge of the cation is localized at sulfur atom in the thiopyrylium ring, whereas a negative charge of TCP anion distrib tributes mainly at four nitrogen atoms. Between N(4) - S, therefore, may be present the specific interaction, which is perhaps electrostatic force. By contrast, the overlaps between π-orbitals of two component ions are

little observed.

The relatively weak contact are observed between TCP^1anion and the benzene ring-B in TPT^2cation as shown in Fig. 4-9. However, the shortest interionic atomic distance, 3.46 Å, indicates that this overlap is usual van der Waals contacts. The large tilt angle of benzene ring-B from thiopyrylium ring may be caused by this overlap. On the contrary, the approximate coplanarity of benzene ring-A with thiopyrylium cation ring is probably maintained by the overlaps between two cations. The tilt angle of benzene ring-C from thiopyrylium ring, about 25°, seems to be nearly in a stable configuration, because the crystal packing did not restrict the rotation of this benzene ring so much.

Unfortunately the author could not find the reason why TPT-TCP salt has such a strange structure. The specific interaction between N(4) - S might affect this structure. However, it can be concluded that the CT interaction has little influence on the crystal structure of TPT-TCP salt.

The presence of the interionic CT interaction in this crystal is demonstrated by its polarized absorption spectrum as shown in Fig. 4-12. Both locally excited band of the cation around 450 nm and a CT absorption band around 540 nm show a remarked dichroism, that is, the optical densities of two absorption bands are both larger in the parpendicular direction than in the parallel direction to the b axis. Since the transition moment of the LE band of the cation is within the plane of thiopyrylium ring which inclines to the b axis by about 70°, the component of the dipole monent perpendicular to the b axis may be fairly larger than the parallel component, as shown in Fig. 4-12. On the other hand, it is fairly difficult to specify the direc- of the CT transition moment in a crystal, because of the complicated relative arrangement between the cation and the anion. Assumed that the direction

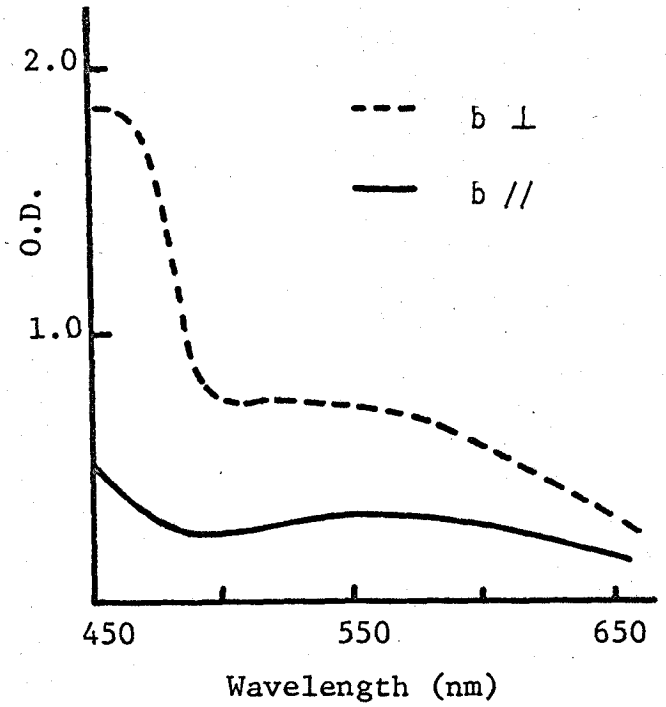

Fig. 4-12. Polarized absorption spectra of TPT-TCP salt.

of the CT transition moment is approximately coincident with that from sulfur atom in TPT cation to a cyano group C(30)-N(4) in TCP anion, the dipole moment would incline to the b axis by about 30 - 35°. This angle could explain the observed dichroism of the CT absorption band.

Summary

The crystal structures of two organic CT salts, 2,4,6-triphenyl-pyrylium-1,1,3,3-tetracyanopropenide (TPP-TCP) and 2,4,6-triphenylthio-pyrylium-1,1,3,3-tetracyanopropenide (TPT-TCP) were determined by means of x-ray diffraction method. In the case of TPP-TCP salt, the cation and the anion are nearly planar, and form an ion-pair, and the crystal is built up from infinite columns stacked by these ion-pairs along the needle, the c axis. By contrast, in the case of TPT-TCP salt, the cation and the anion do not form an ion-pair. The crystal is constructed by infinite columns in

which the same ions are stacked, independently, along the needle, the b axis. Therefore, it can be concluded that an alternating face-to-face arrangement between donor and acceptor characteristic in ordinary molecular CT complexes is not in general in organic CT salts. Moreover, it has been emphasized that the crystal structure of organic CT salt has been influenced by electrostatic force rather than CT interaction between two component ions.

References

1) C. K. Prout and J. D. Wright, Angew. Chem., 80, 688 (1968).

2) H. A. Bent, Chem. Rev., 68, 587 (1968).

3) R. Foster, "Organic Charge-Transfer Complexes", Chapter 8, Academic Press Inc., London, LTD. (1969).

4) A. I. Kitaigorodski, Yu. T. Struchkov, T. L. Khotsyanova, M. E. Vol'pin, and D. N. Kursanov, Izvest. Akad. Nauk. S.S.S.R., Otdl. Khim. Nauk., 1, 32, (1960).

5) K. Nakamura, N. Yasuoka, N. Kasai, H. Mikawa, and M. Kakudo, Chem. Comm. 1135 (1970).

6) S. Sakanoue, Y. Kai, N. Yasuoka, N. Kasai, and M. Kakudo, Bull. Chem. Soc. Japan, 43, 1306 (1970).

7) S. Sakanoue, N. Yasuoka, N. Kasai, and M. Kakudo, ibid., 44, 1 (1971).

8) J. Karle and I. L. Karle, Acta Crystallogra., 21, 849 (1966).

9) H. F. Hanson, F. Hermann, J. D. Lea, and S. Skillman, ibid., 17, 1040 (1964).

10) A. Almennings, O. Bastiansen, and H. Hansen, Acta Chem. Scandi., 9, 1306 (1955).

11) R. Desiderato,and R. L. Sass, Acta Crystallogra., 18, 1 (1965).

12) J. Konnert and D. Britton, Inorg. Chem., 5, 1193 (1966).

13) P. Andersen, B. Klewe, and E. Thom, Acta Chem. Scandi., 21, 1530 (1967).

14) D. A. Bekoe, P. K. Gantzel, and K. N. Trueblood, Acta Crystallogr., 22, 657 (1967).

15) A Streitwieser,Jr., J. Amer. Chem. Soc., 82, 4123 (1960).

16) International Tables for X-Ray Crystallography, Kynoch Press, Birmingham (1962).

PART II

PHOTOPHYSICAL PROCESSES IN PHOTOCONDUCTIVE POLYMERS HAVING LARGE π-ELECTRON CONJUGATED SYSTEMS

INTRODUCTION

The photoconductive polymer is one of the most important material groups among the organic semiconductors. These polymers have been expected as materials for electrophotography, owing to the ability of photoconductive film formation, and many studies on the electric properties of the polymers have been reported, hitherto.[1)]

Among these polymers, the aromatic vinyl-polymers having large π-electron conjugated system as a side chain are most attractive ones, in view of their π-electron system which may be favorable to the photocarrier generation and its migration. Actually, it is well-known that poly-N-vinylcarbazole is utilized as a photoconductive material for electrophotography.[2)]

When a molecule having π-electron conjugated system is photo-excited in its electronic absorption region, at first the singlet excited state is commonly produced, and then the triplet excited state is followed from a part of the singlet excited state by intersystemcrossing.[3)] The photocarriers in these polymers are so far considered to be generated from the singlet

excited state migrating in the solid film of polymer.[1,4,5,6)]

In Part II of this thesis, the author investigated the behaviors of the photo-excited states of the photoconductive vinylpolymers having large π-electron system, by means of fluorescence and phosphorescence spectroscopies, as a fundamental research to understand the mechanism of the photocarrier generation in this kind of polymers. Aromatic vinylpolymers exhibit several kinds of the characteristic dual luminescence from these photo-excited states, together with normal fluorescence and phosphorescence. From the singlet excited state, an excimer fluorescence is found due to the formation of excited singlet dimer.[7)] The excimer fluorescence may be closely related to the photoconduction in the polymers, because the excimer forming site may act as an energy trap for the migration of singlet excited state.[8,9)] Chapter 1 of this part, therefore, will deal with the excimer formation in the vinylpolymers having large π-electron conjugated system. By contrast, little attention has been paid to the contribution of the triplet excited state to the photoconduction in these polymers. In polyvinylnaphthalene, a delayed fluorescence produced by triplet - triplet annihilation was observed at 77°K, which demonstrated the migration of the triplet excited state along the polymer chain.[10,11,12,13)] Therefore, the behavior of the triplet excited state in one of the most photoconductive polymer, PVCz, have been investigated in Chapter 2 of this part.

References

1) K. Okamoto, S. Kusabayashi, and H. Mikawa, Kogyo Kagaku Zasshi, 73, 1351 (1970).

2) K. Morimoto, Y. Murakami, and M. Ikeda, National Technical Reports, 15, 125 (1969).

3) J. B. Birks, "Photophysics of Aromatic Molecules", Wieley-Interscience, London (1970).

4) K. Okamoto, S. Kusabayashi, and H. Mikawa, Bull. Chem. Soc. Japan, 46, 1948 (1973).

5) K. Okamoto, S. Kusabayashi, and H. Mikawa, ibid., 46, 2324 (1973).

6) K. Okamoto, S. Kusabayashi, and H. Mikawa, ibid., 46, 2613 (1973).

7) See the references (1) - (6) in Chapter 2 of Part II of this thesis.

8) K. Klöpffer, J. Chem. Phys., 50, 2337 (1969).

9) K. Okamoto, A. Yano, S. Kusabayashi, and H. Mikawa, Bull. Chem. Soc. Japan, in Press.

10) R. F. Cozzens and R. B. Fox, J. Chem. Phys., 50, 532 (1969).

11) R. B. Fox.and R. F. Cozzens, Macromolecules, 2, 181 (1969).

12) R. B. Fox, T. R. Price, and R. F. Cozzens, J. Chem. Phys., 54, 79 (1971).

13) R. B. Fox, T. R. Price, R. F. Cozzens, and J. R. McDonald, ibid., 57, 2284 (1972).

Chapter 1

EXCIMER FORMATION IN POLYMERS

Introduction

Excimer fluorescence is an emission from the singlet excited dimer which is stabilized by the interaction between an electronically excited chromophore and an identical nearby chromophore in its ground state. Aromatic vinylpolymers such as polystyrene,[1,2] and polyvinylnaphthalene,[3,4,5,6] show excimer fluorescence in addition to the ordinary monomer fluorescence. In aromatic polymers having photoconductivity, the excimer formation may play an important role in the photocarrier generation, because it acts as an energy trap for the singlet excited state.[7,8] The excimer fluorescence may give some significant informations about the behavior of the singlet excited state in polymers. Moreover, it is interesting to elucidate the excimer formation of these polymers in relation to molecular motion or conformation of the polymer chain in solution.[9]

However, the mechanism of the excimer formation in polymer systems does not seem to be clarified well. Especially, it is fairly difficult to decide whether the excimer formation in dilute polymer solution occurs between two neighboring chromophores at a distance of three carbon atoms of the main chain, or between two chromophores in far distant positions in the same polymer chain. Therefore, this problem is particularly important in order to understand the behavior of the singlet excited state in polymers.

In this chapter, the author reports the new observations of excimer fluorescences of several photoconductive aromatic vinylpolymers having large π-electron systems. The author also discusses the excimer forming site of these polymers in solution using following three methods ; (i) the fluorescence study on the corresponding model compounds of the polymers in concentrated solution, (ii) the fluorescence study on the copolymers including 1:1 alternating copolymers in which each chromophore is not at neighboring positions, (iii) the study of the solvent effect on the excimer fluorescence.

Experimental

Materials. The samples of poly-1-vinylpyrene (PVPy)[10], poly-1-pyrenylmethylvinylether (PPMVE)[11], poly-9-vinylacridine (PVAc)[12], and N-vinylcarbazole - fumaronitrile (1:1) alternating copolymer (PVCz/FN)[13] were prepared in the author's laboratory. Polt-N-vinylcarbazole (PVCz) was obtained by radical polymerization using 2,2'-azobisisobutyronitrile (AIBN) as an initiator

Alternating copolymer of 1-vinylpyrene and maleic-anhydride was prepared by radical copolymerization. Equimolar amounts of vinylpyrene and maleic-anhydride in benzene solution containing 1 mol% AIBN were polymerized for an hour at 80°C. Polymer was isolated by pouring the reaction mixture into a large excess of dry petroleum ether, and the precipitate was collected and washed with dry ether. Polymer was purified three times by reprecipitation from tetrahydrofuran (THF) - petroleum ether. This polymer was identified to be 1-vinylpyrene - maleic-anhydride (1:1) alternating copolymer (PVPy/MAh) by the results of elemental analysis and its IR spectrum. Elemental analysis shows C:79.55, H:4.54 %, which agree with the calculated

values for 1:1 copolymer (C:80.9, H:4.3 %). The IR spectrum of this copolymer exhibits the relatively strong absorption bands at 1770 and 1220 cm^{-1} due to succinic acid anhydride and at 720, and 840 cm^{-1} due to pyrene ring, and the charactreristic absorption of vinyl group in 1-vinylpyrene disappears explicitly in polymer. The identification of the alternating 1:1 copolymer was also confirmed by the fact that 1:1 copolymer was obtained even when the ratio of monomer feed was changed. The molecular weight of the copolymer thus obtained is about 1700, corresponding to the pentamer.

The random copolymer of 1-vinylpyrene and N-vinylcarbazole was prepared with AIBN or BF_3-etherate catalyst in toluene at room temperature. The polymer composition was determined by the elemental analysis.

All polymers were purified by reprecipitation at least three times. N-ethylcarbazole (EtCz), 1-ethylpyrene (EtPy), and 9-ethylacridine (EtAc) were prepared in the author's laboratory. The solvents used were purified by ordinary method.

Measurements. Emission spectra were measured with a Hitachi MPF model 3 spectrophotofluorometer, equipped with a xenon arc source and an R-446 photomultiplier tube. Spectra were uncorrected for either source output or detector response. Lifetime measurements were carried out by pulse method with excitation of N_2 gas laser (excitation; 337 nm, 5 nsec half-width).

Results

PVCz and its related compounds.

PVCz. The fluorescence spectra of PVCz in 2MTHF-THF solution at various temperatures are shown in Fig. 1-1. These spectra are identical with those reported in the literature.[14] In fluid solution, PVCz shows both excimer

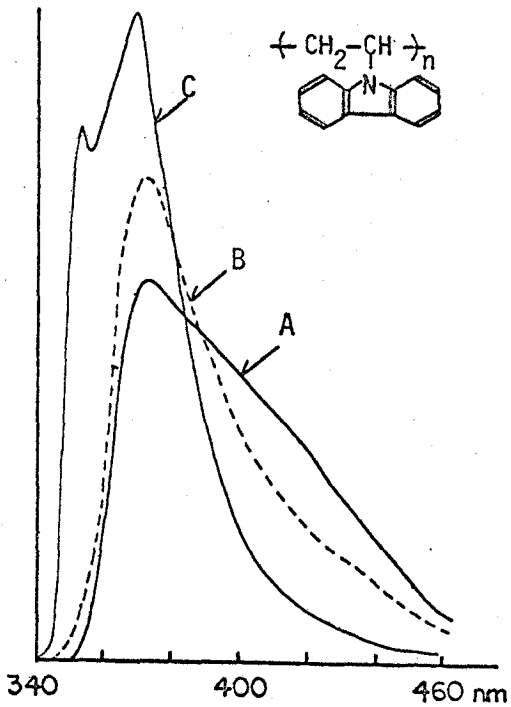

Fig. 1-1. Emission spectra of polyvinylcarbazole 8×10^{-4} mol/l solution in MTHF-THF. A; 300°K, B; 195°K, C; 77°K.

fluorescence around 420 nm and monomer fluorescence at 360 nm. At 77°K, only monomer fluorescence is observed, and excimer emission have no appreciable intensity. This is due to the immobility of carbazyl groups in rigid solution at 77°K. The lifetimes of the excimer fluorescence and monomer fluorescence are about 40 and 20 nsec, respectively.

VCz-FN alternating copolymer. As shown in Fig. 1-2, the alternating copolymer of VCz-FN shows no excimer fluorescence, contrary to PVCz. This fact was confirmed by the lifetime measurements (Fig. 1-2). The fluorescence of the copolymer has an exponential decay with the lifetime of about 25 nsec not only at 350 nm but also at 420 nm, and indicates the absence of emission with longer lifetime.

EtCz. EtCz shows no excimer fluorescence even in concentrated solution.

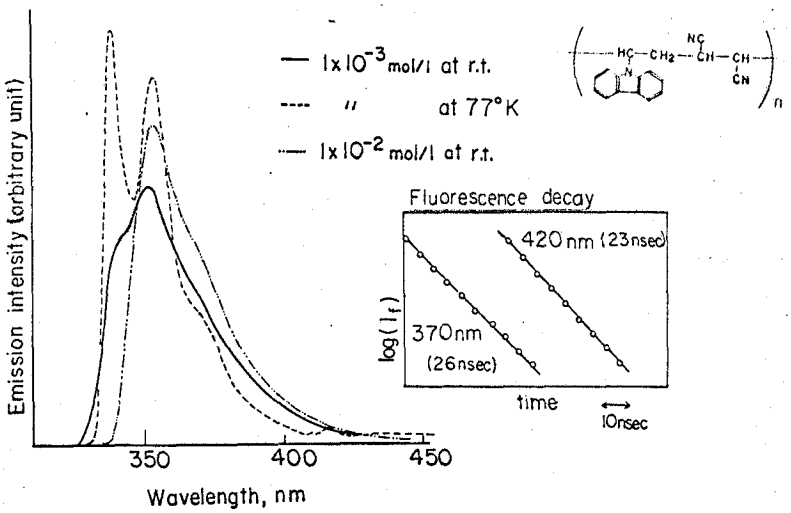

Fig. 1-2. Fluorescence spectra and fluorescence decays of VCz-FN alternation copolymer in 2MTHF-THF solution.

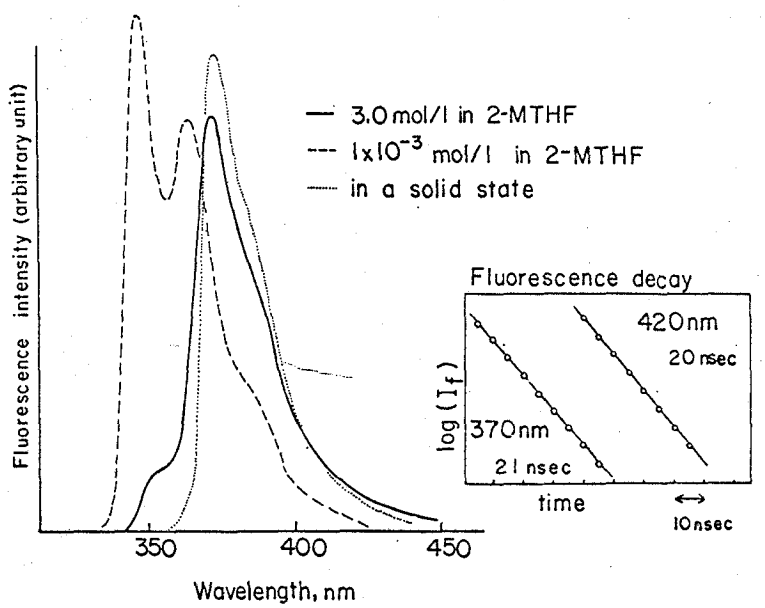

Fig. 1-3. Fluorescence spectra and fluorescence decays of N-ethylcarbazole.

The fluorescence spectra of EtCz in solution and in the solid state are given in Fig. 1-3, together with the fluorescence decay in 3 mol/l solution. The disappearance of the shorter wavelength part of the monomer fluorescence in concentrated solution and in the solid state is due to the reabsorption of the fluorescence. The lifetime of the fluorescence in 3 mol/l solution is constant (25 nsec) in the region of 370 - 430 nm, This result also supports the spectral observation of the absence of excimer fluorescence in EtCz.

PVPy and its related compounds.

PVPy. The fluorescence spectra of PVPy in dilute solution at various temperatures are depicted in Fig. 1-4. At room temperature, only a structureless broad emission band was observed around 480 nm, having the lifetime of 160 nsec. This emission is assigned to the excimer fluorescence of PVPy. The monomer fluorescence of pyrene was not observed in fluid solution, but observed in rigid solution at 77°K. When cyclohexane, a poor solvent for the polymer, was added into the THF solution of PVPy, the excimer emission

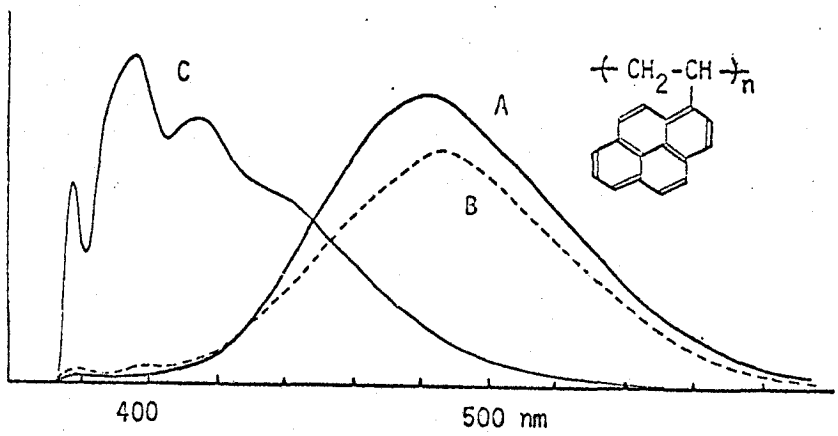

Fig. 1-4. Emission spectra* of poly-3-vinylpyrene 8×10^{-4} mol/l solution in MTHF-THF. A; 300°K, B; 195°K, C; 77°K.

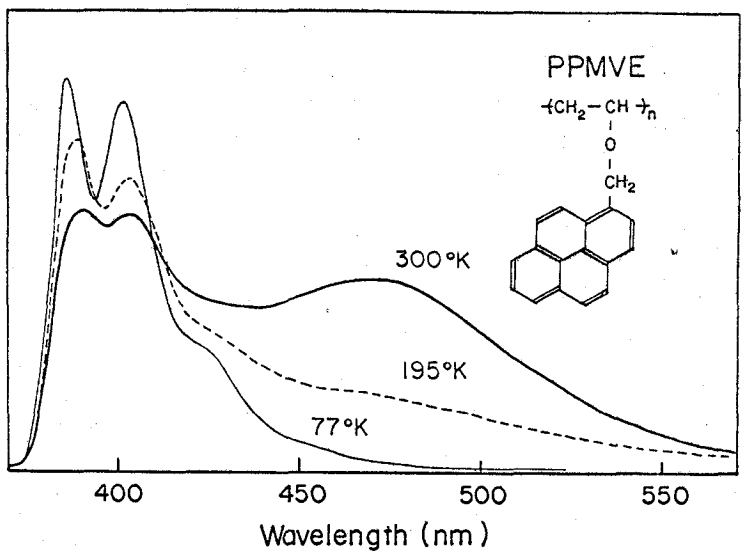

Fig. 1-5. Emission spectra of poly-1-pyrenylmethylvinylether 8×10^{-4} mol/l solution in 2MTHF-THF.

shows no appreciable change.

PPMVE. As shown in Fig. 1-5, PPMVE shows not only excimer fluorescence but also monomer fluorescence in the region of 400 nm in fluid solution. The excimer fluorescence had the lifetime of 66 nsecwhich is much shorter than that of PVPy. In the case of PPMVE, the excimer emission band decreases gradually in intensity with increasing of the monomer emission band as the temperature gets lower, and finally in rigid solution at 77°K, excimer fluorescence shows no appreciable intensity. Since in this polymer the pyrenyl grougs are not connected directly to the skeltal chain of the polymer, the excimer formation is more difficult than in PVPy. The solvent effect on the fluorescence was also not observed in this polymer.

VPy-MAh alternating copolymer. The fluorescence spectra of PVPy/MAh in 10^{-3} mol/l 2MTHF-THF solution at various temperatures are depicted in Fig. 1-6. In the spectrum at room temperature, the excimer fluorescence has approximately the same intensity with that of the monomer fluorescence. This is in sharp contrast with the observation in VCz alternating copolymer. The

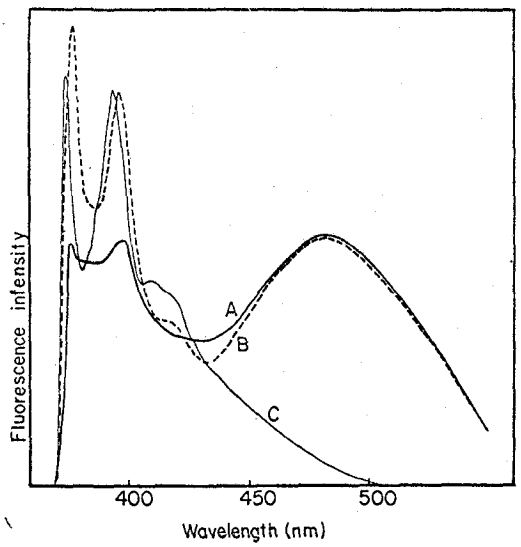

Fig. 1-6. Emission spectra of VPy-MAh alternating copolymer 1×10^{-3} mol/l 2MTHF-THF solution.
(A): 300°K, (B): 213°K, (C): 77°K.

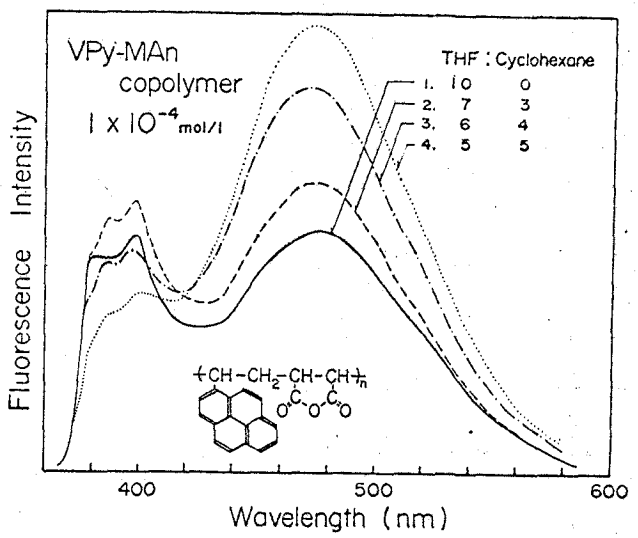

Fig. 1-7. Solvent effect of the fluorescence of VPy-MAh alternating copolymer.

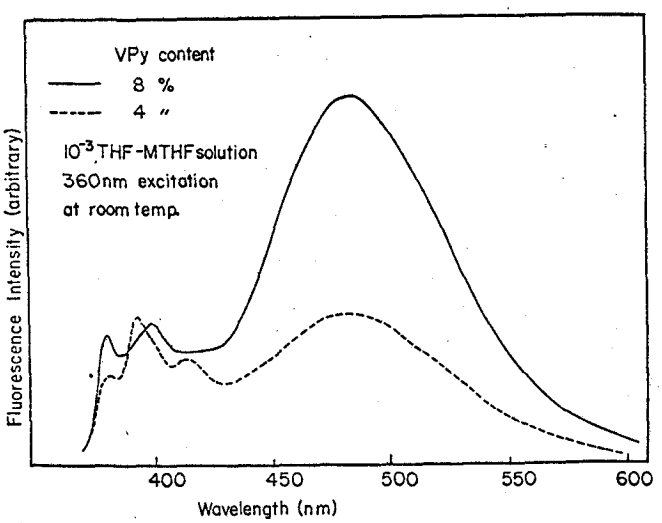

Fig. 1-8. Fluorescence spectra of VPy-VCz random copolymers.

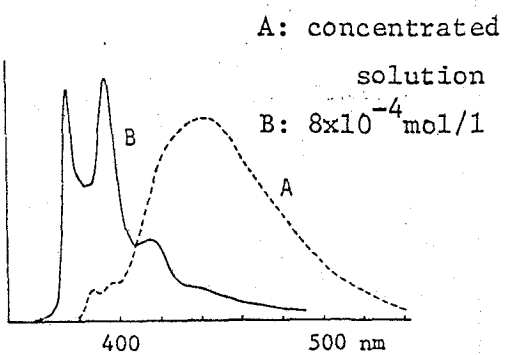

Fig. 1-9. Fluorescence spectra of 1-ethylpyrene in THF solution at room temp.

lifetime of the excimer band in PVPy/MAh is 150 nsec, which is quitely same with that of PVPy. The fluorescence band of this copolymer does not show significant temperature dependence in the region of 300°K - 200°K, but in rigid solution at 77°K excimer fluorescence exhibits no intensity. The variation of the concentration between 10^{-2} - 10^{-5} mol/l gave no change in the fluorescence spectrum, which indicates that the excimer formation is due to the intrachain interaction of two chromophores. Fig. 1-7 shows the fluorescence spectra of this copolymer in various compositions of THF and cyc cyclohexane at 10^{-4} mol/l at room temperature. The fluorescence spectra of this copolymer is considerably affected by the nature of the solvent. As the fraction of cyclohexane increased, the intensity of the excimer fluorescence showed a considerable increase. This may be caused by the result of the deformation of the polymer chain in moor poor solvent.

VPy-VCz random copolymers. In Fig. 1-8 are shown the fluorescence spectra of two kinds of VPy-VCz random copolymers having 8, and 4 % VPy in the copolymer, respectively. When the content of VPy in the copolymer is more than approximately 10 %, the fluorescence band predominantly consists of the excimer fluorescence of pyrene. The copolymer containing VPy about 8 %, shows the monomer fluorescence of pyrene with appreciable intensity, but even in the case of VPy content of only 4 %, the excimer fluorescence is still observed with fairly large intensity. This fact suggests that this copolymer has a similar structure to block-like copolymer, and that the excimer formation occurs easily if two pyrene rings are neighboring to each other.

EtPy. The concentration dependence of the fluorescence spectrum of EtPy, a model compound of PVPy, is shown in Fig. 1-9. In concentrated solution, EtPy easily formed excimer state, and the monomer fluorescence was quenched simultaneously.

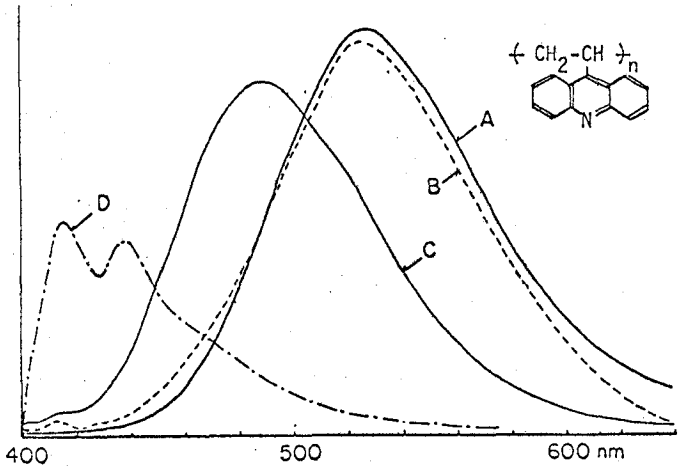

Fig. 1-10. Emission spectra* of poly-9-vinylacridine and 9-ethylacridine. A; 2×10^{-4} mol/l PVAc in $CHCl_3$-5%EtOH at 300°K, B; 195°K, C; 77°K, and D; 10^{-3} mol/l EtAc at 300°K.

PVAc and its related compound.

In Fig. 1-10 are shown the emission spectra of PVAc in 10^{-3}mol/l $CHCl_3$ solution at various temperatures, together with the emission spectrum of EtAc as a model compound of PVAc in 10^{-3}mol/l THF solution. In the case of PVAc, only excimer fluorescence can be observed in the fairly longer wavelength region of 525 nm with the lifetime of 30 nsec. In the film sample the same emission spectrum only consisting of excimer fluorescence was obtained. The temperature dependence above 195°K is quite similar to those of PVPy, but at 77°K the emission spectrum still consists predominantly of excimer fluorescence whose intensity maximum slightly blue-shifts at 500 nm. Since chloroform solidifies into crystalline state under the melting point of -63.5°C, this may be due to the excimer site being frozen by solidification of solvent at relatively high temperature.

Discussion

The excimer forming site in polymer system has not yet been made clear in both solution and solid film. An exceptional case is polyacenaphthylene. In this polymer, the excimer can be considered to be formed between two chromophores in far distance, since two adjacent naphthalene groups cannot be arranged with the planes of the aromatic rings parallel to each other within the distance for excimer formation. In other polymers such as polystyrene and polyvinylnaphthalene, the excimer formation is considered to occur between two neighboring chromophores, but this has never yet been proved. As mentioned above section, the author observed new excimer emissions in some photoconductive polymers having large pendant π-electron conjugated systems. The excimer forming site in solution of these polymers can be made clear by the results of (i) a model compound of the polymer in concentrated solution, (ii) random and alternating copolymers, (iii) solvent effect on the excimer emission.

First, the author would like to discuss the excimer formation in carbazole system. VCz-FN alternating copolymer, in which no carbazole chromophores are separated by a main chain segment of three carbon atoms, does not exhibit excimer fluorescence, although the local concentration of chromophores in the polymer chain is considered to be sufficiently high. N-ethylcarbazole does not also show the excimer fluorescence even in high concentrated solution as much as generally observed in other low molecular aromatic hydrocarbon compounds. These facts indicate that in carbazole system the excimer state cannot be produced even if the local concentration chromophores becomes very high. Namely, there are no excimer formation both between two nearby chromophores belonging to the different polymer chain and between two eventually nearby chromophores in the far distance along the

polymer chain.

However, Klopffer reported that the excimer fluorescence could be observed in the case of 1,3-dicarbazolylpropane, a dimeric model compound of PVCz,[15] and actually, the author also observed the excimer fluorescence of this compound. In this compound, the carbazole chromophores are separated by three carbon atoms just as in PVCz. Therefore, it can be concluded that in carbazole system two carbazole rings, only when they are connected to the alkyl main chain separating three carbon atoms, can form the excimer state which has a sandwitch arrangement of chromophores. In other words, this corresponds to the intramolecular excimer formation between the nearest neighbor chromophores.

On the other hand, in pyrene system, the situation is more complicated, because both 1-ethylpyrene and VPy-MAh (1:1) alternating copolymer emit the excimer fluorescence. The copolymer of VPy-MAh has the structure in which each pyrene group is separated by maleic anhydride unit with rigid skelton. The observed remarked solvent effect on the excimer fluorescence perhaps due to the deformation of this copolymer chain, suggests that the excimer formation occurs even between two chromophores in fairly far distance.

In PVPy, therefore, the excimer formation between non-neighboring chromophores along the polymer chain seems to be possible. However, on the basis of the facts that PVPy shows no solvent effect on the emission spectrum, and that in the random copolymer of VPy-VCz containing only 4 % of VPy, the excimer fluorescence of pyrene has a fairly large intensity, two neighboring pyrene groups easily produce the excimer state in PVPy.

In acridine system, the concentrated solution of EtAc does not exhibit the excimer fluorescence, and only PVAc shows the excimer fluorescence. This situation is quite similar to the case of carbazole system. Therefore, the excimer formation of PVAc probably takes place between two nearest neighbor-

chromophores separated by a main chain segment of three carbon atoms.

Thus, in the vinylpolymers having large π-electron conjugated system, the excimer formation occurs by the interaction between two adjacent chromophores. Such an excimer formation may act as an energy trap for the singlet excited state, and consequently may restrict the migration of singlet exciton. The photocarriers in these polymers are considered to be produced extrinsically from the singlet excitons migrating in the polymer film. Therefore, the excimer formation may be unfavorable to the photocarrier generation. Nevertheless, the photoconductive polymers emit excimer fluorescence with significantly high intensity. Moreover, Okamoto et al.[16] reported that no photoconduction was found in VCz-FN alternating copolymer which, as mentioned above, does not show excimer fluorescence at all. These facts suggest that the sufficiently strong interaction between two adjacent chromophores which enable the excimer formation, is necessary for the charge carrier migration in these polymers.

Summary

New observations of the excimer fluorescences of several photoconductive polymers having large π-electron conjugated system was obtained. On the basis of the results on the model compounds of the corresponding polymers, on the copolymers including 1:1 alternating copolymer, and on the solvent effect of the excimer fluorescence, the excimer forming site in solution of these polymers was discussed. Consequently, the excimer formation almost occurs between two neighboring chromophores separated by three alkyl cabon atoms. The interaction which enable the excimer formation between two adjacent chromophores seems to be unfavorable to the carrier generation in the photoconduction, but may be necessary for the carrier

migration along the polymer chain.

References

1) S. Yanari, T. A. Bovey, and R. Lumry, Nature, 200, 242 (1963).

2) F. Hirayama, J. Chem. Phys., 42, 3163 (1965).

3) M. T. Vala, J. Haebig, and S. A. Rice, J. Chem. Phys., 43, 886 (1965).

4) C. David, W. Demarteau, and G. Geuskens, European Polymer J., 6, 1397 (1970).

5) R. B. Fox, T. R. Price, R. F. Cozzens, and J. R. McDonald, J. Chem. Phys., 57, 534 (1972).

6) Y. Nishijima, M. Yamamoto, S. Katayama, K. Hirota, Y. Sasaki, and M. Ts Tsujisaki, Perts. Progr. Polymer Phys. Japan, 15, 445 (1972).

7) W. Klopffer, J. Chem. Phys., 50, 2337 (1969).

8) K. Okamoto, A. Yano, S. Kusabayashi, and H. Mikawa, Bull. Bhem. Soc. Japan, in press.

9) Y. Nishijima, J. Polymer Sci., Part C, 31, 353 (1970).

10) K. Tanikawa, H. Hirata, S. Kusabayashi, and H. Mikawa, Bull. Chem. Soc. Japan, 42, 2406 (1969).

11) S. Yoshimoto, K. Okamoto, H. Hirata, S. Kusabayashi, and H. Mikawa, ibid., 46, 358 (1973).

12) S. Moriwaki, S. Kusabayashi, and H. Mikawa, Chem. Comm., 407 (1971).

13) Y. Shirota, A. Matsumoto, and H. Mikawa, Polymer J., 3, 643 (1972).

14) C. David, M. Piens, and G. Geuskens, European Polymer J., 8, 1291 (1972).

15) W. Klopffer, Chem. Phys. Letters, 4, 193 (1969).

16) K. Okamoto, K. Kato, K. Murao, S. Kusabayashi, and H. Mikawa, Bull. Chem. Soc. Japan, 46, 2613 (1973).

Chapter 2

TRIPLET EXCITON MIGRATION IN POLY-N-VINYLCARBAZOLE

Introduction

Poly-N-vinylcarbazole (PVCz) shows the largest photoconduction among the polymers investigated so far.[1] The carriers of photoconduction in this polymer have been considered to be generated from its singlet excited state. Recently, Okamoto et al. have investigated the mechanism of electrical conduction in PVCz in detains,[2-6] and they have indicated that the photocarriers are produced extrinsically by the interaction between the electron-accepting impurities and the singlet excitons of PVCz migrating in the polymer film. The migration of singlet excitons in PVCz film have been studied by Klöpffer[7] and Okamoto et al.[8] They suggested that ca. 10^3 of carbazole units are covered with a singlet exciton during its lifetime, and that the excimer forming sites in the solid film act as the most important trap sites for the singlet excitons. Such excimer forming sites in this polymer have been characterized in the previous chapter.

As for the triplet excited state in PVCz, however, no spectroscopic study has been reported yet. Triplet excitons should have much longer lifetime than singlet excitons. In aromatic molecular crystals it was reported that the triplet exciton migrates very fast, and can cover about 10^9 - 10^{12} molecules/sec.[9,10,11] Therefore, the triplet exciton migration may be possi-

ble in the polymer chain, which is considered to be a one-dimensional crystal. It is particular interesting to investigate the spectroscopic behaviors of the excited triplet state of PVCz from the view point whether the triplet excitons contributes to the process of the photocarrier generation, or not.

Fox et al. demonstrated the triplet exciton migration in poly-1-vinylnaphthalene both in rigid solution at 77°K,[12,13,14] and in the solid film.[15] They observed the delayed fluorescence caused by a triplet-triplet annihilation between two migrating triplet excitons along the polymer chain, and suggested that the trap sites in the polymer may significantly affect the T-T annihilation. The similar results were obtained for poly(adenilic acid) in rigid solution at 77°K.[16,17,18] In this case, the triplet excitons migrate over approximately 100 bases, and are readily trapped by the lower energy sites.[17] This value of ca. 100 bases seems to be much smaller than that in aromatic crystals. As mentioned in the previous chapter, between two adjacent chromophores in the aromatic vinylpolymers is there an interaction which enables to form the excimer state. This interaction may be effective on the triplet exciton migration.

In this chapter, the triplet exciton migration in PVCz was investigated in rigid solution at 77°K, and the results will be compared with those on the alternating copolymer of N-vinylcarbazole - fumaronitrile, and N-ethylcarbazole, i.e., a model compound of PVCz in its concentrated solution.

Experimental

Materials. The homopolymer of VCz were prepared with AIBN catalyst in benzene. The alternating copolymer of VCz - fumaronitrile (PVCz/FN), and N-ethylcarbazole (EtCz) were prepared in the author's laboratory. Naphthalene was purified by recrystallization from ether solution, vacuum sublimation and vacuum distillation. The polymers and the solvents used were purified

as described in the previous chapter.

Measurement. All polymers having adequate concentrations with 2-methyltetrahydrofuran (2MTHF) - THF solutions in a pyrex tube (2mm diameter) were sealed in vacuum. The measurements of the emission spectra were carried out as described in Chapter 2 of Part I in this thesis. Phosphorescence lifetimes were traced on an X-t recorder, and delayed fluorescence decays were determined from oscilloscope traces. The exciting light intensity was controlled by neutral filters.

Results

PVCz. In Fig. 2-1 are shown the total and delayed emission spectra of PVCz (M.W. = 21000) in 2MTHF-THF rigid solution at 77°K. The delayed emission in longer wavelength region (> 410 nm), which has an exponential decay with the lifetime of 7.6 sec, is identified with phosphorescence from the carbazole chromophores in PVCz. The delayed emission band around 360 nm

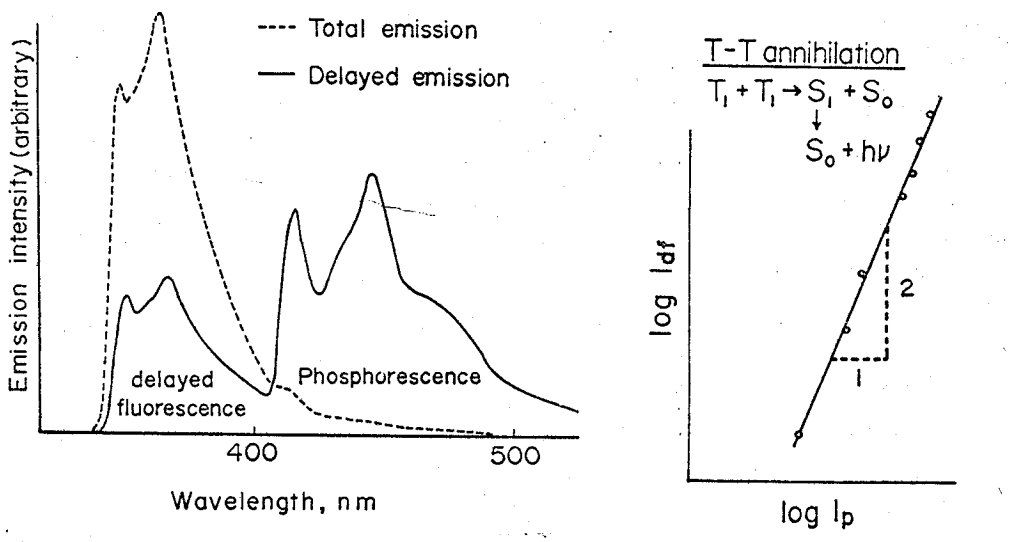

Fig. 2-1. Emission spectra of poly-N-vinylcarbazole in rigid solution of 2MTHF-THF at 77°K, and the light intensity dependence of delayed emissions of poly-N-vinylcarbazole. [1×10^{-3} mol/l].

can be assigned to the delayed fluorescence, because this band locates in the same position as the normal prompt fluorescence, and has a long lifetime about 20 msec. The light intensity dependence study revealed that the delayed fluorescence intensity increased as the square of the phosphorescence intensity, as shown in Fig. 2-1. This fact indicates that the delayed fluorescence is the biphotonic process. Triplet quenchers, such as piperylene and naphthalene, quenched in high efficiency both fluorescence and phosphorescence emissions. Therefore, this delayed fluorescence is emitted from the singlet excited state generated as the result of triplet - triplet annihilation of two triplets in a polymer chain. The experimental result that the lifetime of the delayed fluorescence is much shorter than a half of the phosphorescence lifetime, is also found in polyvinylnaphthalene[12] and poly(adenylic acid) [16] This is characteristic of T-T annihilation in aromatic vinylpolymers.

[Quenching by naphthalene] The delayed emission of PVCz is effectively quenched by naphthalene. In carbazole - naphthalene system, whose energy

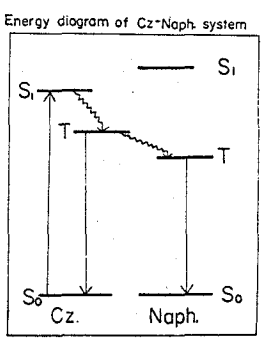

Fig. 2-2 (a).
Energy diagram of carbazole-naphthalene system.

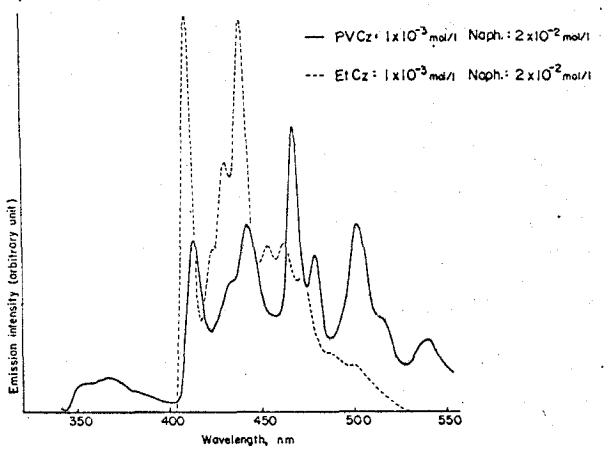

Fig. 2-2(b). Delayed emission spectra of PVCz and EtCz in the presence of naphthalene.

diagram is shown in Fig. 2-2(a), the sensitized phosphorescence of naphthalene must be observed by the excitation of carbazole, if triplet - triplet energy transfer occurs from carbazole to naphthalene. In Fig. 2-2(b) are shown the delayed emissions of 10^{-3} mol/l solutions of PVCz and of EtCz, both containing 2×10^{-2} mol/l of naphthalene. In the case of EtCz, the phosphorescence of EtCz was little quenched and no sensitized phosphorescence of naphthalene was observed. However, the delayed emission of PVCz was considerably quenched, and the phosphorescence of naphthalene appeared clearly around 460 - 520 nm. These results proved that the triplet state of PVCz is migrating in a polymer chain as an exciton.

The Stern-Volmer plots for the intensities of phosphorescence and delayed fluorescence of PVCz are given in Fig. 2-3. Although the both plots deviate from the linear relation at high concentration of the quencher, the plot for the phosphorescence shows approximately linear dependence and that for the delayed fluorescence shows a second order dependence upon the naphthalene concentration, respectively. This result implies that two triplet excitons are necessary for the T-T annihilation. The lifetime of the delayed fluorescence decreased considerably with the quencher concentration, whereas the phosphorescence lifetime remained unchanged independently of the naphthalene concentration, in spite of the decrease of the phosphorescence intensity. The phosphorescence of PVCz, therefore, is emitted from trap sites of triplet excitons, and not from the free

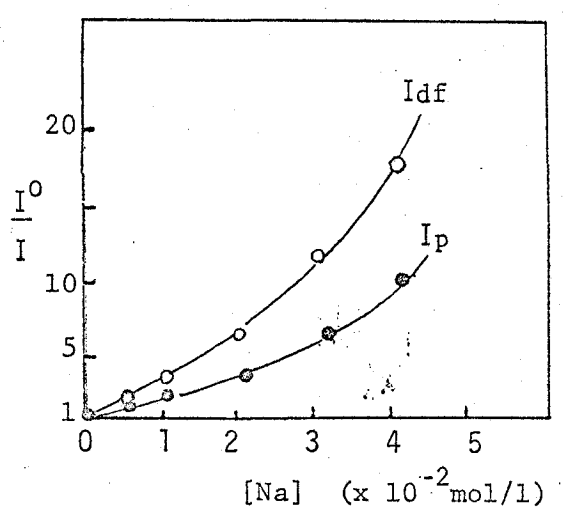

Fig. 2-3. Stern-Volmer plots for the delayed emissions of PVCz in the presence of Naphthalene. [PVCz] = 1×10^{-3} mol/l

migrating triplet excitons, and naphthalene can quench only the freely migrating triplet excitons.

[Molecular weight dependence] Table 2-1 gives the intensity ratio (I_{df}/I_p) of delayed fluorescence and phosphorescence, and the lifetime (τ_{df}) of delayed fluorescence of PVCz, each having different molecular weight.

Table 2-1 Molecular weight dependence of delayed fluorescence of PVCz.

Sample	M. W.	I_{df}/I_p[1]	τ_{df} (msec)
PVCz(commercial)[2]	> 100,000	10	12 - 15
PVCz (A)	80,000	3.6	18 - 20
PVCz (B)	35,000	0.9	20
PVCz (C)	21,000	0.5	28 - 30
PVCz (D)	14,000	0.4	-
PVCz (E)	8,000	0.0	-
PVCz (F)	5,000	0	-

[1] measured with almost constant excitation light intensity.
[2] Luvican M-170 (BASF Co. Ltd.).

Under an ordinary light intensity condition (150 w Xe lamp, 340 nm excitation, excitation slit of 5 nm), the delayed fluorescence could not be detected with an appreciable intensity in the homopolymer with molecular weight less than about 10,000 (50 carbazole units). The intensity ratio (I_{df}/I_p) gradually increases with the increase of molecular weight, whereas the lifetime of delayed fluorescence slightly decreases.

VCz-FN alternating copolymer. The behavior of triplet exciton migration in in VCz-FN alternating copolymer is quite different from that in PVCz. The total and delayed emissions of VCz-FN copolymer (M.W. = 6,200) in 2MTHF-THF rigid solution at 77°K are shown in Fig. 2-4. The 0-0 band of the normal fluorescence of the copolymer is located at 339 nm, which is blue shifted

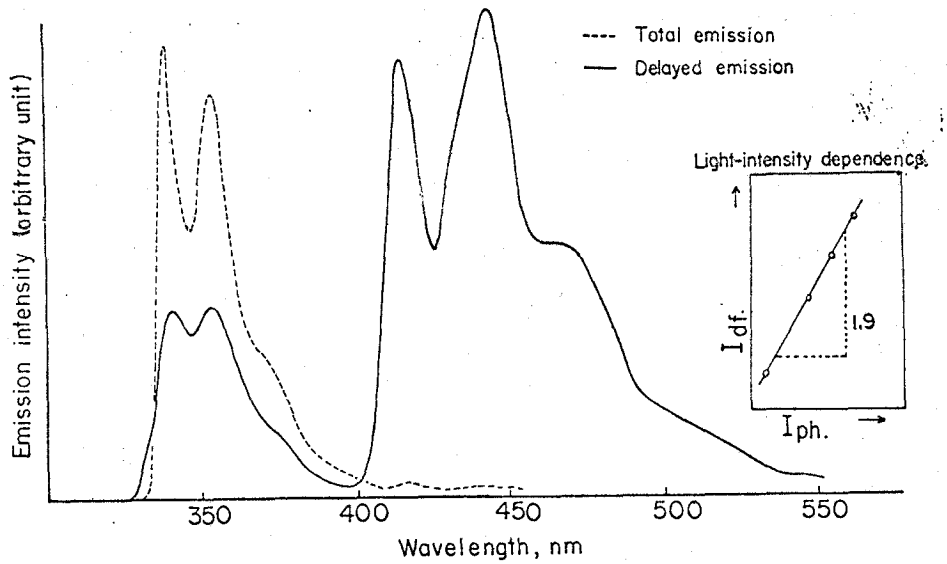

Fig. 2-4. Total and delayed emission spectra at 77°K for PVCz/FN in 1 x 10^{-3}mol/l 2MTHF-THF solution; excitation: 330 nm.

ca. 12 nm relative to that of PVCz. This blue shift may be caused by the effect of electron-withdrawing CN groups in FN unit. In the delayed emission spectrum of this copolymer, the delayed fluorescence was also observed as well as the phosphorescence from the carbazole units. The phosphorescence in this copolymer did not show such a large shift from that of PVCz as could be found in the delayed fluorescence.

The studies on the light intensity dependence and the quenching of the delayed emission indicate that the delayed fluorescence is also due to T-T annihilation in the polymer chain. The emission lifetimes, however, differ from those of PVCz. The decay curves of the delayed fluorescence and phosphorescence of PVCz/FN are drawn in Fig. 2-5. The phosphorescence exhibits a non-exponential decay with apparent lifetime of about 4.5 sec, which is considerably shorter than that of PVCz showing restrictively exponential decay. On the other hand, the delayed fluorescence of this copolymer has also marked non-exponential decay with the apparent lifetime of about 200 msec. This value of the lifetime is much longer than that of

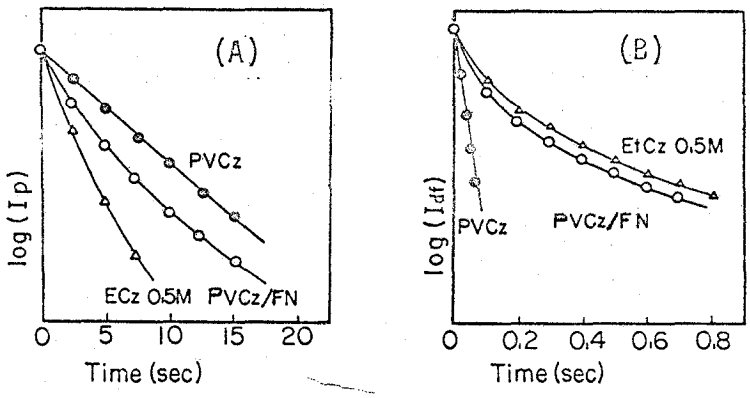

Fig. 2-5. Delayed emission decays of PVCz, PVCz/FN, and EtCz 0.5 mol/l in rigid solution at 77°K.
(A): phosphorescence decay, (B): delayed fluorescence decay.

PVCz. This results suggest that the migration of triplet exciton in the alternating copolymer is fairly slower than in the homopolymer.

[Quenching by naphthalene] Naphthalene effectively quenches the delayed emission of this copolymer, and alternatively the sensitized phosphorescence of naphthalene can be observed. The behavior of the quenching is different from that in the homopolymer. The Stern-Volmer plots of two delayed emission are given in Fig. 2-6. In the copolymer, the delayed fluorescence was quenched more effectively rather than the phosphorescence. In Figure 2-7 are shown the change in decay curve with the quencher concentration. The decay curves of both delayed fluorescence and phosphorescence are always non-exponential, and the apparent life-times become short with increasing

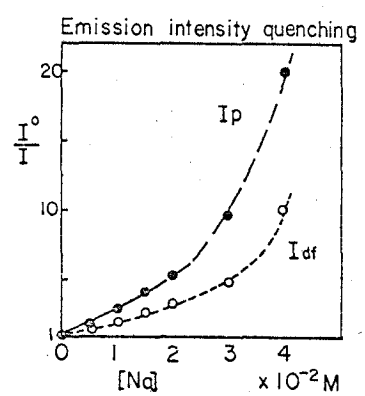

Fig. 2-6. Stern-Volmer plots for the delayed emissions of PVCz/FN in the presence of naphthalene.

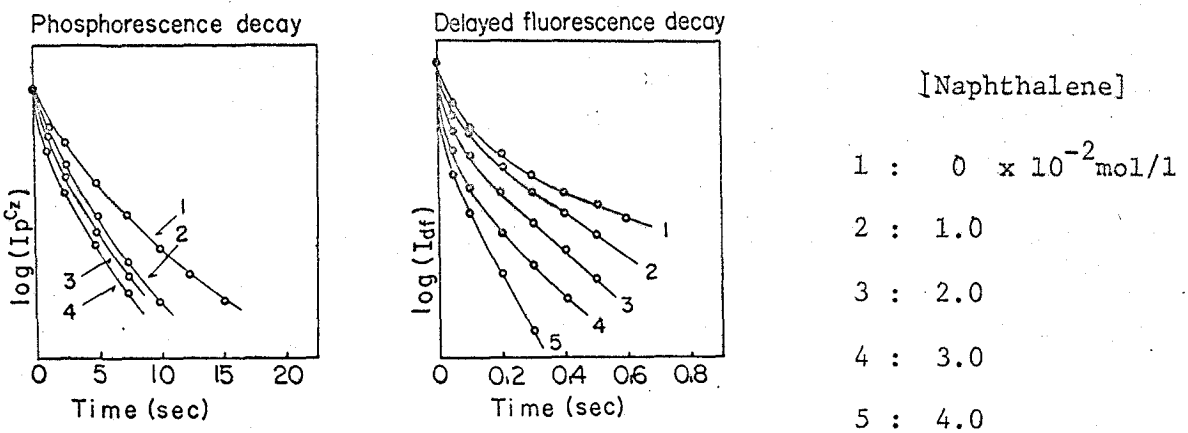

Fig. 2-7. The dependence of delayed emission decays of PVCz/FN on the concentration of naphthalene. [PVCz/FN] = 1 x 10^{-3}mol/l.

the concentration of naphthalene. The apparent lifetime and the intensity of delayed fluorescence in the presence of 4 x 10^{-2}mol/l of naphthalene decrease by factors of ca. 7 and 10, respectively, compared with those in the absence of the quencher. On the other hand, under the same condition the phosphorescence intensity is reduced by a factor of ca. 20, while the phosphorescence lifetime in the presence of 4 x 10^{-2}mol/l naphthalene is estimated to be 1.9 sec, being nearly a half of 4.5 sec in the absence of naphthalene. In PVCz the phosphorescence lifetime is 7.6 sec regardlessly of the quencher concentration. These experimental results suggest that in the alternating copolymer the phosphorescence emission may occur not only from the trapped triplet but also from the freely migrating triplet excitons, which can be quenched by naphthalene. Therefore, the rate of the free triplet migration of the copolymer is considered to be very slow, and comparable to the rate of the phosphorescence emission.

[Molecular weight dependence] The ratios, Idf/Ip, of four alternating copolymers of VCz-FN having different molecular weight were measured under

the constant light intensity condition, and the results are given in Table 2-2. The molecular weight does not seem to affect the delayed fluorescence of this copolymer, contrary to the case of VCz homopolymer. It is somewhat surprising that even in the copolymer with molecular weight of only 4,000 (ca. 15 carbazole units in a polymer chain), the delayed fluorescence can be observed with a significant intensity.

Table 2-2. Molecular weight dependence of the delayed fluorescence of PVCz/FN.

Sample	M.W.	Idf/Ip
PVCz/FN (A)	8,000	0.62
PVCz/FN (B)	6,200	0.65
PVCz/FN (C)	4,200	0.59
PVCz/FN (D)	4,000	0.83

EtCz. The delayed fluorescence of EtCz, a model compound of PVCz, in rigid solution at 77°K is not found in relatively low concentrations, but can be found in higher concentrations. In Fig. 2-8 are shown the delayed emission spectra of EtCz at 0.5 and 1 x 10^{-4} mol/l.. In 0.5 mol/l solution the delayed fluorescence due to T-T annihilation was observed. The delayed fluorescence can be observed in > about 0.25 mol/l solution under the present experimental condition, and in 0.5 mol/l the intensity ratio (Idf/Ip) is approximately comparable to that observed in VCz-FN alternating copolymers.

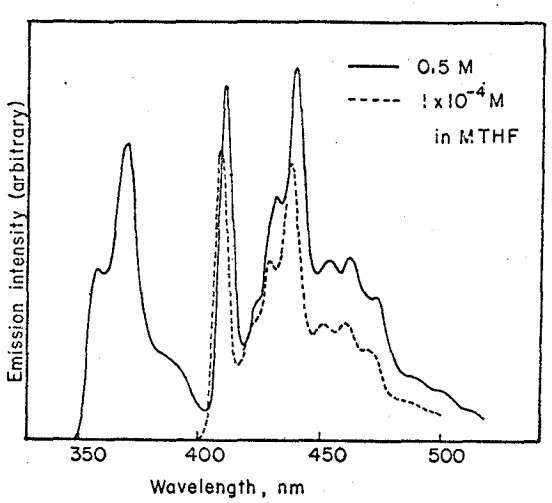

Fig. 2-8. Delayed emission spectra of N-ethylcarbazole in 2MTHF rigid solution at 77°K.

In 1 mol/l solution the delayed emission spectrum predominantly consists of the delayed fluorescence. The phosphorescence lifetimes in 10^{-4}, 10^{-1}, 0.25, 0.5, and 1.0 mol/l solutions are 7.6, 7.6, 7.2, 4.0, and 1.8 sec, respectively. The delayed fluorescence of 0.5 mol/l solution shows a marked non-exponential decay with a apparent lifetime of 1.9 sec, as shown in Fig. 2-5. The results in the case of 0.5 mol/l EtCz, therefore, are very similar to that of the alternating copolymer rather than that of the homopolymer.

Discussion

Parker indicated that a T-T energy transfer in rigid solution is possible at the distance less than 15 Å by electron exchange mechanism.[19] The rate of T-T energy transfer can be considered to depend on the distance between two chromophores, and the shorter is the distance, the easier the energy transfer can occur. In aromatic vinylpolymers, such as polyvinylnaphthalene and PVCz, triplet exciton migration may be nearest neighbor event. The distance between two carbazole ring in PVCz may be approximately 3 Å, whereas in the copolymer of VCz-FN, this may be at least 5 - 6 Å. Therefore, the rate of triplet exciton migration in the copolymer is expected to be fairly slower than in the homopolymer.

Triplet excitons in polymers produced from singlet excited state by intersystem-crossing are depleted by the following photophysical processes:

(1)	$Tf \longrightarrow Tt$		Trapping of free triplet exciton
(2)	$Tf + Tf \longrightarrow S_1 + S_0$		Tf-Tf annihilation
(3)	$Tf + Tt \longrightarrow S_1 + S_0$		Tf-Tt annihilation
(4)	$Tf \longrightarrow S_0 + h\nu_p$		Phosphorescence emission from Tf
(5)	$Tt \longrightarrow S_0 + h\nu_p$		Phosphorescence emission from Tt
(6)	$Tf + Q \longrightarrow S_0 + Q^*$		Quenching of free triplet

(7) $Tf + Q \longrightarrow S_0 + Q^*$ Quenching of trapped triplet

, where Tf and Tt are freely migrating and trapped triplet states, respectively, and Q represents triplet quencher.

Among these processes, the quenching of trapped triplets (precess 7) is negligible, because the concentration of the trap site may be much lower compared with that of the total carbazole units. The freely migrating triplet excitons of PVCz are almost depleted mainly via the processes of (1), (2), (3), and (6), before emitting the phosphorescence, since the rate of migration is considerably fast. In other words, the rate of the triplet exciton migration in PVCz is much larger than the rate of phosphorescence radiation, and therefore, the phosphorescence emission originates only from the trapped triplets. This consideration can be reasonably confirmed by the fact that the phosphorescence lifetime remains unchanged in various conditions of measurement. On the other hand, from the differences in the delayed fluorescence lifetime and in the steady-state concentration of free triplets between the homopolymer and the alternating copolymer, the rate of triplet exciton migration in the copolymer can be considered to be about 10 - 100 times slower than the homopolymer, and consequently the phosphorescence in the copolymer originate from both Tf and Tt. The phosphorescence from Tf must have significantly smaller lifetime than that from Tt (7.6 sec), because the other processes can compete for the depletion of Tf with the phosphorescence emission. The total phosphorescence decay, therefore, must be non-exponential, and its lifetime must be significantly shorter. The presence of the phosphorescence not only from Tf but also from Tt in the copolymer can be demonstrated by the facts that the phosphorescence lifetime is quenched by naphthalene and that the long lifetime component of the phosphorescence can be detected.

In the copolymer, the phosphorescence from both Tf and Tt are quenched

by naphthalene molecule. The quenching of τ_f occurs directly, but the quenching of τ_t probably occurs during the process of the trapping of free triplets (process 1). The decrease in the phosphorescence lifetime shown in Fig. 2-7 is caused by the former quenching process. The fact that in the copolymer the phosphorescence is more effectively quenched than the delayed fluorescence, may be accounted for by these dual quenching of phosphorescence by naphthalene. Thus, in the alternating copolymer, most of all τ_f may be depleted by the processes of (1), (2), (3), and (4), before reaching the end of the polymer chain which can be considered as a trapping site, and consequently, the molecular weight dependence is not observed in the copolymer. By contrast, the molecular weight dependence observed in the homopolymer can be understood in terms of the increase of free triplet concentration with the increase of molecular weight.

Although in the copolymer with molecular weight of only 4000, the total triplet concentration produced in a polymer chain is sufficient for the occurrence of T-T annihilation, it seems to be very strange that no delayed fluorescence is observed in the homopolymer having the molecular weight less than about 10,000. If the τ_f-τ_t annihilation (process 3) could take place, a delayed fluorescence would have to appear, because τ_t is available for 7.6 sec. The results in Table 2-1, therefore, suggest that T-T annihilation can only take place between two freely migrating triplet excitons, and that trapped triplets cannot participate in T-T annihilation. This consideration is supported by the fact that even when the exciting light intensity is so strong that the delayed fluorescence intensity is fairly large than that of the phosphorescence, the phosphorescence lifetime of PVCz still remains unchanged. If this consideration is true, a considerable part of triplet excitons in PVCz is easily trapped because of the large rate of migration, and cannot contribute to T-T annihilation. As the

molecular weight decreases, the concentration of free triplet excitons available for T-T annihilation becomes small and the delayed fluorescence cannot be observed with an appreciable intensity.

However, the reason why the trapped triplets are unable to participate in T-T annihilation in PVCz is unknown.

Assumed that the energy of the host triplet exciton level in PVCz is equal to the energy of the phosphorescence 0-0 band of EtCz (24,510 cm^{-1}), the depth of the triplet trap sites can be estimated from the 0-0 band of the phosphorescence of PVCz to be only 530 cm^{-1}. The energy of trapped triplet, therefore, may be sufficient for T-T annihilation. These trapping sites seem to be located at unique structures in the polymer, perhaps some are located at the end of the polymer chain, other at defects. The carbazole rings acting as these trapping sites may have different steric configuration from those of the majority of carbazole rings. If in order to take place T-T annihilation, particular steric configurations would be necessary between two interacting chromophores, the trapped triplet could not contribute to T-T annihilation.

It is well-known that P-type delayed fluorescence in rigid medium at 77°K produced by T-T annihilation can be observed with many aromatic hydrocarbons at their fairly high concentrations.[19] Also with EtCz, the delayed fluorescence was observed at 0.5 mol/l so that the intensity ratio of this emission to the phosphorescence was approximately the same with those observed in the copolymers or in the homopolymer with molecular weight of 20,000. The ratios of apparent lifetime of the delayed fluorescence to that of the phosphorescence were compared among these three cases, being about 0.4, 0.045, and 0.003 for EtCz, the copolymer, and the homopolymer, respectively. These values suggest that the alternating copolymer has the nature of both the monomer and the homopolymer. A most decisive difference

in T-T annihilation between the monomer and the homopolymer may be seen in the presence of the trap sites of triplet excitons in the homopolymer. In the alternating copolymer these trap sites may play a less important role in triplet exciton migration because of the slow rate of migration.

Thus, it has been shown that the triplet excited states can effectively migrate along the polymer chain. Therefore, it seems to be possible that the migrating triplet exciton produces the photocarrier by the interaction with the electron-accepting impurities present in the polymer film, as well as singlet excitons. The energy of the triplet excited state of atomatic molecules are usually much lower than that of the singlet excited state. However, in the case of PVCz, the energy difference between the singlet and triplet excited states is fairly small as compared with other aromatic compounds.

The halogenated PVCz such as poly-3,6,dichloro-N-vinylcarbazole, and poly-3,6,dibromo-N-vinylcarbazole, also show photoconduction and are utilized as a material for electrophotography.[20] These polymers seem to have higher triplet yield than PVCz, due to the heavy atom effect of the halogene atoms. Actually, Yokoyama et al. observed that in poly-3,6-dibromo-N-vinylcarbazole there appears only phosphorescence emission, and no emission from the singlet excited state.[21]

These facts suggest that the carrier generation from the triplet excited state is possible not only in the halogenated PVCz but also in PVCz.

Summary

In this chapter, the behavior of the triplet excited state of PVCz was investigated. New observations of the delayed fluorescence due to T-T annihilation between two migrating triplet excited states were obtained in

rigid solution at 77°K. Triplet exciton migration in PVCz was compared with those in VCz-FN alternating copolymer and in 0.5 mol/l EtCz, and consequently, The rate of triplet exciton migration is about 10 - 100 times faster in the homopolymer than in the copolymer, and in monomer. Tacking into consideration that the energy of the triplet state of PVCz are relatively high, and that the lifetime of triplet state is much longer than that of singlet state, the possibility was suggested that the triplet state produces the carriers in the photoconduction of PVCz, as well as singlet excited state.

References

1) K. Okamoto, S. Kusabayashi, and H. Mikawa, Kogyo Kagaku Zasshi, 73, 1351 (1970).

2) K. Okamoto, S. Kusabayashi, and H. Mikawa, Bull. Chem. Soc. Japan, 46, 1948 (1973).

3) K. Okamoto, S. Kusabayashi, and H. Mikawa, ibid., 46, 1957 (1973).

4) K. Okamoto, S. Kusabayashi, and H. Mikawa, ibid., 46, 2324 (1973).

5) K. Okamoto, K. Kato, K. Murao, S. Kusabayashi, and H. Mikawa, ibid., 46, 2883 (1973).

6) K. Okamoto, S. Kusabayashi, and H. Mikawa, ibid., 46, 2613 (1973).

7) W. Klopffer, J. Chem. Phys., 50, 2337 (1969).

8) K. Okamoto, A. Yano, S. Kusabayashi, and H, Mikawa, Bull. Chem. Soc. Japan, in Press.

9) G. W. Robinson and R. P. Frosch, J. Chem. Phys.,38 , 1187 (1969).

10) P. Avakian, E. Abramson, R. G. Kepler, and J. C. Caris, ibid., 39, 1127 (1963).

11) V. Ern, P. Avakian, and R. E. Merrifield, Phys. Rev., 148, 862 (1966).

12) R. F. Cozzens and R. B. Fox, J. Chem. Phys., 50, 532 (1969).

13) R. B. Fox and R. F. Cozzens, Macromolecules, 2, 181 (1969).

14) R. B. Fox, T. R. Price, and R. F. Cozzens, J. Chem. Phys., 54, 79 (1971).

15) R. B. Fox, T. R. Price, R. F. Cozzens, and J. R. McDonald, 57, 2284 (1972).

16) W. Longworth and M. D. C. Battista, Photochem. Photobiol., 1, 207 (1970).

17) J. Eisinger and R. G. Schulman, Proc. Natl. Acad. Sci. U.S., 55, 70 (1970).

18) C. Herene and W. Longworth, J. Chem. Phys., 57, 399 (1972).

19) C.A. Parker, "The Triplet State", 353, Cambridge University Press (1967).

20) H. Kitaichi, Electronics (Japan) 18, 1197 (1973); K. Morimoto, ibid., 17, 1370 (1972).

21) M. Yokoyama, M. Funaki, and H. Mikawa, Private Communication .

CONCLUSION

The purpose of this thesis is to present information with regard to the structures and the optical and electrical properties of two types of important material group among organic semiconductors.

In Part I, organic CT salts, that is, organic ionic compounds in which a CT interaction is present between two component ions, were picked up as a new organic material group. Several new organic CT salts composed of a pyrylium or thiopyrylium cation and a polycyano-acid anion (1,1,3,3-tetracyanopropenide, or tricyanomethanide) were synthesized.

The presence of CT interaction in these salts both in solution and in solid state, have been demonstrated by the observations of CT absorption (Chapter 1) and CT fluorescence bands (Chapter 2). It has also been shown that interionic CT transitions of these salts are remarkedly sensitive to the nature of solvent and the temperature, because of the ionic ground state being strongly solvated.

In Chapter 3, the photoconductive and magnetic properties of these salts were examined. All the CT salts showed relatively large photoconduction with a good reproducibility. On the basis of the results on the electrical and magnetic properties, the mechanism of the electrical conduction was discussed in order to elucidate the relationship between the photoconduction and the interionic CT interaction. It has been suggested that the CT interaction contributes intrinsically to the photoconduction, and that this photoconduction can be explained in terms

of the carrier generation by CT interaction and carrier migration by trapping conduction.

In Chapter 4, the crystal structures of two organic CT salts, 2,4,6-triphenylpyrylium-1,1,3,3-tetracyanopropenide (TPP-TCP) and 2,4,6-triphenylthiopyrylium-1,1,3,3-tetracyanopropenide (TPT-TCP), were determined by x-ray structure analysis, in order to elucidate the role of interionic CT interaction in the crystal. These two salts have quite different crystal structure. It has been suggested that the crystal structure of organic CT salt has been influenced by electrostatic force rather than CT interaction between the cation and the anion.

It can be concluded that the characteristic features mentioned above in organic CT salts are caused by the CT salts having ionic ground state and neutral CT excited state. In future, more attention will be paid to this kind of ionic compounds as new photoconductive materials.

Part II of this thesis has dealt with the potoconductive aromatic vinylpolymers which are most important photoconductive materials. The photophysical processes of several photoconductive polymers having large π-electron conjugated system as a side chain were examined in order to obtain information on the photocarrier generation in these polymers.

The excimer formation in these polymers have been discussed in Chapter 1. New observations of the excimer fluorescences were obtained. It has been indicated that the excimer formation in these polymers occur by the interaction between two adjacent chromophores along the polymer chain and this interaction seems to be necessary for the carrier migration in these polymers.

In Chapter 2, the behaviors of triplet excited state in poly-N-vinylcarbazole, a most photoconductive polymer, were investigated. It has been

shown that the triplet excited state of poly-N-vinylcarbazole can migrate effectively along the polymer chain. This result suggests that the carrier generation is possible from the triplet excited state, and the mechanism of photocarrier generation in poly-N-vinylcarbazole must be re-examined from this point of view.

The informations obtained in this part may contribute to the development of the photoconductive polymers in giving new guiding principles for the future study.